How Did Government Bonds Become Safe? *

Juan Antolin-Diaz
London Business School

January 22, 2025

CLICK HERE FOR THE LATEST VERSION

Abstract

Government bonds in advanced economies shifted their comovement with aggregate stock returns at the end of the 1990s, from moving in sync with stocks to acting as "safe" hedges, then reverting to being "risky" after 2022. An analysis of twelve countries over the postwar period shows these shifts occurred simultaneously across countries and are not well explained by changes in output and inflation dynamics. Using a Dynamic Factor Model and a novel identification strategy combining heteroskedasticity with narrative information, I find that the data point instead to the increased importance after 1998 of financial shocks leading to flight-to-safety dynamics. A model of financial intermediaries in the stock and bond market formalizes how the rise of levered funds constrained by risk limits propagate such shocks, altering the aggregate return comovement and the perceived safety of government bonds.

Keywords: Macro finance, stock-bond covariance, historical data, narrative information, Bayesian methods.
JEL Classification Numbers: E32, E44, Q35, G12.

*Department of Economics, London Business School, 26 Sussex Pl, London NW1 4SA. Email: jantolindiaz@london.edu.
I am deeply grateful to Hélène Rey and Paolo Surico for many discussions, and to Lucrezia Reichlin, Joseba Martinez, Vania Stavrakeva, Richard Portes, Francisco Gomes, Gertjan Vliege, Thomas Drechsel, Ivan Petrella, Juan Rubio-Ramirez, Diego Känzig, Michele Andreolli, and Jesus Fernandez-Villaverde for helpful comments.

1 Introduction

Government bonds in the United States and other advanced economies are generally thought to be "safe", not only because they are subject to little or no risk of default, but also because their prices tend to increase in bad times, such as recessions and financial crises, when risky asset prices fall. The negative comovement between government bond and stock returns, however, is a relatively new phenomenon that became apparent only at the turn of the last century, as first documented by Li (2002) and Fleming et al. (2003). Indeed, for much of the century prior to the late 1990s, and after 2022, treasuries behaved not as hedges but as "risky" assets, with their prices appreciating or depreciating in sync with those of corporate equities and the broader business cycle.

Why the returns on safe government bonds switch from behaving pro- to counter-cyclically is of first-order concern for our understanding of asset pricing, for the asset allocation decisions of investors, and for the conduct of monetary and debt management policies. Focusing mostly on the post-1980 US experience, an extensive literature has linked these switches to changes in the covariance between output and inflation during the same period (Burkhardt and Hasseltoft, 2012; David and Veronesi, 2013; Campbell, Sunderam, and Viceira, 2017; Campbell, Pflueger, and Viceira, 2020). Higher unexpected inflation lowers nominal and real bond returns, and higher output raises stock returns, so changes in the cyclicality of inflation are a prime candidate for explaining the flip of the bond-stock correlation from positive to negative. However, the global financial system has undergone a large number of simultaneous technological, regulatory, and macroeconomic changes since the early 1990s (see, e.g. Rey, 2013), which make it difficult to distinguish between alternative theories of what drives these switches.

This paper widens the lens by studying the international and historical dimension of the question, and advances the hypothesis that the structure of financial markets is key to understanding the changes in the comovement between safe and risky assets. Using a panel of twelve advanced economies for the entire postwar period, I first show that bonds co-moved mostly positively with stocks for the majority of the sample, with the covariance only turning significantly negative after the 1998 Financial Crisis, earlier than previously estimated. This switch was persistent, simultaneous across countries, and does not align well with the patterns of output and inflation comovement in the time series or the cross section.[1] Instead, I show that a financial shock leading to

[1] A supplementary dataset going as back as 1890 confirms this picture. Part of this evidence is also discussed by Laarits (2020) and Chernov et al. (2021).

flight-to-safety dynamics in international markets is the leading driver of the negative stock-bond covariance, and that the importance of this shock increased dramatically after the late 1990s, changing the covariance unconditionally.[2] I then provide a theory of how market dynamics induced by levered financial intermediaries in the equity and fixed-income markets, which became prominent during this period, are consistent with the new set of facts. In my model, levered funds subject to value-at-risk constraints amplify and propagate flight to safety episodes, and a rise in their market share drives a switch in the aggregate return covariance.

A key contribution of this paper is to develop an empirical strategy that can identify the nature of the macroeconomic shocks that account for the changes in the stock-bond covariance across countries and over time. I use a Dynamic Factor Model (DFM) specifically designed to summarize the comovement among a broad set of time series that includes not just stock and bond returns, but also short-term interest rates, commodities, exchange rates, as well as output, consumption and inflation, and tease out the changing importance of different types of macroeconomic shocks. Building on ideas from the macroeconomics literature on the identification of structural vector autoregressions (VAR), I exploit heteroskedasticity in the data, complemented with a-priori narrative knowledge that certain types of structural shocks were more volatile in certain periods, to identify the model. For example, knowledge that oil supply shocks were more prevalent during the 1970s or during the 1990 Gulf War helps separate these from other types of demand and supply shocks. This new approach, which extends the narrative sign restrictions method of Antolín-Díaz and Rubio-Ramírez (2018) (see also Ludvigson et al., 2018; Giacomini et al., 2021) to a case with conditional heteroskedasticity along the lines of Sentana and Fiorentini (2001), Rigobon (2003) and Brunnermeier et al. (2020), helps overcome weak identification concerns associated with identification via heteroskedasticity only (Montiel Olea et al., 2022).

My results show that the shocks that are responsible for the volatility of output and inflation across developed countries are not the ones accounting for the flips in the stock-bond covariance, simultaneously across countries, from positive to negative in 1998, and back from negative to positive in 2022. Instead, a 'financial shock', identified from narrative information as having unusually high variance during the stock market crashes of October 1987, August 1998, and September 2008, appears as the main driver of the negative stock-bond covariance. I show that the volatility of this shock was on average, three times higher after 1998 than before 1998, and

[2]For brevity, I will refer to this shock as a 'flight-to-safety' shock. Baele et al. (2020) empirically document flgight-to-safety episodes in international financial markets.

that it leads to a 'flight to safety' in international financial markets: a simultaneous fall in the prices of stock markets around the world, a decline in nominal and real long-term interest rates, and an appreciation of the US dollar against risky currencies such as the Australian dollar but a depreciation against safe currencies such as the Japanese Yen or the Swiss Franc.

Finally, I provide a theory that links the rise of levered financial intermediaries in the late 1990s to the increased importance of financial shocks consistent with the facts. I present a stylized model of financial intermediation in the spirit of Vayanos and Vila (2021), Greenwood et al. (2018, 2023a) and Gourinchas et al. (2024) in which specialist levered traders subject to value-at-risk constraints amplify and propagate flight to safety episodes in stock and bond markets. In the model, a shock to the risk-taking capacity of specialist funds, interpreted as hedge funds or broker-dealers, interacts with the convenience demand for long-term bonds of a separate class of market participants, interpreted as pension funds, to produce a temporary flight towards long-term bonds. My model reproduces the flight towards long-maturity instruments, rather than to a safe one period bond, observed in the data and critical to explain the switch in the covariance between stock and bond returns. As the importance of levered intermediaries increases in the market, driven by regulation and/or financial innovation, shocks leading to opposite-sign movements in stock and bond returns become more volatile, leading to a change in the aggregate return comovement.

Related literature. An active literature in macro-finance has explored why the relationship between government bond and stock returns has changed over time. The switch from positive to negative covariance was documented and discussed by Li (2002), Fleming et al. (2003) and Ilmanen (2003). Baele et al. (2010), Campbell et al. (2017, 2020), Burkhardt and Hasseltoft (2012), and David and Veronesi (2013) all link the changing stock-bond covariance to changes in the cyclical behavior of inflation and consumption. They argue that inflation was counter-cyclical during the 1970s and 1980s but became pro-cyclical during the Great Moderation, affecting the riskiness of nominal bonds. Consistent with my findings, Baele et al. (2010) find that macroeconomic fundamentals contribute little to explaining stock and bond return correlations. A few papers have explored alternative explanations, all within the framework of consumption-based asset pricing. Song (2017), proposes that a shift toward more counter-cyclical monetary policy in the late 1990s accounts for the observed changes, whereas Chernov et al. (2021) link them to changes in the autocorrelation of consumption growth, and Li et al. (2022) links them to the fiscal policy regime. Consistent with

my findings, Acharya and Laarits (2023) document the important linkage between the stock-bond covariance and convenience yields on long-term treasuries, and Laarits (2020) emphasizes the importance of a precautionary savings motive. Duffee (2018, 2023) challenges existing theories by showing that they all imply that volatile expected inflation is a primary driver of bond yields. He shows instead that in the data, expected inflation is relatively stable and does not significantly impact bond yields. My evidence confirms that shocks not directly linked to inflation are important to explain the stock-bond covariance, and I provide a purely real model in which the latter can switch without a significant role for inflation.

I depart from consumption-based pricing and instead build on a strand of theories emphasizing the importance of financial intermediaries and market structure on asset pricing. Krishnamurthy and Vissing-Jorgensen (2012) analyze how the demand for safe assets affects Treasury yields, emphasizing the impact of the supply and demand dynamics of government bonds on asset prices. Vayanos and Vila (2021) and Greenwood and Vayanos (2014) discuss how demand pressures and supply factors influence the yield curve through the behavior of preferred-habitat investors. In a closely-related contribution to my own, Kekre and Lenel (2021) investigate how value-at-risk constraints on levered intermediaries affect asset prices and contribute to flight-to-safety episodes. My model is closest to Greenwood et al. (2018, 2023a) and Gourinchas et al. (2024), with the key difference that I focus the attention on arbitrage across stock and bond markets, and shocks to levered intermediaries risk-taking capacity. On the empirical front, the literature on the "global financial cycle" (Rey, 2013; Miranda-Agrippino and Rey, 2020, 2022) connects these intermediary effects to the movements in risky asset prices. These papers document the synchronization of financial cycles across countries and highlight the role of global financial intermediaries in transmitting shocks internationally. I contribute to this body of work by showing that safe assets such as bonds are also affected by the synchronized movements in prices associated to the actions of global financial intermediaries.

On the econometric front, the paper contributes to the literature on dynamic factor models and identification of structural vector autoregressions (VARs). Sentana (1998), and Sentana and Fiorentini (2001) explore identification in conditionally heteroskedastic factor models, while Rigobon (2003) introduces identification through heteroskedasticity in structural VARs, a strategy that has become increasingly popular (see, e.g. Brunnermeier et al., 2020; Lewis, 2021). Identification via heteroskedasticity offers the promise of sharp inference by exploiting the differences in volatility,

but is subject to concerns about interpretability, sensitivity, and weak identification, as discussed by Montiel Olea et al. (2022). To address these concerns, I introduce a new identification strategy that combines heteroskedasticity with narrative information about periods where the volatility of certain types of shocks is known a-priori to be elevated, an approach that I label "volatility narratives" and that builds on the concept of narrative sign restrictions introduced in Antolín-Díaz and Rubio-Ramírez (2018) (see also Ludvigson et al., 2018; Giacomini et al., 2021).

Organization of the paper. The rest of the paper is organized as follows. Section 2 discusses the data and presents an initial set of stylized facts. Section 3 discusses the econometric approach to identification, and presents the idea of volatility narratives. Section 4 applies the model to the data and discusses the results. I formalize the mechanism behind the empirical results in section 5, and section 6 concludes.

2 Data and Stylized Facts

2.1 Baseline dataset.

The main dataset underlying the empirical analysis comprises 99 time series at the monthly frequency from January 1955 to June 2024 and covers twelve advanced economies: Australia, Canada, France, Germany, Italy, Japan, New Zealand, Norway, Sweden, Switzerland, the United Kingdom, and the United States. I outline here the variables included and the main sources, and give full details in Appendix A. The dataset includes stock returns, 3-month and 10-year interest rates, exchange rates against the US dollar, core and headline inflation, and GDP and consumption growth for each country, as well as four series of commodity prices aggregated at the level of broad categories (energy, agriculture and livestock, industrial metals, and precious metals). Stock return data comes from Morgan Stanley Capital International (MSCI) from December 1969 onward, and from Global Financial Data (GFD) prior to that date. Because data on government bonds differs greatly in terms of time span and maturity availability across countries, the creation of consistent series of government bond yields requires specifying and estimating an empirical model of the term structure of interest rates for each country. I apply the model of Diebold and Li (2006), adjusted to allow for arbitrary patterns of missing data, to raw data from Thomson Reuters Datastream and GFD, and construct homogeneous series of zero-coupon bond yields at the

1-month, 2-year and 10-year maturity for all the countries in my sample.[3] Bond returns are then computed following the approximation of Campbell et al. (1998). All return series are denominated in their domestic currency and converted into excess returns by subtracting the one-month bill return of the respective country. Foreign Exchange rates are from the International Monetary Fund (IMF).[4] Commodity futures returns are from S&P Goldman Sachs Commodity Indices. Whenever necessary, these are extended backwards using historical data from GFD. Inflation rates, both headline and core (excluding food and energy), as well as quarterly real GDP and consumption growth rates, are from the OECD Main Economic Indicators. These are interpolated to monthly frequency using the growth rates of industrial production and retail sales, also from the OECD.[5]

2.2 Additional data

I complement the main dataset with an extension covering a longer historical period starting in 1890. This is achieved by merging three distinct sources. The first is the study by Dimson, Marsh, and Staunton (2009) (DMS), which compiles annual data on stock, bond, and bill returns, as well as inflation since 1901 for a large cross section of countries. Second, the one of Barro and Ursúa (2008), whose main source is Global Financial Data (GFD). An advantage of the latter source is that much of the return data is also available at monthly frequency. More recently, Jordà, Schularick, and Taylor (2017) (JST) and Jordà et al. (2019) updated, revised and combined these data sources to create a comprehensive database at the annual frequency for 17 advanced economies. Combining these data sources, I can re-construct monthly series of stock and bond returns for the 12 countries of interest going back to 1890.[6]

A summary of the data is displayed in Figure 1. In the figure, each blue circle represents one country-year observation for the stock-bond correlation, computed as the correlation within the twelve months of the year, using monthly stock and return data. The solid black line represents the correlation, computed in the same way, of equally weighted global averages of stock and bond returns, respectively. It is already possible to see a key stylized fact from the figure: although each country and year is noisy, the stock bond correlation was mostly positive throughout the

[3] Further details are provided in Appendix A.

[4] For France, Germany and Italy, the Franc, Mark, and Lira are used prior to the introduction of the euro, and spliced with the euro thereafter.

[5] The empirical model which I present below can easily be extended to handle mixed frequencies, at the cost of increased computation time. To avoid this, I use the method of Chow and Lin (1971) to transform these series to monthly frequency prior to estimation.

[6] Additional details of this reconstruction are presented in Appendix A.

Figure 1: INTERNATIONAL STOCK-BOND CORRELATION: 1890-2024

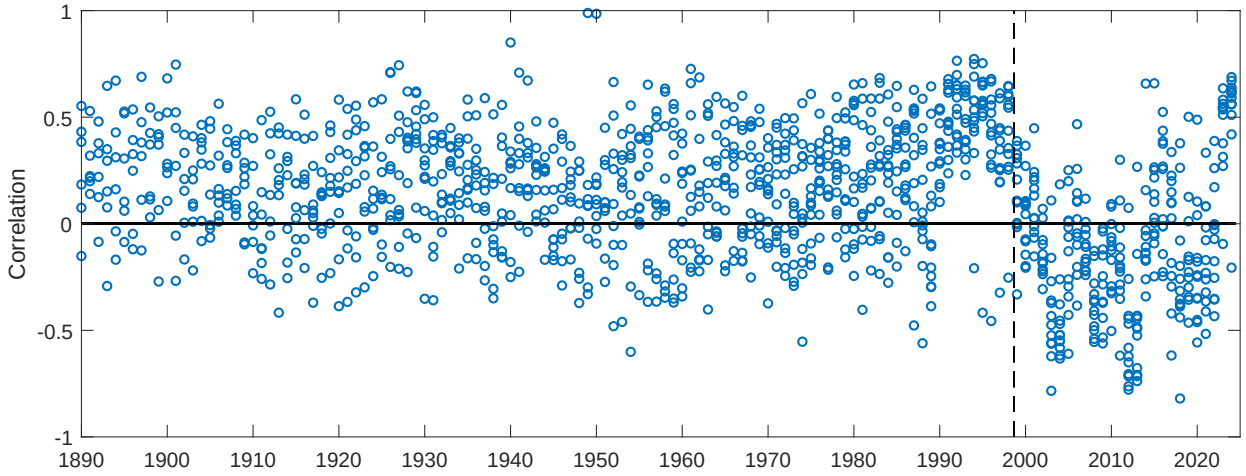

Notes. In the figure, each blue circle represents one country-year observation for the stock-bond correlation, computed as the correlation within the twelve months of the year, using monthly stock and return data. The solid black line represents the correlation, computed in the same way, of equally weighted global averages of stock and bond returns, respectively. Vertical dashed line marks failure of LTCM in August 1998.

century prior to 1998, and only turned clearly and persistently negative after that year. Moreover, periods of large macroeconomic fluctuations, such as the 1930s and the 1970s, characterized by very different cyclical behavior of inflation (pro-cyclical during the 1930s, counter-cyclical during the 1970s) barely stand out.

Figure 2 presents a second important stylized fact. The figure displays the average pairwise correlation among stocks and bond returns of different countries. As can be seen in the figure, international asset comovement increased dramatically starting in the decade of the 1980s, and in particular during the 1990s. At the end of the 20th century, advanced-economy stock and government bond markets had become highly integrated, a fact that has been highlighted before by Rey (2013) and Jordà et al. (2019). Taken together, these two facts suggest the need for an empirical framework that is capable of capturing changes in the importance of global and country-specific factors affecting asset returns and macro variables, as well as changes in their conditional correlations.

A final stylized fact concerns the behavior of real (inflation-linked) interest rates. As originally pointed out by Campbell et al. (2009, 2017) and Liu (2018) returns on U.S. Treasury Inflation-Protected Securities (TIPS) co-move negatively with stocks returns in a similar manner than nominal

Figure 2: INTERNATIONAL ASSET COMOVEMENT: 1890-2024

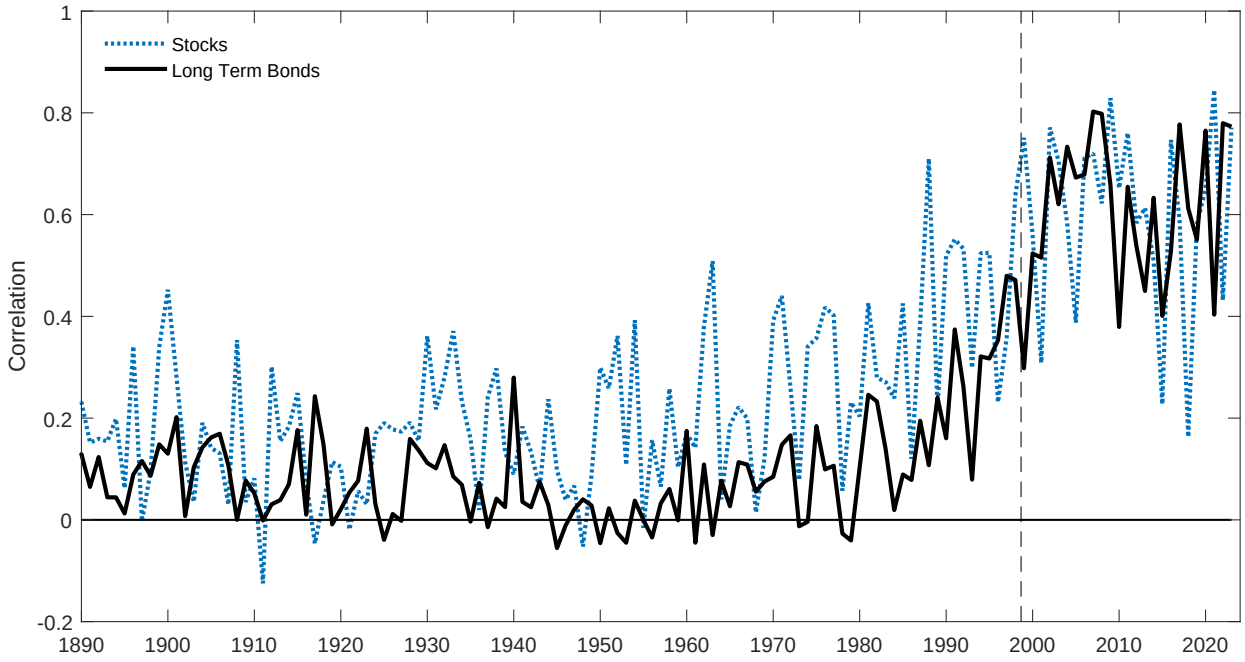

Notes. The figure represents the average pairwise correlation, computed on non-overlapping 12-month windows, of bonds and stocks of the twelve countries included in the sample. Vertical dashed line marks failure of LTCM in August 1998.

bonds. An important limitation is that TIPS are available only since 1997, so it is not possible to understand whether the switch in the correlation observed around this time for nominal bonds occurred as well for real bonds. Figure 3 presents new evidence for three advanced economies which started issuing inflation-linked bonds prior to 1997. Data is available since 1985 for the United Kingdom, since 1990 for Canada, and since 1995 for Australia. In the three cases, we observe a striking similarity between the patterns observed in the nominal and inflation-linked bond returns. As is the case with the nominal bonds, the switch in the real bond-stock covariance appears simultaneous across countries and centered around the time of the financial crises of 1997-1998. This seems to suggest that changes in the covariance of expected inflation with aggregate stock returns is less important for understanding fluctuations in the stock-bond covariance. As discussed by Duffee (2018, 2023) this challenges existing theories, the majority of which imply that volatile expected inflation is a primary driver of bond yields.

Figure 3: INTERNATIONAL INFLATION-LINKED BOND RETURN CORRELATION WITH STOCKS

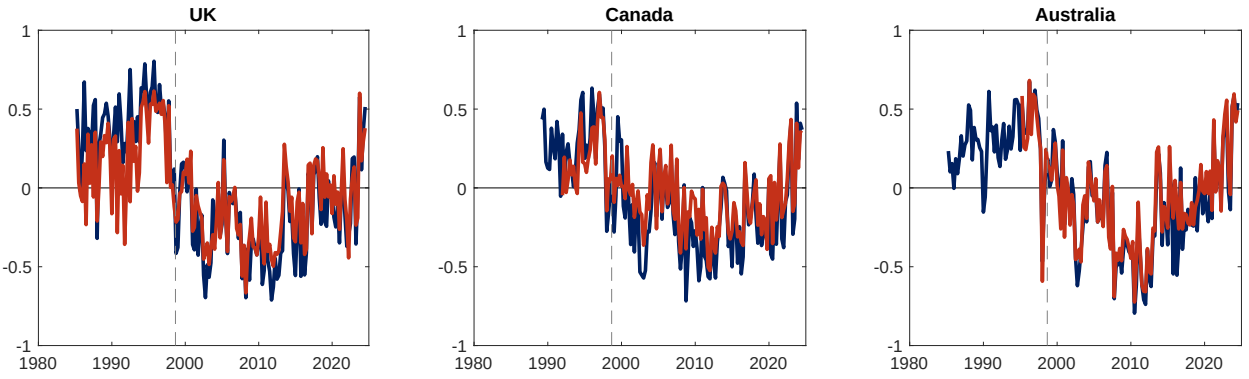

Notes. The figure represents the correlation of stock and inflation-linked bonds, at the 10-year maturity, computed using daily data over quarterly windows. The solid blue lines represent the correlation of stocks with nominal bond returns, whereas the red lines represent the correlation of stocks with inflation-linked bond returns. Vertical dashed line marks failure of LTCM in August 1998.

3 Econometric Framework

This section introduces the econometric model I use to further analyze the data described above. The panel-like structure of the data, which contains different economic concepts for 12 integrated economies, and the stylized patterns described above, suggest a Dynamic Factor Model with time-varying volatilty. This type of model is well suited to capture common and country-specific movements among financial and macroeconomic variables. To identify structural shocks, I propose an identification strategy that combines heteroskedasticity-based methods with "volatility narratives"using periods where certain shocks are known to have elevated volatility based on historical events. I present a Bayesian algorithm to conduct inference on the parameters of the model.

3.1 The structural factor model

Let $\mathbf{y}_t$ be a $N \times 1$ vector of observable time series at t. It is assumed that the variation in the data is originating from $k < N$ common macroeconomic shocks, collected in the vector $\boldsymbol{\varepsilon}_t$, as well as N variable-specific innovations, collected in the vector $\boldsymbol{\nu}_t$. The propagation of the k macroeconomic shocks can be described in terms of k common latent variables, denoted $\mathbf{x}_t$, which jointly follow an autoregressive process of order p, and n idiosyncratic terms, denoted $\mathbf{u}_t$, which follow independent

autoregressive process of order q:

$$\mathbf{x}_t = \mathbf{\Phi}_1 \mathbf{x}_{t-1} + \ldots + \mathbf{\Phi}_p \mathbf{x}_{t-p} + \mathbf{A}_0^{-1} \varepsilon_t \tag{1}$$

$$\mathbf{u}_t = \boldsymbol{\rho}_1 \mathbf{u}_{t-1} + \ldots + \boldsymbol{\rho}_q \mathbf{u}_{t-q} + \boldsymbol{\nu}_t \tag{2}$$

with $\boldsymbol{\rho}_\ell$ diagonal for $\ell = 1 \ldots q$. The common and idiosyncratic processes map into observable variables according to the measurement equation

$$\mathbf{y}_t = \mathbf{\Lambda}_0 \mathbf{x}_t + \mathbf{\Lambda}_1 \mathbf{x}_{t-1} + \mathbf{u}_t. \tag{3}$$

The inclusion of a lag of the factors in the measurement equation has been advocated by Antolín-Díaz et al. (2024) as necessary to capture the heterogeneous dynamics present in many macroeconomic time series. Pre-multiplying the factors by the matrix $\mathbf{A}_0$, and defining $\tilde{\mathbf{x}}_t \equiv \mathbf{A}_0 \mathbf{x}_t$, $\tilde{\mathbf{\Phi}}_\ell \equiv \mathbf{A}_0 \mathbf{\Phi}_\ell \mathbf{A}_0^{-1}$, $\tilde{\mathbf{\Lambda}}_0 \equiv \mathbf{\Lambda}_0 \mathbf{A}_0^{-1}$, $\tilde{\mathbf{\Lambda}}_1 \equiv \mathbf{\Lambda}_1 \mathbf{A}_0^{-1}$, we can re-write the model in structural form:

$$\tilde{\mathbf{x}}_t = \tilde{\mathbf{\Phi}}_1 \tilde{\mathbf{x}}_{t-1} + \ldots + \tilde{\mathbf{\Phi}}_p \tilde{\mathbf{x}}_{t-p} + \varepsilon_t \tag{4}$$

$$\mathbf{y}_t = \tilde{\mathbf{\Lambda}}_0 \tilde{\mathbf{x}}_t + \tilde{\mathbf{\Lambda}}_1 \tilde{\mathbf{x}}_{t-1} + \mathbf{u}_t. \tag{5}$$

This formulation of the dynamic factor model will be particularly useful for discussing identification, and is flexible enough to encompass a wide class of macroeconomic models.[7] The common shocks and idiosyncratic innovations are conditionally Gaussian, have mean zero, and are uncorrelated with each other, but their variances are possibly time-varying, i.e.,

$$\begin{bmatrix} \varepsilon_t \\ \boldsymbol{\nu}_t \end{bmatrix} \sim N\left(\begin{bmatrix} \mathbf{0}_{k\times 1} \\ \mathbf{0}_{N\times 1} \end{bmatrix}, \begin{bmatrix} \mathbf{D}_t & \mathbf{0}_{k\times N} \\ \mathbf{0}_{N\times k} & \mathbf{V}_t \end{bmatrix} \right). \tag{6}$$

Moreover, it is assumed that $\mathbf{D}_t$ and $\mathbf{V}_t$ are diagonal matrices. Diagonality of $\mathbf{D}_t$ is a standard assumption which is necessary for the shocks ε_t to be interpreted as primitive sources of variation, whereas diagonality of $\mathbf{V}_t$ identifies these innovations as purely specific to each variable. Indeed,

[7] In particular, it nests structural vector autoregressive (VAR) models, and the 'ABCD' representation of linearized dynamic, stochastic, general equilibrium (DSGE) models (see Fernández-Villaverde et al., 2007), with the addition of serially correlated measurement errors.

the conditional covariance matrix of the observables can be written

$$\text{Var}_t(\mathbf{y}_t|\mathbf{x}_{t-1}, \mathbf{u}_{t-1}, \ldots, \mathbf{u}_{t-q}) = \mathbf{\Lambda}_0 \mathbf{D}_t \mathbf{\Lambda}_0' + \mathbf{V}_t,$$

which highlights that any correlation between the variables originates from their loading on the common shocks, ε_{t+1}. For this reason, I refer to them as "macro" shocks. In turn, the idiosyncratic innovations $\boldsymbol{\nu}_{t+1}$ affect only one variable each. They can be interpreted as measurement error in the macroeconomic variables or market micro-structure-driven movements in returns that do not spill over to other variables.

Denote $\delta_{t+1}^{(j)}$ the square root of the j-th diagonal element of the matrix $\mathbf{D}_{t+1}$, and by $\nu_{t+1}^{(i)}$ the square root of the i-th diagonal element of the matrix $\mathbf{V}_{t+1}$, i.e. the volatilities of the macro and idiosyncratic shocks. I assume that the logarithm of these volatilities evolve according to autoregressive latent processes:

$$\log \delta_{t+1}^{(j)} = \mu_\delta^{(j)} + \phi_\delta^{(j)} \log \delta_t^{(j)} + \omega_\delta^{(j)} v_{\delta,t+1}^{(j)}, \quad v_{\delta,t+1}^{(j)} \overset{iid}{\sim} N(0,1) \quad j = 1, \ldots, k \tag{7}$$

$$\log \nu_{t+1}^{(i)} = \mu_\nu^{(i)} + \phi_\nu^{(j)} \log \nu_t^{(i)} + \omega_\nu^{(i)} v_{\nu,t+1}^{(i)}, \quad v_{\nu,t+1}^{(i)} \overset{iid}{\sim} N(0,1) \quad j = 1, \ldots, n \tag{8}$$

This completes the description of the model. I now turn to the issue of identification of its structural parameters.

3.2 Identification and Weak Identification

The model in (4)-(6) is a dynamic factor model with heteroskedasticity in the innovations to the factors and idiosyncratic components. It nests the setup of Bai and Wang (2014, 2015) by allowing for conditional heteroskedasticity, and the one of Sentana (1998) and Sentana and Fiorentini (2001) by allowing autoregressive dynamics in both factors and idiosyncratic components, as well as the idiosyncratic components (rather than just the common factors) to be heteroskedastic.

It is well known that the structural DFM is in general not identified. In particular, because the common factors are unobserved, rotations of factors and loadings by a $k \times k$ invertible matrix $\mathbf{Q}$

lead to an observationally equivalent model:

$$\mathbf{Q}\tilde{\mathbf{x}}_t = \mathbf{Q}\tilde{\mathbf{\Phi}}_1\mathbf{Q}^{-1}\mathbf{Q}\tilde{\mathbf{x}}_{t-1} + \ldots + \mathbf{Q}\tilde{\mathbf{\Phi}}_p\mathbf{Q}^{-1}\mathbf{Q}\tilde{\mathbf{x}}_{t-p} + \mathbf{Q}\boldsymbol{\varepsilon}_t \tag{9}$$

$$\mathbf{y}_t = \tilde{\mathbf{\Lambda}}_0\mathbf{Q}^{-1}\mathbf{Q}\tilde{\mathbf{x}}_t + \tilde{\mathbf{\Lambda}}_1\mathbf{Q}^{-1}\mathbf{Q}\tilde{\mathbf{x}}_{t-1} + \mathbf{u}_t. \tag{10}$$

Identifying the system means placing restrictions on the parameters to ensure that $\mathbf{Q} = \mathbf{I}_k$ is the only admissible rotation. Bai and Wang (2015) discuss the identification problem in the context of homoskedastic factor models, and show that we require a minimum of k^2 restrictions on the loading matrix $\mathbf{\Lambda}_0$ or the covariance matrix $\mathbf{D}_t$ of the common shocks. We start the discussion on identification by stating the general assumptions on the dynamic factor model:

Assumption 1 (A1). *$\mathbf{x}_t$ and $\mathbf{u}_t$ are stationary processes with $\mathbb{E}(\mathbf{x}_t) = \mathbb{E}(\mathbf{u}_t) = \mathbf{0}_k$, $Var(\mathbf{x}_t) < \infty$ and $Var(\mathbf{u}_t) < \infty$.*

Assumption 2 (A2). The common shocks, $\boldsymbol{\varepsilon}_t$, and idiosyncratic innovations, $\boldsymbol{\nu}_{t+1}$, are mutually independent, and serially uncorrelated, i.e. $\mathbb{E}(\varepsilon_{j,t}\varepsilon_{j,s}) = \mathbb{E}(\nu_{i,t}\nu_{i,s}) = \mathbb{E}(\varepsilon_{j,t}\nu_{i,s}) = 0\ \forall i, j$ and $\forall t \neq s$.

Assumption 3 (A3). The loading matrix $\mathbf{\Lambda}_0$ has full column rank, the covariance matrices $\mathbf{D}_t$ and $\mathbf{V}_t$ are positive definite for all t.

Under these conditions, Bai and Wang (2015) propose two alternative identification schemes that are sufficient to identify the reduced-form factor model:

Identification Scheme 1 (DFM1). *If $var(\boldsymbol{\varepsilon}_t) = \mathbf{I}_k$ and the upper $k \times k$ block of $\mathbf{\Lambda}_0$ is a lower-triangular matrix with strictly positive diagonal elements, the factor model is identified.*

Notice that the requirement that the unconditional variance of the shocks, $\text{var}(\boldsymbol{\varepsilon}_t) = \mathbf{I}_k$ imposes $k(k+1)/2$ restrictions, whereas the requirement that the upper block of $\mathbf{\Lambda}_0$ is lower-triangular imposes an additional $k(k-1)/2$ restrictions, a total of q^2 restrictions. This still leaves the model invariant to sign flips, hence the requirement to fix the sign of the diagonal elements of the upper block of $\mathbf{\Lambda}_0$. Alternatively, one could specify $\text{var}(\boldsymbol{\varepsilon}_t)$ as a diagonal matrix and the upper block of $\mathbf{\Lambda}_0$ has 1's on the diagonal.

Identification Scheme 2 (DFM2). *The upper $k \times k$ block of $\mathbf{\Lambda}_0$ is an identity matrix $\mathbf{I}_k$.*

This is also sufficient to identify the factor model. Notice that DFM2 does not impose any

restrictions on the unconditional covariance matrix of ε_t, in principle allowing this to be a full matrix $\mathbf{\Sigma}$. The upper k variables provide 'labels' to the factors, and structural analysis can be carried out by further decomposing $\mathbf{\Sigma} = \mathbf{A}_0^{-1}(\mathbf{A}_0^{-1})'$ with a combination of zero and sign restrictions (see Rubio-Ramirez et al., 2010).

While both DFM1 and DFM2 impose k^2 restrictions on either the loadings or the covariance matrix of the factor innovations, DFM 2 leaves the structural matrix $\mathbf{A}_0^{-1}$ unrestricted, whereas DFM 1 has the peculiarity of simultaneously identifying the reduced-form and the structural form of the factor model. It is reminiscent of the Cholesky identification strategy in the structural VAR literature as it imposes a recursive structure to the impact of the structural shocks. Indeed, it is easy to see that DFM1 is equivalent to DFM2 plus the additional requirement that $\mathbf{A}_0^{-1}$ is lower triangular, which amounts to $n(n-1)/2$ additional restrictions. Critically, the need for these restrictions disappears under conditional heteroskedasticity of the structural shocks. This leads to a new identification scheme.

Identification scheme 3 (DFM3). *Under independent AR(1) processes for the common volatilities in* (8)*, if* $\mathbf{D}_t$ *and* $\mathbf{V}_t$ *are diagonal matrices, with* $\mathbb{E}(v_{\delta,t}^{(j)}, v_{\delta,t}^{(l)}) = 0, \forall j \neq l$ *and* $\mu_\delta^{(j)} = 0 \; \forall j$*, the model is statistically identified up to column permutations and sign flips.*

The restrictions $\mu_\delta^{(j)} = 0$ fixes the scale of the shocks, giving us k restrictions, whereas the diagonality of $\mathbf{D}_t$ gives an additional $k(k-1)/2$ restrictions, as in DFM1. The remaining $k(k-1)/2$ restrictions that are necessary in the case of a homoskedastic model are made redundant by the presence of conditional heteroskedasticity. This is easiest to see in the simplified case of Rigobon and Sack (2003), in which the heteroskedasticity is described by two regimes: the empirical covariance matrix of the second regime provides $k(k-1)/2$ additional moments. This "identification via heteroskedasticity" holds under a variety of stochastic processes for the time-varying variances in $\mathbf{D}_{t+1}$ (Sentana and Fiorentini, 2001; Lewis, 2021).[8]

In practice however, estimation of the model above can be challenging. This is for two reasons. First, economic time series display common trends in their volatilities (e.g., the 'great moderation' described in McConnell and Perez-Quiros (2000)), such that the independence assumption is frequently violated. While, in theory, weaker assumptions are required for statistical identification (Lewis, 2021), in small samples, the degree of commonality in the volatilities is sufficient to lead to

[8]Moreover, Sims (2020) argues that identification can be quite robust to misspecification of the volatility process.

weak identification. Second, even if the patterns of volatilities are sufficiently distinct, the model is still only identified only up to permutations and sign switches. This presents practical challenges whenever two or more shocks display similar patterns of sign impact on the variables. Monte Carlo Markov Chain algorithms, in practice, will tend to randomly permute the shocks across columns.

Figure 4: THREE CASES OF IDENTIFICATION VIA HETEROSKEDASTICITY

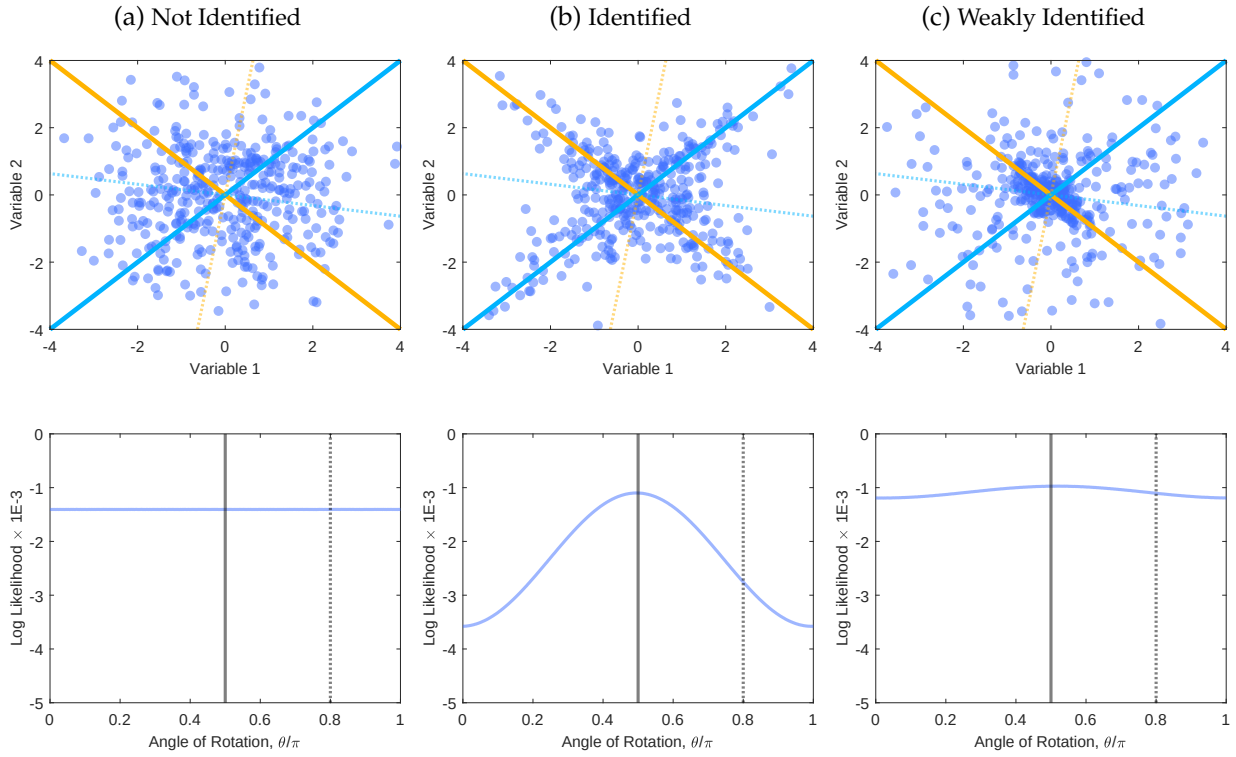

Note: The figure illustrates three cases of identification via heteroskedasticity. In all cases the data generating process underlying the figure is $\mathbf{y}_t = \mathbf{\Lambda}\boldsymbol{\varepsilon}_t$, with the dimension of $\mathbf{y}_t$ is of size $n = 2$ for $T = 1, \ldots, T$, $\mathbf{\Lambda} = [1, 1; -1, 1]$ and $\boldsymbol{\varepsilon}_t) \sim \mathcal{N}(\mathbf{0}_n, \mathbf{\Sigma}_1)$ for $t \leq T/2$ and $\boldsymbol{\varepsilon}_t) \sim \mathcal{N}(\mathbf{0}_n, \mathbf{\Sigma}_2)$ for $t > T/2$. In panel (a), $\mathbf{\Sigma}_1 = \mathbf{\Sigma}_2 = \mathbf{I}_2$. In panel (b), $\mathbf{\Sigma}_1 = diag([1.2, 0.4])$ and $\mathbf{\Sigma}_2 = diag([0.3, 1.5])$. In panel (c), $\mathbf{\Sigma}_1 = diag([1.2, 0.4])$ and $\mathbf{\Sigma}_2 = diag([1.2, 0.2])$. The first row plots each of $T = 400$ observations drawn from the respective D.G.P., together with the true coefficients of $\mathbf{\Lambda}$ (solid lines) and an arbitrary rotation at angle $0.8/\pi$ (dotted lines). The second row plots the value of the conditional log likelihood for angles of rotation $\theta/\pi, \theta \in [0, 1]$. The horizontal lines mark the true parameters ($\theta = 0$, solid line) and the rotation $\theta = 0.8$ (dotted line). As can be seen from the figure, the structural parameters of the model in panel (a) are not identified, whereas they are identified in panels (b) and (c), but only weakly so in the latter case.

Figure 4 illustrates the intuition behind the problem of weak identification for a simple bi-variate model with two shocks: one that moves both variables in the same direction and one that moves them in opposite direction, as in a textbook demand and supply model. In the top panels, the solid lines are the true demand and supply schedules, with their slopes equal to the inverse elasticities 1

and -1. Each circle represents an observation resulting from simultaneous shocks that shift the supply and demand curves. In the familiar case with constant shock volatilities (Panel A), it is not possible to discriminate between the true parameters and an arbitrary rotation (thin dotted lines), because their likelihood is the same, as seen in the lower panel. The model is not identified and additional, theoretically-motivated restrictions are needed. In the case in which the volatilities of the structural shocks are time-varying (Panel B), periods of high volatility of each shock trace out the elasticities, and the true structural model maximizes the likelihood without need for additional restrictions. In this case, the model is identified (up to permutations and sign switches) and all that remains is to attach labels to the shocks ex-post. While this statistical approach to identification can be appealing, in practice for the reasons discussed above, identification will be very weak and the likelihood will become close to flat across different structural parameters (Panel C).

3.3 Introducing additional identifying information: volatility narratives

I now introduce the idea of volatility narratives in order to ameliorate the weak identification problem described above. The idea of volatility narratives involves the possibility that for certain dates $\tau \in \tau_1, \tau_2, \ldots, \tau_m$, the researcher might have external knowledge about the volatilities of the macroeconomic shocks being higher or lower than usual. For instance, one could think that the variance of monetary policy shocks was higher than usual during the tenure of Paul Volcker, or the volatility of financial shocks higher during the fall of 2008. This external knowledge can be encoded in the form of a prior

$$p(\log \delta_{\tau}^{(j)}) \sim N(\kappa_{\tau}^{(j)}, \xi_{\tau}^{(j)}) \quad \text{for} \quad \tau \in \tau_1, \tau_2, \ldots, \tau_m \quad \text{and} \quad j \in 1, \ldots, k. \tag{11}$$

where $\kappa_{\tau}^{(j)}$ represents the a priori level of the log volatility of shock j during period τ, and $\xi_t^{(j)}$ captures a priori uncertainty around this level. Notice that given that the steady state log-volatilities are zero, this implies that the volatility of shock j is believed to be $\exp(\kappa_{\tau}^{(j)})$ higher than usual during period τ. Equivalently, one can think of the researcher as having access to a *volatility proxy*, z_t that is observed, with a measurement error whose variance is equal to $\xi_t^{(j)}$, to take the values $\kappa_{\tau}^{(j)}$ on dates $\tau \in \tau_1, \tau_2, \ldots, \tau_m$, and is not observed on other dates.

Volatility narratives extend the idea of narrative sign restrictions (Antolín-Díaz and Rubio-Ramírez, 2018; Ludvigson et al., 2018) to models featuring heteroskedasticity. Narrative sign re-

strictions constrain the structural shocks and/or the historical decomposition around key historical events, ensuring that they agree with the established narrative account of these episodes. Volatility narratives extend the idea of a shock being particularly important for the history of a variable during a specific period by incorporating that information into the estimation of the time-varying shock volatilities. The existing literature (see also Giacomini et al., 2021) has employed them in the context of VARs with fixed volatilities, and therefore, like traditional sign restrictions, narrative sign restrictions can only achieve set identification of the structural parameters.[9] Moreover, existing algorithms for inference, such as the one developed by Antolín-Díaz and Rubio-Ramírez (2018), rely on rejection sampling and can be computationally quite intensive. Volatility narratives provide many of the same advantages as narrative sign restrictions in the context of point identification and, as we shall see below, can be implemented by means of a straightforward Gibbs sampler.

3.4 Inference under volatility narratives

This section describes the estimation of the model in Equations (4)-(8) under the existence of volatility narratives as described in (11). Our objective is to draw from the joint posterior distribution of the underlying shocks ε_t, idiosyncratic errors $\mathbf{u}_t$, the autoregressive parameters governing the dynamics of the factors, $\mathbf{\Phi} = \{\mathbf{\Phi}_1, \ldots, \mathbf{\Phi}_p\}$, the structural impact matrix, $\mathbf{A}_0^{-1}$, the loading matrices $\mathbf{\Lambda}_0$ and $\mathbf{\Lambda}_1$, the time-varying volatilities $\boldsymbol{\delta} = \{\boldsymbol{\delta}_1, \ldots, \boldsymbol{\delta}_T\}$ and $\boldsymbol{\nu} = \{\boldsymbol{\nu}_1, \ldots, \boldsymbol{\nu}_T\}$, together with the vectors of autoregressive parameters and standard deviations for the log-volatilities, $\boldsymbol{\phi}_\delta, \boldsymbol{\phi}_\nu, \boldsymbol{\omega}_\delta$, and $\boldsymbol{\omega}_\nu$. This posterior is in general unknown but can be approximated by means of a Gibbs sampling algorithm that iteratively draws from the known conditional distributions of each block of parameters. Many of the steps required are standard and have been described before, e.g by Bai and Wang (2015); Antolín-Díaz et al. (2024), so this section focuses on the new elements and provides only a brief sketch.[10]

Conditional on an arbitrary initialization of the parameters, a first draw of the factors $\mathbf{x}_t^{(1)}$ is obtained. Using the previous draw of $(\mathbf{A}_0^{-1})^{(0)}$, these can be orthogonalised into $\tilde{\mathbf{x}}_t^{(1)} = \mathbf{A}_0^{(0)}\mathbf{x}_t^{(1)}$. Each of the k factor autoregressions can now be treated as a series of unrelated regressions with

[9] An exception is Carriero et al. (2023), which uses traditional and narrative sign restrictions to refine the identification in SVARs identified via heteroskedasticity.

[10] Full details are available in Appendix C.

heteroskedastic errors:

$$\tilde{x}_{j,t}^{(1)} = \tilde{\phi}_{j,1}\tilde{\mathbf{x}}_{t-1}^{(1)} + \ldots + \tilde{\phi}_{j,p}\tilde{\mathbf{x}}_{t-p}^{(1)} + \varepsilon_{j,t} \quad , \varepsilon_{j,t} \sim N(0, \delta_{j,t}^2) \quad \text{for} \quad j = 1 \ldots k, \tag{12}$$

where $\tilde{\phi}_{j,\ell}$ is the j-th row of $\tilde{\mathbf{\Phi}}_\ell$. Further dividing each equation by the previous estimate of $\delta_{j,t}$ allows us to draw the rotated coefficients $\tilde{\mathbf{\Phi}}_\ell \equiv \mathbf{A}_0 \mathbf{\Phi} \mathbf{A}_0^{-1}$ under a standard Normal-Inverse Wishart prior. The posterior can then be rotated back using $(\mathbf{A}_0^{-1})^{(0)}$ to obtain a new draw $\mathbf{\Phi}^{(1)}$.

Next, we can calculate a new estimate of the structural shocks, $\varepsilon_t^{(1)} = (\mathbf{A}_0^{-1})^{(0)}[\mathbf{x}_t^{(1)} - \mathbf{\Phi}_1{}^{(1)}\mathbf{x}_{t-1}^{(1)} - \ldots - \mathbf{\Phi}_p{}^{(1)}\mathbf{x}_{t-p}^{(1)}]$ which can be projected onto $[\mathbf{x}_t^{(1)} - \mathbf{\Phi}_1{}^{(1)}\mathbf{x}_{t-1}^{(1)} - \ldots - \mathbf{\Phi}_p{}^{(1)}\mathbf{x}_{t-p}^{(1)}]$ element-by-element to obtain a new draw of $(\mathbf{A}_0^{-1})^{(1)}$.[11] Sign restrictions can be imposed on the elements of $\mathbf{A}_0^{-1}$ using the truncated normal sampler proposed by Korobilis (2022). At this stage, the columns of $\mathbf{A}_0^{-1}$ are permuted to maximize the conditional likelihood $p(\varepsilon_t|\delta_t^{(0)})$.

Then, we need to drawing from the log-volatilities $\log \delta_t^{(j)}$ and $\log \nu_t^{(j)}$, while incorporating prior information about the volatility narratives at dates $\tau \in \tau_1, \ldots, \tau_m$. This can be achieved easily by modifying the standard auxiliary mixture sampler of Kim et al. (1998) in order to incorporate the proxy variable z_t.

Finally, we need to draw the remaining parameters of the reduced-form factor model, including the latent factors. These steps are standard and have been described in detail by Antolín-Díaz et al. (2024). This completes a full iteration of the Gibbs sampler, which can be then iterated until convergence.

4 Empirical Results

Given that the variables in my panel comprise the same economic concepts (such as stock returns, long- and short-term interest rates, inflation, etc.) for each of the twelve countries in the sample, it is natural to group them by economic concept and impose a block structure on the reduced-form factor loadings, ensuring that each set of conceptually similar variables loads on the same factor across countries. This greatly reduces the number of free parameters to be estimated and delivers a clearer, more interpretable representation of the underlying factors. For example, consider a simplified model in which the only economic concepts included in the dataset are stock returns,

[11] I use an independent Normal-Inverse Wishart centered at an identity matrix with each element having a variance of 100, making the prior essentially uninformative.

bond yields, and inflation, each of which is observed for several countries in the panel. The structure of the loadings would be as follows:

$$\mathbf{y}_t = \begin{pmatrix} \text{stock}_t^{USA} \\ \text{stock}_t^{UK} \\ \vdots \\ \text{bond}_t^{USA} \\ \text{bond}_t^{UK} \\ \vdots \\ \text{infl}_t^{USA} \\ \text{infl}_t^{UK} \end{pmatrix}, \quad \mathbf{\Lambda}_0 = \begin{pmatrix} \lambda_0^{(\text{stock,USA})} & 0 & 0 \\ \lambda_0^{(\text{stock,UK})} & 0 & 0 \\ \vdots & \vdots & \vdots \\ 0 & \lambda_0^{(\text{bond,USA})} & 0 \\ 0 & \lambda_0^{(\text{bond,UK})} & 0 \\ \vdots & \vdots & \vdots \\ 0 & 0 & \lambda_0^{(\text{infl,USA})} \\ 0 & 0 & \lambda_0^{(\text{infl,UK})} \end{pmatrix}, \quad \mathbf{\Lambda}_1 = \begin{pmatrix} \lambda_1^{(\text{stock,USA})} & 0 & 0 \\ \lambda_1^{(\text{stock,UK})} & 0 & 0 \\ \vdots & \vdots & \vdots \\ 0 & \lambda_1^{(\text{bond,USA})} & 0 \\ 0 & \lambda_1^{(\text{bond,UK})} & 0 \\ \vdots & \vdots & \vdots \\ 0 & 0 & \lambda_1^{(\text{infl,USA})} \\ 0 & 0 & \lambda_1^{(\text{infl,UK})} \end{pmatrix}.$$

In this case, the first factor would be interpreted as the global stock factor, capturing the co-movement of equity returns across all countries, while the second factor would represent a global bond factor, and so on. It should be clear that because the structural impact matrix $\mathbf{A}_0^{-1}$ is full, the block structure in the loadings does not preclude cross-factor interactions or dynamic linkages across blocks, since shocks can still propagate among them through the structural equations; denoting $a_{i,j}$ the elements of $\mathbf{A}_0$, we see that each shock can affect multiple factors simultaneously:

$$\mathbf{A}_0^{-1} = \begin{pmatrix} a_{1,1} & a_{1,2} & a_{1,3} \\ a_{2,1} & a_{2,2} & a_{2,3} \\ a_{3,1} & a_{3,2} & a_{3,3} \end{pmatrix}, \quad \mathbf{\Lambda}_0 \, \mathbf{A}_0^{-1} = \begin{pmatrix} \lambda_0^{(\text{stock,USA})} a_{1,1} & \lambda_0^{(\text{stock,USA})} a_{1,2} & \lambda_0^{(\text{stock,USA})} a_{1,3} \\ \lambda_0^{(\text{stock,UK})} a_{1,1} & \lambda_0^{(\text{stock,UK})} a_{1,2} & \lambda_0^{(\text{stock,UK})} a_{1,3} \\ \vdots & \vdots & \vdots \\ \lambda_0^{(\text{bond,USA})} a_{2,1} & \lambda_0^{(\text{bond,USA})} a_{2,2} & \lambda_0^{(\text{bond,USA})} a_{2,3} \\ \lambda_0^{(\text{bond,UK})} a_{2,1} & \lambda_0^{(\text{bond,UK})} a_{2,2} & \lambda_0^{(\text{bond,UK})} a_{2,3} \\ \vdots & \vdots & \vdots \\ \lambda_0^{(\text{infl,USA})} a_{3,1} & \lambda_0^{(\text{infl,USA})} a_{3,2} & \lambda_0^{(\text{infl,USA})} a_{3,3} \\ \lambda_0^{(\text{infl,UK})} a_{3,1} & \lambda_0^{(\text{infl,UK})} a_{3,2} & \lambda_0^{(\text{infl,UK})} a_{3,3} \end{pmatrix}.$$

I consider one factor per each of the groups of variables in the panel (stock returns, long-term bond yields, short-term interest rates, inflation, core inflation, output, consumption, exchange rates and commodities), plus an extra factor to capture additional variation in the short-term rates across European countries, leading to ten factors. Additionally, I consider two additional factors per each of the countries, restricted so that they are country-specific. These additional factors

allow for the possibility that correlation among variables arises from shocks purely specific to each country. Subject to these restrictions, the dynamic factor model is estimated using 7000 draws of the algorithm above, discarding the first 2000 as burn-in. Posterior inference is carried out on the remaining 5000 draws of the parameters and latent structural shocks.

4.1 Accounting for the Stock-Bond Correlation

Figure 5 displays the first key results of the model. Starting with the top panel, the figure reports the time-varying correlation between the global bond factor and the global stock factor. The thick solid line is the posterior median correlation along with the associated 68% and 90% highest posterior density (HPD) intervals. For reference, a simple 12-month rolling estimate of the correlation is also presented. As can be seen, the time-variation in the factor volatilities is able to explain the secular patterns in the stock-bond correlation, in particular, the values close to zero or positive between 1955 and 1975, the generally positive value between 1975 and the late 1990s, and the switch to negative territory until after the 2020 pandemic. The vertical reference lines mark October 1987 (the "Black Monday" stock market crash), August 1998 (the failure of LTCM and associated financial turmoil), the first month in which the correlation becomes significantly negative with 90% confidence, and June 2022 (the start of an aggressive monetary tightening by the Federal Reserve), a point after which the correlation becomes significantly positive again.[12]

Panels (b) and (c) of Figure 5 display the posterior estimates of the average pairwise correlations *within* stocks and bonds, respectively. Again, a simple rolling estimate is also reported for reference. This figure is the model analogue for the postwar period of the longer-term estimates reported in Figure 3. As can be seen, the model is successful at capturing the increased synchronization in bond yields and returns that ocurred between the end of the 1980s and the early 2000s. This correlation has increased further after the pandemic, reaching an average level of between 70 and 80 percent. Though less dramatic, the pairwise correlation between stocks of different countries displays a similar secular increase, as reported by Jordà et al. (2019).

Next, I compute the stock-bond correlation of individual countries implied by the global factors in Figure 6. For reference, a rolling 12-month estimate of the correlation is reported for each country as a dotted gray line. Deviations between this estimate and the one implied by the global factors,

[12]The tightening process by the Federal Reserve started in March of 2022 with a 25 basis point hike and continued in May with a 50 basis point hike. In their analysis of available policy records, Romer and Romer (2023) conclude that the announcements of June or July 2022 meet their criteria for a contractionary monetary policy shock.

Figure 5: COMOVEMENT OF INTERNATIONAL ASSET PRICES

(a) Correlation of Global Stock Return and Global Bond Returns

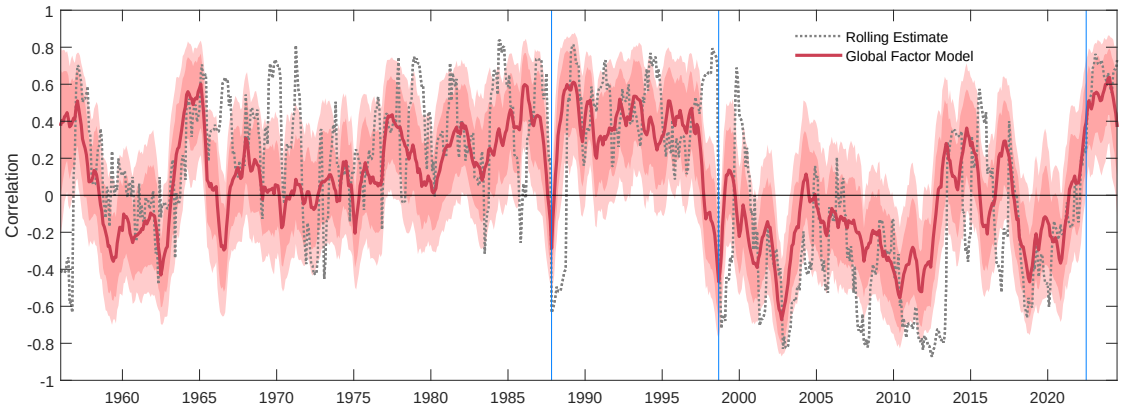

(b) Bond Returns: Average Pairwise Correlation Across Countries

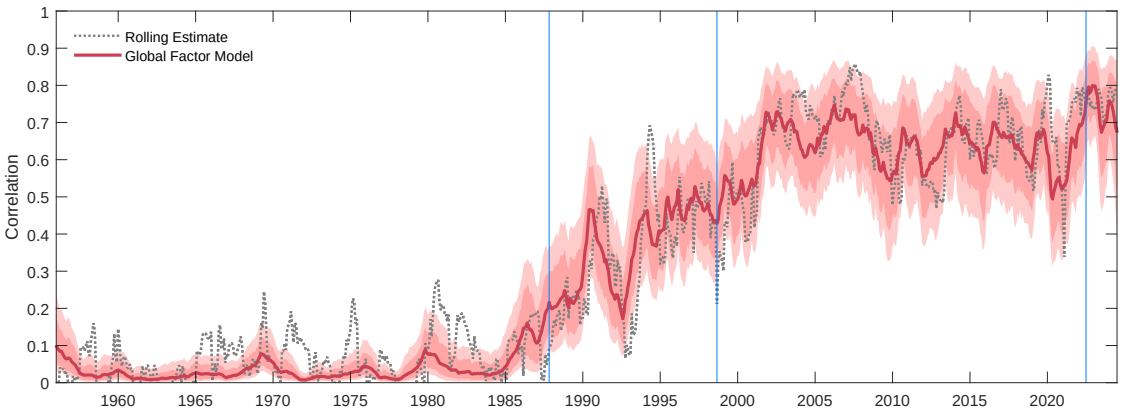

(c) Stock Returns: Average Pairwise Correlation Across Countries

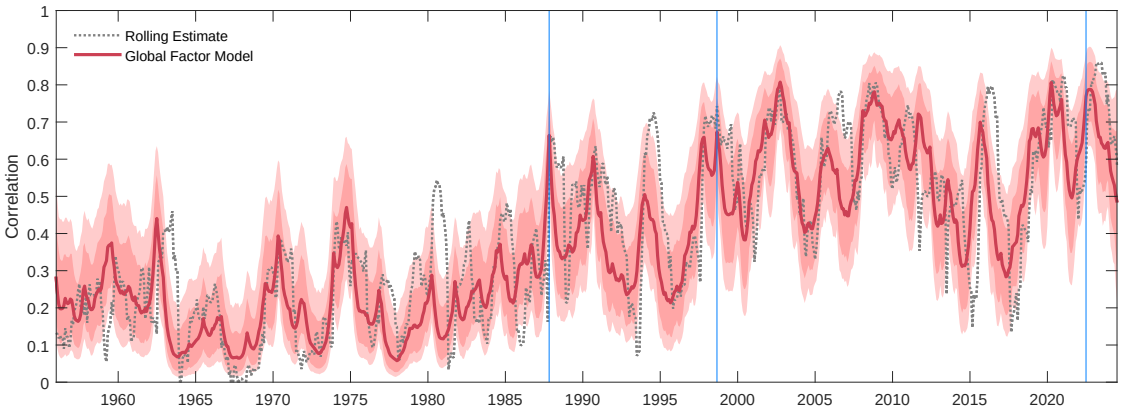

Note: Estimates of stock-bond correlation across twelve advanced economies from January 1955 to June 2024, using monthly data. Each panel presents the posterior median correlation (thick solid line) along with the associated 68% highest posterior density (HPD) interval and 90% interval derived from the global factor model. The posterior estimates account for the portion of the correlation explained by global shocks. The dotted line represents a simple 12-month rolling correlation.

Figure 6: GLOBAL VARIATION IN THE STOCK-BOND CORRELATION ACROSS COUNTRIES

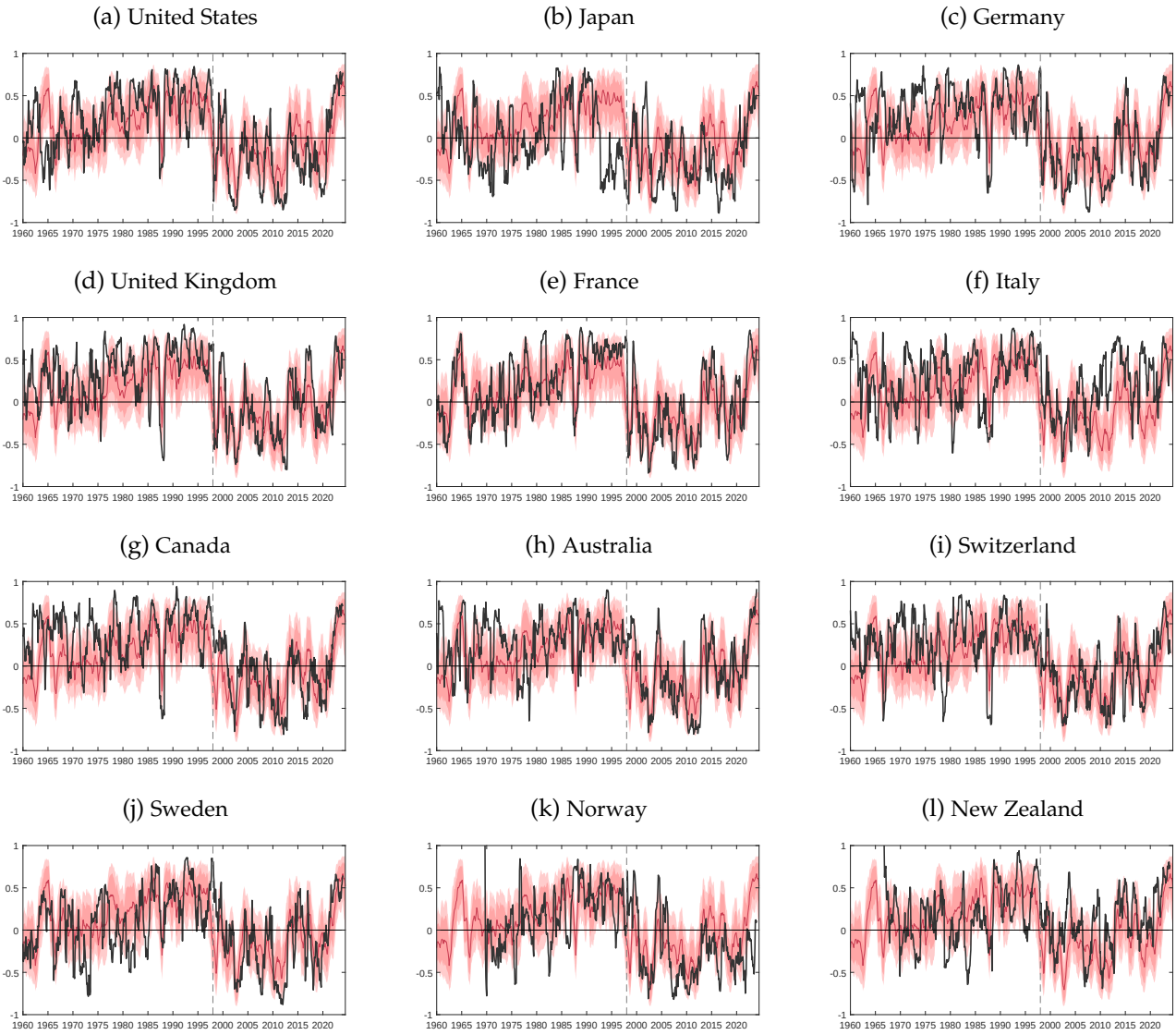

Note: Estimates of stock-bond correlation across twelve advanced economies from January 1955 to June 2024, using monthly data. Each panel presents the posterior median correlation (thick solid line) along with the associated 68% highest posterior density (HPD) interval and 90% interval derived from the global factor model. The posterior estimates account for the portion of the correlation explained by global shocks. The dotted line represents a simple 12-month rolling correlation.

reported in thick solid red with associated 68% and 90% HPD confidence bands, represent the influence of country-specific factors. The conclusion is clear: the changes in correlation between stock and bonds across countries are highly synchronized across countries. In other words, the time-variation in the correlation across countries represents the time-varying correlation of the global stock and bond factors.

Two persistent deviations from this pattern are worth noting. First, Italy, where the comovement is largely similar to that of other European countries until the sovereign debt crisis of 2010, after which point Italian bonds systematically comoved positively with Italian stocks, reflecting a heightened risk of government default. Second, Japan, where the correlation switched to negative in early 1993. Interestingly, this year saw the Financial System Reform Act –passed one year earlier– come into effect. It partially dismantled the strict firewall regulations in Japans financial sector (akin to those under the U.S. Glass-Steagall Act), thereby allowing allowing financial institutions to diversify their activities into securities trading, including the issuance and trading of derivatives.

We will return to the relationship between financial intermediation and the stock bond covariance in the next subsection. To make further progress, I require identification assumptions to give economic meaning to the global sources of variation responsible for international asset price comovements.

4.2 Identification Assumptions

To identify the structural shocks in the empirical Dynamic Factor Model, I use three sources: heteroskedasticity in the data, volatility narratives, and sign restrictions. Heteroskedasticity allows me to exploit periods when the variances of certain shocks change, aiding in their identification. Volatility narratives involve historical events where specific shocks had elevated (or reduced) volatility, helping to isolate those shocks. I also apply a small set of normalizing sign restrictions on the immediate responses of certain variables to specific shocks, which help prevent the algorithm from cycling through random sign switches of the structural parameters.

I identify four key shocks. Two U.S. monetary policy shocks are identified. First a "short rate" shock using the period from October 1979 to December 1982, when the Federal Reserve implemented significant policy changes that led to higher interest rate volatility, as well as the zero lower bound period between January 2009 and December 2015 where the federal funds rate was effectively fixed; the U.S. T-bill rate and the U.S. 10-year bond yield are restricted to have a

positive response on impact to this shock. A "long-rate" or term premium shock is identified during the "Taper Tantrum" in June 2013, when indications of tapering quantitative easing led to rising long-term interest rates; the U.S. T-bill rate is restricted to have a positive response on impact, and the U.S. 10-year bond yield is restricted to have a stronger positive response on impact. An oil price shock is associated with significant oil price fluctuations in January 1974, January 1986, and August 1990; oil prices are restricted to have a positive response on impact. A financial or flight-to-safety shock is identified during periods of financial market stress, such as October 1987, August 1998, and September 2008; stock prices are restricted to have a positive response on impact. By combining heteroskedasticity, volatility narratives, and sign restrictions, this identification strategy allows me to effectively disentangle the structural shocks in the model.

I find that once these four key shocks are identified, the remaining six global shocks in the model appear to be robustly identified by the heteroskedasticity in the data alone. In order to give them a label, I examine the implied Impulse Responses on GDP and Inflation, and label a shock as an "aggregate demand" shock if it leads to a significantly positive comovement of output and inflation at the one year horizon, an "aggregate supply" shock if it leads to negative comovement, and "other" of there is no significant comovement.

4.3 The identified shocks and their contribution

Figure 7 displays the time series of the realization (in black solid line, left axis) and the volatility (plotted as a blue area, right axis) of the four shocks identified via volatility narratives. Appendix Figure E.1 is the analogue for the remaining shocks. The flight-to-safety shock is displayed in panel (a). It is clear from the figure that this shock was virtually non-existent prior to the early 1970s, and that its volatility has increased over time. Moreover, it displays discrete spikes during the market crashes of 1987 and 1998, a result that derives from the identification assumptions. The fact that its volatility is persistently higher after 1998 than before that date is instead a feature of the data rather than an assumption. Panels (b) and (c) display the two monetary policy shocks. By assumption, the short rate monetary policy shock displays large fluctuations during the reserve-targeting period of 1979-1982, and almost no realizations during the zero lower bound period of 2009-2015.

Figure 8 carries out a historical decomposition of the contribution of different structural shocks to the historically observed deviations of several variables from their unconditional mean. Historical decompositions can be computed for every draw; the figure reports the posterior mean

Figure 7: TIME SERIES AND VOLATILITIES OF KEY SHOCKS

(a) Flight-to-Safety Shock

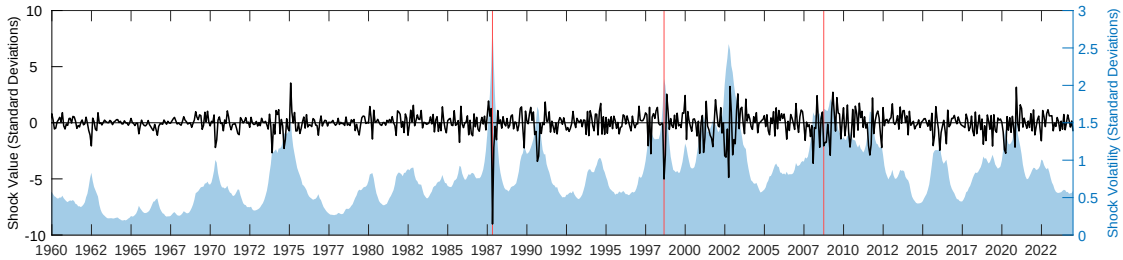

(b) Short-Rate Monetary Policy Shock

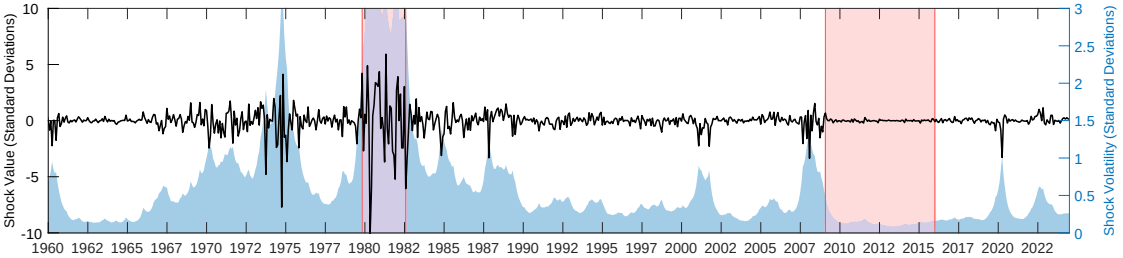

(c) Long-Rate Monetary Policy Shock

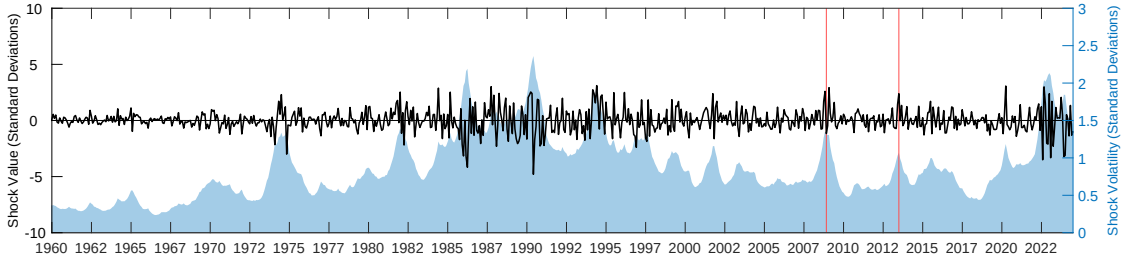

(d) Oil Supply Shock

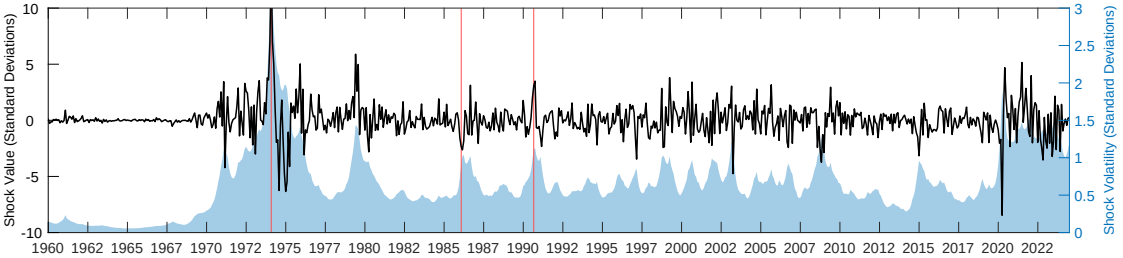

Note: Each panel displays the time series (in black solid line, left axis) of the realization of the identified structural shock, and its estimated time-varying volatility (blue area, right axis). The reference lines mark the following events. Panel (a): Black Monday (October 1987), collapse of LTCM (August 1998), failure of Lehman Brothers (September 2008); Panel (b): Reserve Targeting period (October 1979 to July 1982), Zero Lower Bound period (January 2009 to December 2015); Panel (c): first announcement of Quantitative Easing (November 2009), "Taper Tantrum" (June 2013); Panel (d) Iranian Revolution (January 1974), collapse of OPEC (January 1986), Gulf War (August 1990). Results based on posterior mean.

Figure 8: HISTORICAL DECOMPOSITION

(a) Global Inflation (annual, % 12 month change)

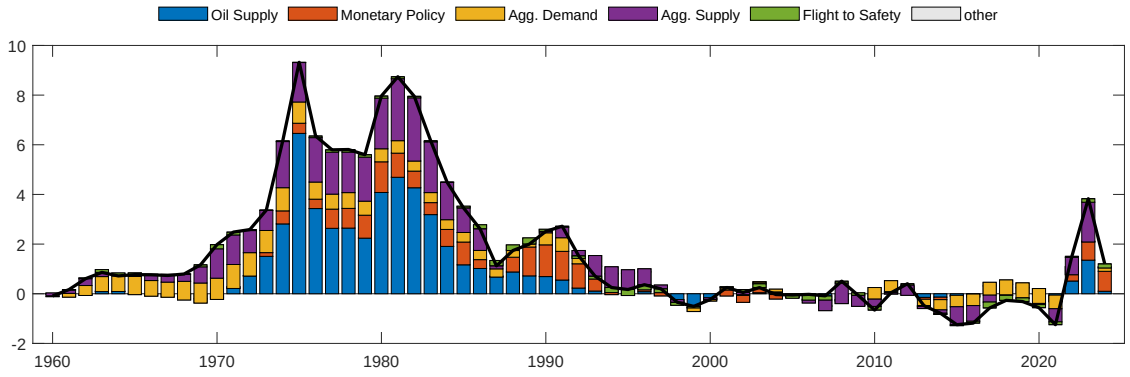

(b) Global Stock Returns (annual, % 12 month return)

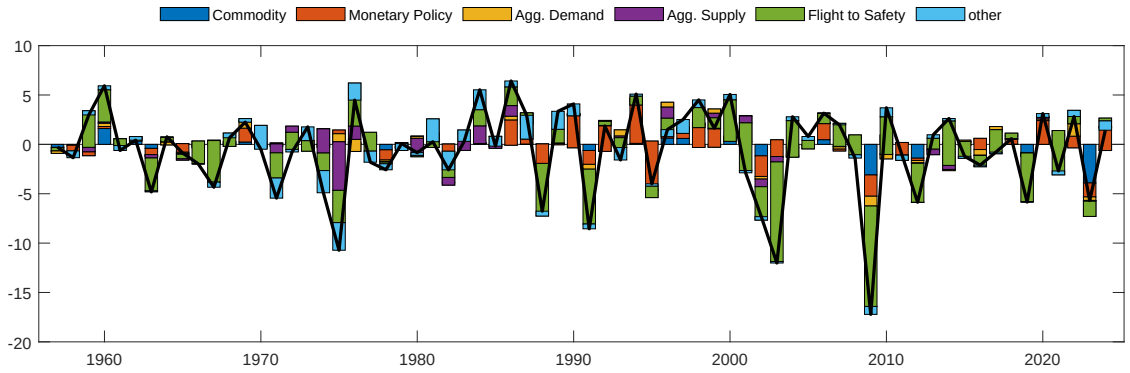

(c) Global Bond Returns (annual, % 12 month return)

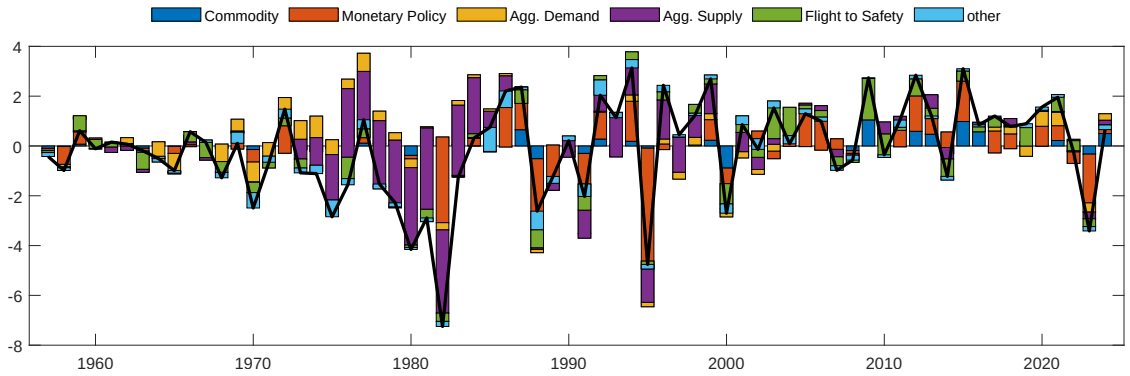

Note: Estimates of the historical contribution of different structural shocks to the deviations of each variable from its unconditional mean. Results based on posterior mean.

decomposition. This allows to trace out visually which shocks were important for which variables during different periods. Starting with panel (a), which examines the movements of global inflation, intuitively we observe that the identified oil shock displays an important impact on inflation during the 1970s, and then fades until the post-pandemic period. In any event, panels (b) and (c) of Figure 8 already show a key result of this paper: the changing volatilities of energy shocks that dominated inflation fluctuations during the postwar period were not important for stock return fluctuations, which were instead were dominated by flight-to-safety shocks. Bond returns reflect a mixture of influences, but only those shocks that strongly affect stocks *and* bonds, such as monetary policy and flight-to-safety shocks, can account changes in their correlation.

Figure 9 more formally carries out a historical correlation decomposition. Since the shocks are orthogonal to each other, we can write the one-step ahead conditional correlation between any two variables, i and j, as:

$$\text{Corr}(y_{i,t}, y_{j,t}|\mathbf{y}_{t-1}, \ldots, \mathbf{y}_1) = \sum_{r=1}^{k} \frac{\mathbf{A_0}^{-1}_{(i,r)} \delta^2_{t,r} \mathbf{A_0}^{-1}_{(j,r)}}{\sqrt{\mathbf{A_0}^{-1}_{(i,\cdot)} \delta^2_t \mathbf{A_0}^{-1}_{(j,\cdot)}}} \tag{13}$$

which can be computed additively for each shock $r = 1 \ldots k$. Each of these terms represents the contribution of each structural shock to the total correlation.[13] Confirming the visual impression discussed above, Figure 9 shows that the monetary policy and the flight-to-safety shocks are responsible for esentially all of the correlation and its movements over time. In particular, the flight-to-safety shock (panel (a)) is responsible for the negative comovement, and its importance increases over time, whereas the monetary policy shock –in particular the long-rate shock– accounts for most of the positive covariance. The latter shock increases in importance during the second half of the 1980s, then declines at the end of the 1990s until the post-pandemic period. All the other shocks taken together have a limited influence on the stock-bond correlation.

Appendix Figure G.1 performs the equivalent decomposition of the output and inflation correlation. This "Phillips curve" correlation is mostly positive except for the 1970s and 1980s period. Moreover, aggregate demand and supply shocks are mostly responsible for changes in this correlation. Thus, contrary to the existing literature, the shocks that are responsible for the changes in the output-inflation correlation are distinct from those responsible for the changes in the stock-bond correlation. Moreover, a flight-to-safety shock largely disconnected from output and inflation is the

[13] This formula can be generalized to the correlation at any horizon by substituting $\mathbf{A}_0^{-1}$ by the matrix of impulse responses at horizon h.

Figure 9: HISTORICAL CORRELATION DECOMPOSITION: STOCK-BOND CORRELATION

(a) Stock-Bond Correlation: Fraction Attributed to Flight-to-Safety Shocks

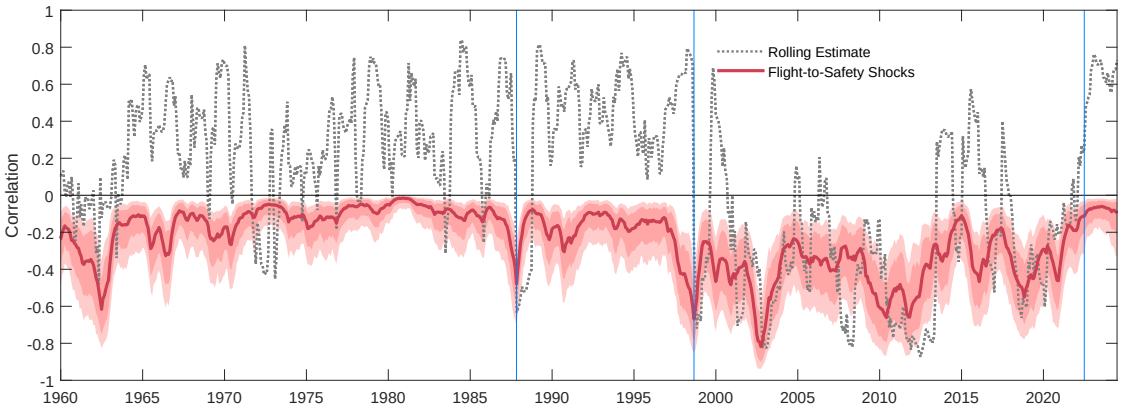

(b) Stock-Bond Correlation: Fraction Attributed to Monetary Policy Shocks

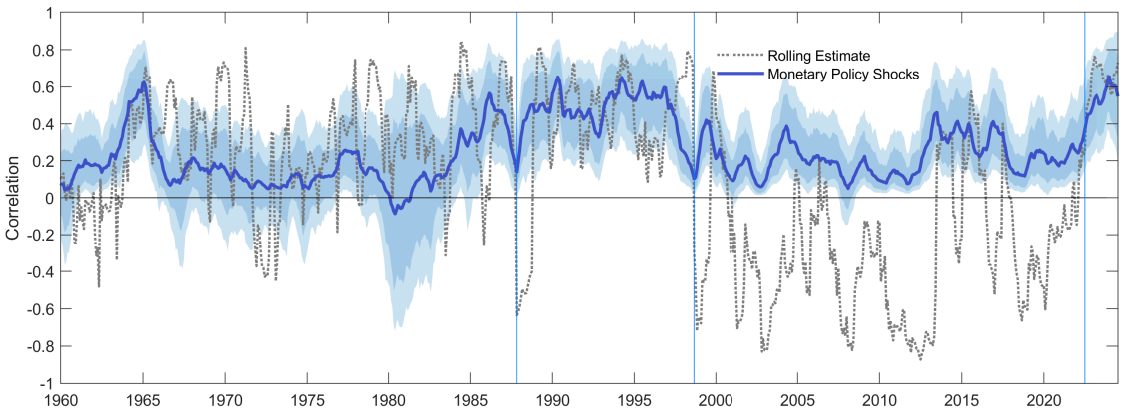

(c) Stock-Bond Correlation: Fraction Attributed to All Other Shocks

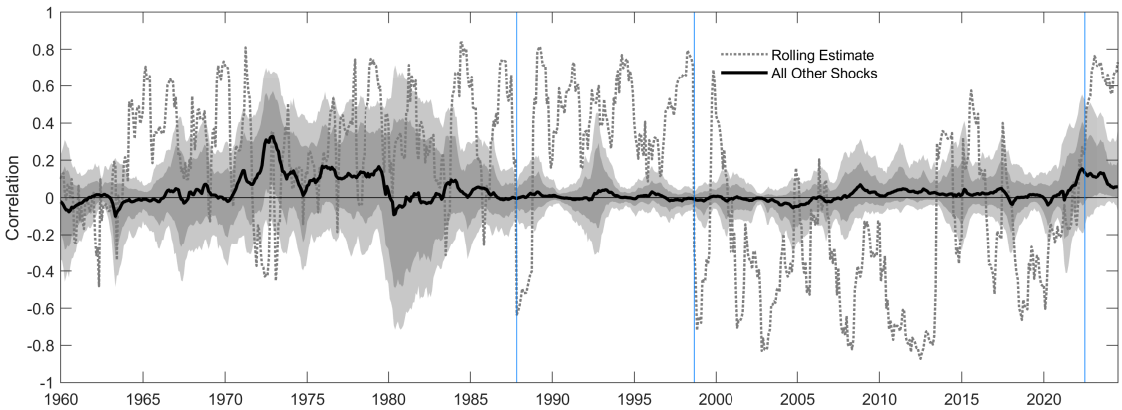

Note: Estimates of the contribution of different structural shock to the observed correlations between the global stock and bond return factors. Each panel presents the posterior median correlation (thick solid line) along with the associated 68% highest posterior density (HPD) interval and 90% interval derived from the global factor model, attributable to the shocks highlighted. The posterior estimates account for the portion of the correlation explained by global shocks. The dotted line represents a simple 12-month rolling correlation.

key shock that drives a negative stock-bond correlation. I now examine this shock in more detail.

Figure 10 displays the impulse responses of selected variables in the panel to a one standard deviation innovation in the flight to safety shock.[14] As can be seen from the figure, the shock leads to a simultaneous decline in the global stock markets, and a decline in global bond yields. The flight-to-safety shock is not entirely disconnecte from macroeconomic variables: it leads to a short-term decline in output and inflation. Interestingly, the response of short term rates across major economies is not significant. This point is further seen in Figure 11, which compares the implied responses of the average short term interest rates (blue impulse reponses) with the decline in bond yields (red responses). The significant differences between the two indicate a decline in the bond term premium for all countries. Figure 12 looks at the response of currencies. As can be seen, risky currencies such as the Australian, New Zealand, or Canadian dollar depreciate against the US dollar, whereas the Euro, Japanese Yen and the Swiss Franc appreciate. This is consistent with the results of Baele et al. (2020), who empirically document and classify flight-to-safety episodes using a different methodology. Thus, the flight-to-safety shock responsible for the negative stock-bond-comovement is peculiar in two ways. First, it leads to a *decline* in long-term term premia, contrary to other episodes of flight towards cash, and second it does not lead to an homogeneous appreciation of the dollar, but instead appears to have a significant effect on the carry factor (Lustig et al., 2011).

Finally, Figure 13 plots the responses of additional indicators not included in the model. These are computed using Local Projections of each variable on the shock, controlling for 48 lags of each. Indicators of risk aversion, such as the VIX volatility index, the MOVE index of treasury implied volatility, or the spread between BAA corporate bonds and treasuries, both spike in a consistent manner. These patterns are consistent with the findings of Acharya and Laarits (2023), who document that the stock-bond covariance is strongly negative when convenience yields on long-term treasuries are highest, and of Laarits (2020), who emphasizes the importance of a precautionary savings motive. The figure also shows the response of the intermediary capital ratio of He et al. (2017). This variable reflects the financial strength of intermediaries and their capacity to absorb shocks. It is constructed as the market equity of broker-dealers divided by the sum of their market equity and book leverage, capturing the intermediary's capital constraints. This measure is crucial in their asset pricing framework, as it proxies for intermediary risk-bearing

[14] The full set of impulse responses is available upon request.

Figure 10: Impulse Responses to a Flight-to-Safety Shock

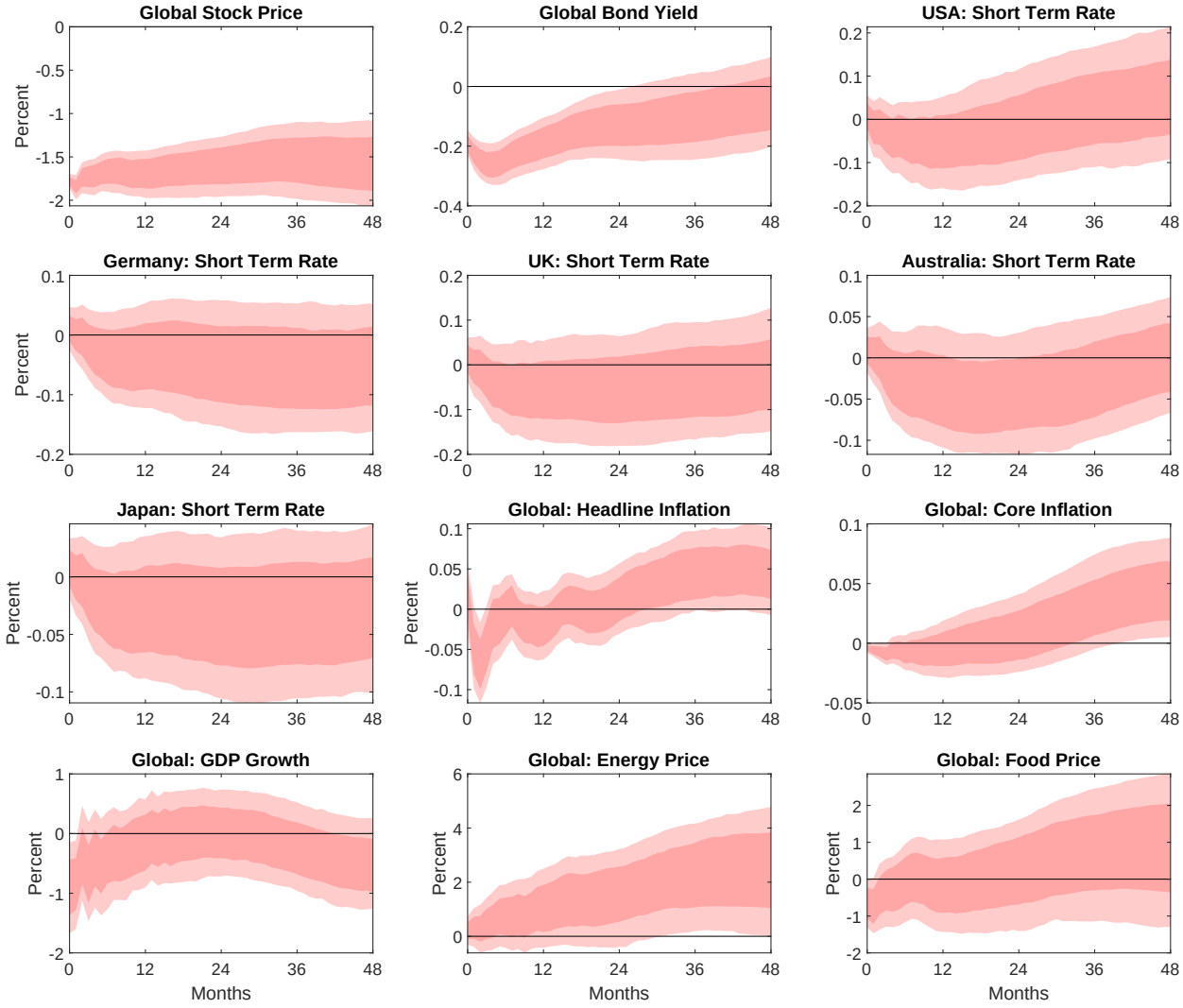

Note: Responses of selected variables to the flight-to-safety shock.

Figure 11: Impulse Responses of Interest Rates to a Flight-to-Safety Shock

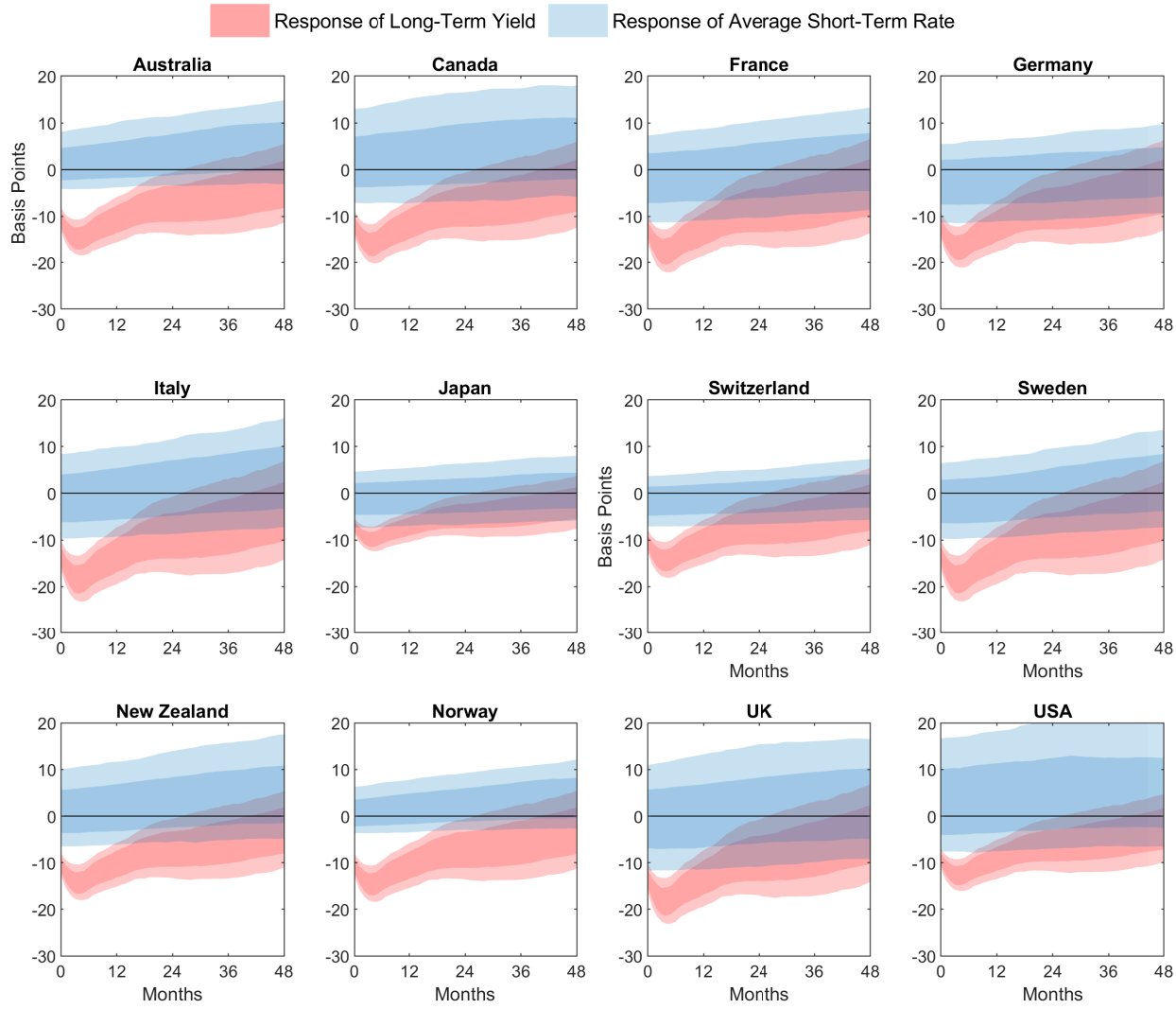

Note: Responses of selected variables to the flight-to-safety shock.

capacity, which varies countercyclically and helps explain fluctuations in risk premia. The response shows a significant and persistent decline in the ratio following the shock, with the trajectory indicating an immediate and pronounced drop that disipates after about one year. The sharp drop in the intermediary capital ratio reflects a contraction in the ability of broker-dealers to absorb risk, as their equity buffers shrink relative to their total or risk-weighted assets. Such a reduction in financial resilience constrains intermediaries capacity to provide liquidity and extend credit, limiting their ability to support financial markets during periods of stress. Moreover, panel (f) looks at the response of actual bond holdings by primary dealers, using data collected by Fleming et al. (2024). Primary dealers, which were generally net short during this sample, typically respond to the impairment in their risk taking capacity by undoing these short positions, i.e. buying back bonds. This dynamic highlights the intrinsic connection between the identified financial shock and the ability of broker-dealers to take on risk. These patterns are all consistent with the traditional flight to safety mechanism, in which risky assets simultaneously sell off to the benefit of bonds and safe-haven currencies. Importantly, this shock, which accounts for the negative comovement between stocks and bonds, has a modest impact on inflation but appears strongly connected to the risk taking capacity of intermediary broker-dealers. The next section presents a stylized model that rationalizes these responses from the perspective of the risk taking capacity of levered financial intermediaries.

Figure 12: Impulse Responses of Currencies to a Flight-to-Safety Shock

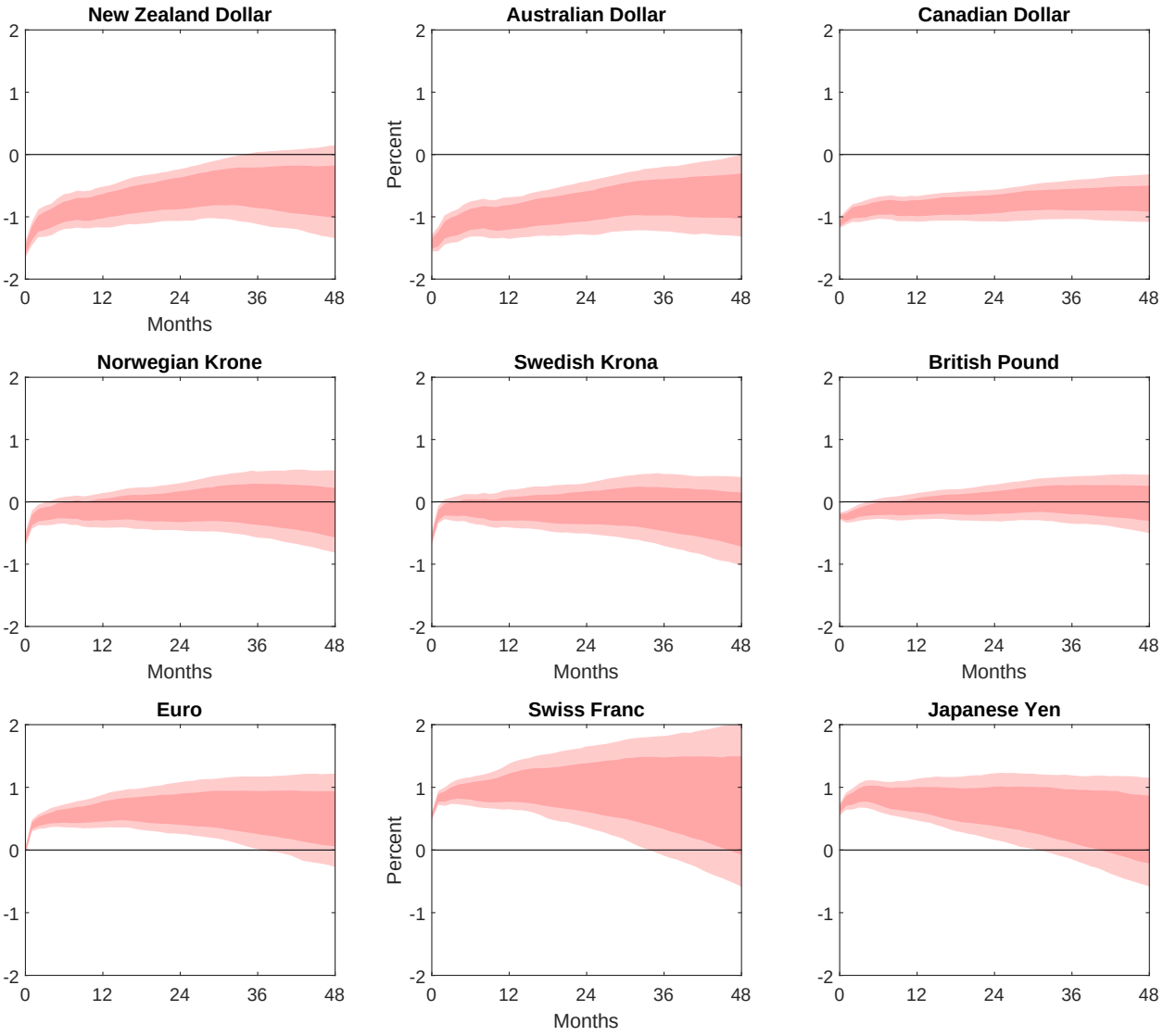

Note: Responses of selected variables to the flight-to-safety shock.

Figure 13: RESPONSES OF ADDITIONAL FINANCIAL VARIABLES

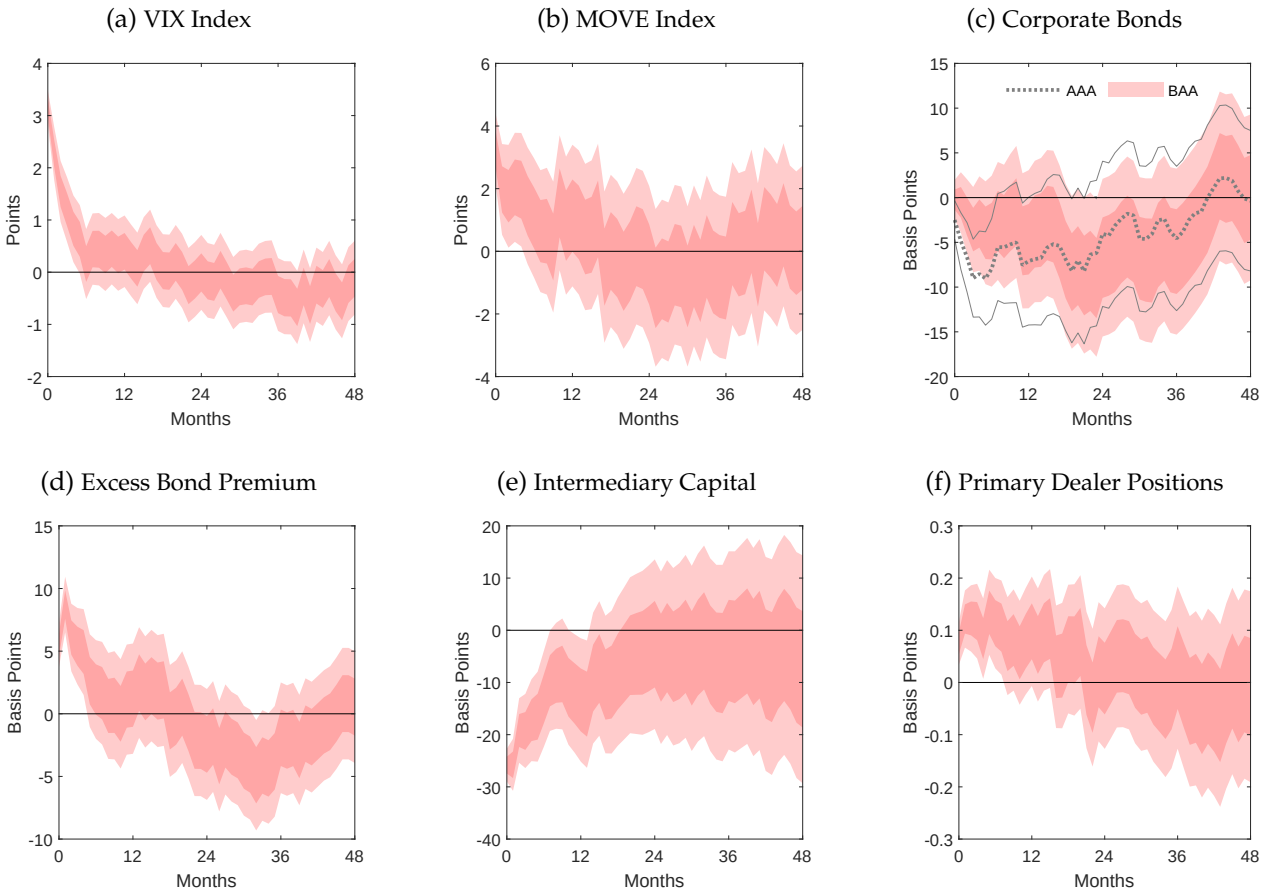

Note: Estimates of stock-bond correlation across twelve advanced economies from January 1955 to June 2024, using monthly data. Each panel presents the posterior median correlation (thick solid line) along with the associated 68% highest posterior density (HPD) interval and 90% interval derived from the global factor model. The posterior estimates account for the portion of the correlation explained by global shocks. The dotted line represents a simple 12-month rolling correlation.

5 A Stylized Model of Flight to Safety

This section presents a stylized equilibrium model that formalizes the link between the increased importance of financial shocks and flight to safety episodes observed in the data to the rise of levered financial intermediaries. A key challenge is to generate a flight to safety towards *long-term* bonds. In frictionless models, when a short-term risk-free asset is available, an increase in risk aversion leads investors to reduce holdings in both stocks and long-term bonds in favor of the short-term asset (Merton, 1972). This limitation suggests the need to move beyond representative agent models.

I build upon models of quantity-driven asset prices (Vayanos and Vila, 2021; Greenwood et al., 2018, 2023a) and incorporate three key elements: segmented markets, a preference for long-term bonds, and slow-moving capital (Duffie, 2010). Segmented markets introduce heterogeneity among investors, allowing shifts in the marginal investor to influence equilibrium prices. Some investors derive a convenience yield from holding long-term bonds, whereas others require to hold cash instruments, creating differential preference for these assets. Slow-moving capital means that trading frictions amplify the impact of demand shifts on prices. In my model, a shock to the risk-taking capacity of levered intermediaries, subject to value-at-risk constraints, interacts with the demand for long-term bonds from other market participants. This interaction leads to a temporary flight towards long-maturity bonds. As the presence of levered intermediaries increases due to exogenous changes in regulation or financial innovation, shocks causing opposite movements in stock and bond returns become more and more prominent, altering the aggregate return comovement.

5.1 Set-up

Primitives. The model is set in discrete time, and describes the dynamics of real asset prices, abstracting from nominal shocks. There are three types of assets –a risk-free, one period bond, a long-term bond, and a stock which represents a claim to the aggregate dividend– and four underlying sources of risk in the model, which are described in turn. First, an exogenous system

governs the dynamics of dividend growth and the real interest rate:

$$\Delta d_{t+1} = (1-\phi_d)\bar{d} + \phi_d \Delta d_t + \varepsilon^d_{t+1} \tag{14}$$

$$r_{t+1} = \bar{r} + \beta_d(\Delta d_{t+1} - \bar{d}) + \eta^r_{t+1}, \tag{15}$$

where $\bar{d}$ and $\bar{r}$ are the steady-state dividend growth and real interest rates, ϕ_d dividend growth autocorrelation and ε^d_{t+1} is an $i.i.d.$ innovation, whereas $\eta^r_{t+1} = \phi_r \eta^r_t + \varepsilon^r_{t+1}$. In this equation, ϕ_r is an autocorrelation coefficient, and ε^r_{t+1} is an i.i.d. innovation. The parameter $\beta_d \geq 0$ captures an endogenous, contemporaneous reaction of the interest rate to dividend growth. The term η^r_t is an exogenous shock to the real interest rate. This formulation is a reduced-form representation that stands in for a more involved structure where monetary policy endogenously sets the real interest rate in line with the growth of aggregate output or consumption, which in turn is correlated to dividend growth, but subject to exogenous real interest rate shocks captured by ε^r_{t+1}.

In addition, following Vayanos and Vila (2021), the supplies of both long term bonds and stocks, denoted s^b_{t+1} and s^s_{t+1} respectively, is subject to random fluctuations, with

$$s^j_{t+1} = (1-\phi_{s^j})\bar{s}^j + \phi_{s^j} s^j_t + \varepsilon^{s^j} \quad \text{for } j \in \{s, b\}. \tag{16}$$

This formulation accommodates shocks coming from issuers of the assets including governments and the corporate sector, net of the demands from "preferred habitat" investors operating in either market. These supply shocks represent additional sources of risk which arbitrageurs must absorb, as we describe next.

To model the excess returns of bonds and stocks, we will follow the tradition of Campbell and Shiller (1988a,b), and approximate them by the following linear relationships:

$$r^{xb}_{t+1} = -\frac{\theta}{1-\theta} y_{t+1} + \frac{1}{1-\theta} y_t - r_t, \tag{17}$$

$$r^{xs}_{t+1} = \kappa - \rho dp_{t+1} + dp_t + \Delta d_{t+1} - r_t, \tag{18}$$

where y_t and dp_t are the yield on the long-term bond and the stock dividend-price ratio at time t, respectively, θ is a parameter that determines the duration of the bond, and the κ and ρ are approximation constants that arise from the linearization of stock returns.

Market structure. We consider two classes of arbitrageurs, distinguished by their ability to operate in different markets. First, a class of generalists are active both in stock and bond markets. They are subject to two frictions: they face costs to adjust their portfolios, and they have a preference or convenience yield for long-term bonds. This preference is motivated by unmodelled regulatory requirements and/or liability matching motives. These features make pension and sovereign wealth funds close empirical analogue of these actors, so we will refer to them as 'pension funds' from now on.

Pension funds are mean-variance investors, trading off the one-period ahead expected return of their portfolio against its variance, and also taking into account adjustment costs and their convenience yield for bonds. Denote by $\mathbf{D}_t = [D_t^b, D_t^s]'$ the asset demands, expressed as shares of pension funds' total portfolio held in bonds and stocks, with any residual wealth held in the risk free rate.

$$\max_{\mathbf{D}_t} \mathcal{U}(W_{t+1}) = r_t + \mathbf{D}_t' \mathbb{E}_t \mathbf{r}_{t+1}^x - \frac{1}{2\tau} \mathbf{D}_t' \mathbf{\Sigma}^x \mathbf{D}_t - g(\mathbf{D}_t - \mathbf{D}_{t-1}) + \nu(D_t^b), \tag{19}$$

where $\mathbb{E}_t \mathbf{r}_{t+1}^x = \left[\mathbb{E}_t \left(r_{t+1}^{xb}\right), \mathbb{E}_t \left(r_{t+1}^{xs}\right)\right]'$ is the vector of expected excess returns on bonds and stocks, $\mathbf{\Sigma}^x$ is the covariance matrix of excess returns, τ is the risk tolerance parameter, $g(\mathbf{D}_t - \mathbf{D}_{t-1}) = \frac{\psi}{2}(\mathbf{D}_t - \mathbf{D}_{t-1})' \mathbf{\Sigma}^x (\mathbf{D}_t - \mathbf{D}_{t-1})$ captures a quadratic cost of adjusting the portfolio shares with $\psi > 0$, and $\nu(D_t^b) = \lambda D_t^b$ with $\lambda > 0$ is the convenience yield from holding long-term bonds. Given their objectives, the optimal demands for bonds and stocks satisfy

$$\mathbf{D}_t = (1-\beta)\tau(\mathbf{\Sigma}^x)^{-1}\left(\mathbb{E}_t \mathbf{r}_{t+1}^x + \lambda \mathbf{e}_b\right) + \beta \mathbf{D}_{t-1} \tag{20}$$

where $\mathbf{e}_b$ is a selection vector and $\beta = \frac{\tau\psi}{1+\tau\psi}$ arises from the presence of transaction costs. With quadratic adjustment costs, the optimal portfolio shares are a linear combination of the optimal mean-variance solution in the absence of adjustment costs, and the previous-period shares.

The second class of agents in the model are differentiated by the fact that they do not face adjustment costs, but can only invest in either of the two asset classes (they can both invest in the risk-free one period bond). Similar to Greenwood et al. (2018), these agents are fast-moving specialists that perform arbitrage within but not across markets. Their empirical counterparts of the fast-moving specialists are hedge funds and proprietary trading desks of banks and broker-dealers, which are typically segmented across asset class lines and conduct highly leveraged arbitrage

trades. I therefore label these agents 'hedge funds' for short, although it should be understood that they are meant to capture a wider class of levered specialists. I introduce two features which will be key to generate the flight to safety dynamics observed in the data. First, the levered hedge funds will face a cost of holding long positions in their respective risky assets, interpreted as a balance sheet cost. Second, their risk bearing capacity will be subject to stochastic shocks, common across the hedge fund sector. Formally, the problem of the hedge fund in sector $j \in \{b, s\}$ is

$$\max_{d_t^j} \mathcal{U}_j(W_{t+1}^j) = d_t^j \mathbb{E}_t[r_{t+1}^{xj}] - \frac{1}{2\gamma}(d_t^j)^2 V_j - \nu_j d_t^j,$$

which gives rise to the optimal portfolio weights:

$$d_t^j = \gamma_t \frac{\mathbb{E}_t[r_{t+1}^{xj}] - \nu_j}{V_j}. \tag{21}$$

where $\gamma_t = \bar{\gamma} + \phi_\gamma(\gamma_{t-1} - \bar{\gamma}) + \varepsilon_t^\gamma$, and $\epsilon_t^\gamma \sim \mathcal{N}(0, \sigma_\gamma^2)$. One-period optimization subject to time-varying risk limits, such as Value-at-Risk constraints, naturally gives rise to portfolio rules such as (21), (see, e.g. Danielsson and Zigrand, 2001; Danielsson, Shin, and Zigrand, 2004). A more complicated structure could link the realization of ε_t^γ to the aggregate dividend, linking the risk taking capacity of the levered intermediaries to the state of the aggregate stock market. For simplicity, and for now, ε_t^γ is assumed to be uncorrelated to the other primitive shocks.

Market clearing. Assume now that there is a continuum of pension funds with overall size ω and a continuum of hedge funds with size $1 - \omega$ in each market. Collect the demands of the hedge funds in each sector into the vector $\mathbf{d}_t = \left[d_t^b, d_t^s\right]'$. Market clearing in the stock and bond markets imply:

$$\omega \mathbf{d}_t + (1 - \omega)\mathbf{D}_t = \mathbf{s}_t, \tag{22}$$

where $\mathbf{s}_t = \left[s_t^b, s_t^s\right]'$. The demands from hedge funds can be collected in the vector $\mathbf{d}_t = \gamma_t \mathbf{V}^{-1}\left(\mathbb{E}_t \mathbf{r}_{t+1}^x - \boldsymbol{\nu}\right)$, where $\mathbf{V} \equiv diag(\boldsymbol{\Sigma}^x)$ is the matrix of variances of excess returns, and $\boldsymbol{\nu} \equiv [\nu_b, \nu_s]'$.

Equilibrium risk premia and prices. Combining this with equations (20) and (22), we can obtain the following expression for risk premia

$$\mathbb{E}_t \mathbf{r}_{t+1}^x = \boldsymbol{\Omega}_t^{-1}(\mathbf{s}_t - \omega\gamma_t \mathbf{V}^{-1}\boldsymbol{\nu} - (1 - \omega)(1 - \beta)\tau(\boldsymbol{\Sigma}^x)^{-1}\lambda \mathbf{e}_b - (1 - \omega)\beta \mathbf{D}_{t-1}), \tag{23}$$

where

$$\mathbf{\Omega}_t = \omega\gamma_t \mathbf{V}^{-1} + (1-\omega)(1-\beta)\tau(\mathbf{\Sigma}^x)^{-1},$$

is the market-wide effective level of risk tolerance. As can be seen in equation (23), the model features two sources of time variation in risk premia. First, shocks that increase supply increase risk premia, as both classes of arbitrageurs require compensation for absorbing additional supply. Second, shocks to the risk bearing capacity of the specialist hedge funds also increase risk premia, by lowering $\mathbf{\Omega}_t$, but also through the second term in equation (23). Moreover, with adjustment costs, risk premia depend as well on the past pension fund allocations. Given risk premia, bond yields and the price-dividend ratio can be retrieve from the Campbell-Shiller relationships:

$$y_t = (1-\theta)\sum_{j=0}^{\infty}\theta^j \mathbb{E}_t\left(r_{t+j} + r^{xb}_{t+j+1}\right) \tag{24}$$

$$dp_t = -\frac{\kappa}{1-\rho} + \sum_{j=0}^{\infty}\rho^j \mathbb{E}_t\left(r_{t+j} - \Delta d_{t+j+1} + r^{xs}_{t+j+1}\right) \tag{25}$$

5.2 Solution method.

An equilibrium in this model is defined as a fixed point for the covariance matrix of excess returns,

$$\mathbf{\Sigma}^x = \begin{bmatrix} V_b & C_{bs} \\ C_{bs} & V_s \end{bmatrix}.$$

At this fixed point, both generalist investors (such as pension funds) and specialist investors (such as hedge funds) satisfy their optimal demand functions, and markets clear, given the stochastic processes governing dividends, real interest rates, asset supplies, and the risk tolerance of specialists. The equilibrium is found numerically by iterating through the following steps:

1. Start with an initial guess for V_b, V_s, and C_{bs}.
2. Given this initial guess, calculate the policy functions for equilibrium prices using a second-order perturbation method around the 'risky steady state' (Coeurdacier et al., 2011).
3. Using these policy functions, compute the implied values of V_b, V_s, and C_{bs}.
4. Iterate the process by updating the guess in step 2 and continue until the covariance matrix converges, indicating that the equilibrium has been reached.

This numerical procedure ensures that the resulting covariance matrix satisfies the equilibrium conditions, reflecting the interaction between asset supplies, investor preferences, and the stochastic environment. Moreover, as discussed by Greenwood et al. (2018), models with stochastic supply can feature multiple rational expectations equilibria, with a unique stable equilibrium that does not explode as $\sigma_s^2 \to 0$. Like most of the literature, I focus on analyzing the properties of the stable equilibrium, which the numerical procedure above is guaranteed to converge to.

5.3 Calibration.

The table below presents the calibrated parameters used in the model, which are carefully chosen to reflect realistic economic conditions and investor behaviors. These parameters include steady-state values for key variables such as the risk-free rate, dividend growth rate, and asset supplies, as well as critical behavioral parameters like risk tolerance and the convenience yields associated with holding bonds and stocks.

Table 1: Model Parameters and Their Descriptions

Parameter	Description	Value	Comments
$\bar{r}$	Steady-state risk free rate	0.0025	Implies 1% annual real rate
$\bar{d}$	Steady-state dividend growth rate	0.0075	Implies 5% annual dividend growth rate
$\bar{s}_b$	Steady-state bond supply	10	
$\bar{s}_s$	Steady-state stock supply	15	
κ	Stock return approx. constant	0	
ρ	Stock return approx. discount rate	0.97	
ϕ_r	Risk free rate autocorrelation	0.9	
ϕ_d	Dividend growth autocorrelation	0.7	
ϕ_{sb}	Bond supply autocorrelation	0.9	
σ_r	S.D. risk free innovation	0.003269	Implies 1.5% annualised S.D. of r_t
σ_d	S.D. dividend innovation	0.01785	Implies 5% annualised S.D. of r_t
σ_{sb}	S.D. bond supply innovation	1	
θ	Bond discount rate	0.95	
τ	Generalist risk tolerance	2.5	
γ	Specialist risk tolerance	10	
α	Generalist demand inertia	0.1	
β_d	Interest rate response to dividends	0.0-0.2	
ω_b	Fraction of specialists	0.0-0.5	

Figure 14: Responses of Returns to Exogenous Shocks

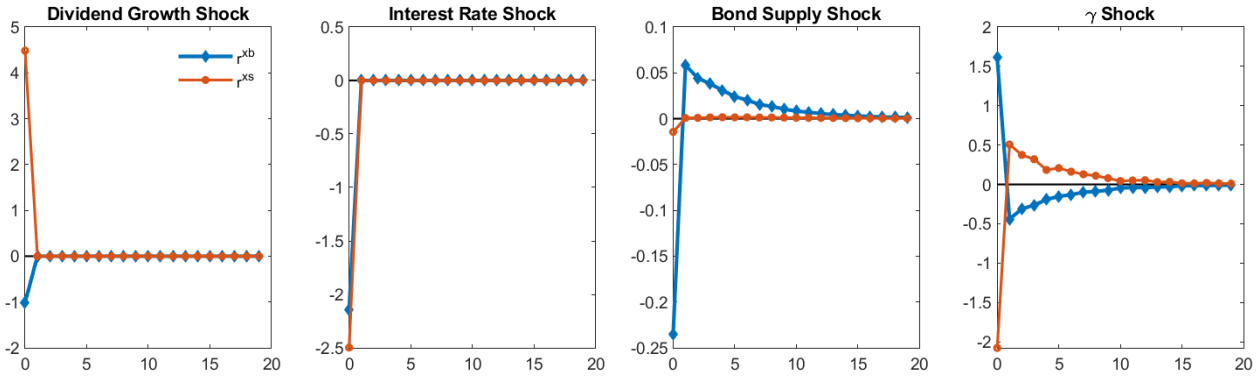

Note: Responses of returns to one-standard deviation shocks to dividend growth, interest rates, bond supply and specialist risk tolerance.

5.4 Results.

Figure 14 shows the responses of returns to the different shocks in the model. Starting with the first panel, a positive shock to dividend growth results in an immediate increase in stock prices, reflecting higher expected future cash flows. Through the endogenous response of the short-term interest rate, bonds decline in value, experiencing a negative return. The impulse response functions show that this shock is priced instantaneously in both asset prices, with no movements in returns beyond the impact horizon. In other words, risk premia do not change in response to the shock, and neither of the agents in the model vary their allocations in response to the shock.

A similar picture emerges in response to a positive shock to the risk-free rate (second panel), the impulse response functions indicate an instantaneous decrease in both stock and bond prices. Of note, a risk-free rate shock moves returns of both assets in the same direction, so it will be important that this shock does not dominate the unconditional distribution of shocks for a negative stock-bond covariance to emerge. Finally, as was the case with the dividend growth shock, the interest rate shock does not lead to a movement of risk premia beyond the instaneous impact.

The third panel shows the responses to a bond supply shock.[15] As is typical of this class of models (see, e.g., Greenwood et al., 2023b), an unanticipated increase in bond supply leads to a negative instantaneous bond return, as well as a movement in risk premia in the opposite direction.

[15]The responses to a stock supply shock look like the mirror image of the bond supply shock, with a strong instantaneous impact on stock returns followed by a movement in the opposite direction, and a muted impact on bond returns in the same direction.

This is seen as a positive response beyond impact horizon. The response propagates to the equity market as well, although in a muted way. Like the response to the interest rate shock, an increase in bond supply leads to movements in returns of stocks and bonds in the same direction, so this shock cannot be an important driver of a negative stock-bond covariance.

Finally, the last panel of Figure 14 shows the effect of a γ-shock, an unanticipated decline in the risk tolerance of the specialist sector. As can be seen in the figure, this leads to a strong response of stocks and bonds instantaneously, followed by a movement in risk premia in the opposite direction. Figure 15 looks at the responses to this shock in more detail, focusing on movements in demands.

An unexpected increase in the supply of bonds leads to a decline in bond prices, as indicated by the impulse response functions. The increased supply results in higher yields, which in turn raises the risk premia for bonds. The pension fund, which has a significant allocation to long-term bonds, reduces its bond holdings in response to the lower prices and higher yields. Similarly, hedge funds specializing in bonds adjust their portfolios by demanding a higher expected return to hold the increased supply. The impact on stocks is relatively muted, although there may be some indirect effects if the bond supply shock alters the overall risk perception in the market.

Figure 16 displays the impact of increasing ω, the share of specialists in stock and bond markets, on the unconditional stock-bond correlation. As the share of specialists in the market increases, shocks to their risk tolerance (γ shocks) become more significant, leading to a decrease in the equilibrium correlation between stock and bond returns. This decline in correlation is non-monotonic: a small increase in the share of specialists exerts a strong downward pressure on the stock-bond correlation, sufficient to flip the sign of the stock-bond covariance even for a small share –about 5% of specialists in the market. However, as the share increases, the decline slows down and eventually reverses.

To see why, recall the equilibirum expression for risk premia, Eq. (23). When ω is small, specialists are a minor part of the market and have little impact on prices. As ω increases, the effects of shocks to specialists' risk tolerance become larger, amplifying their influence on asset prices and reducing the stock-bond correlation. However, if ω becomes too large, the convenience yield term $\nu'(D_t^b)$ decreases because the demand from other investors diminishes. This reduction lessens the flight-to-safety effect, potentially reversing the decline in correlation.

Figure 15: Impulse Responses to a Risk Tolerance Shock

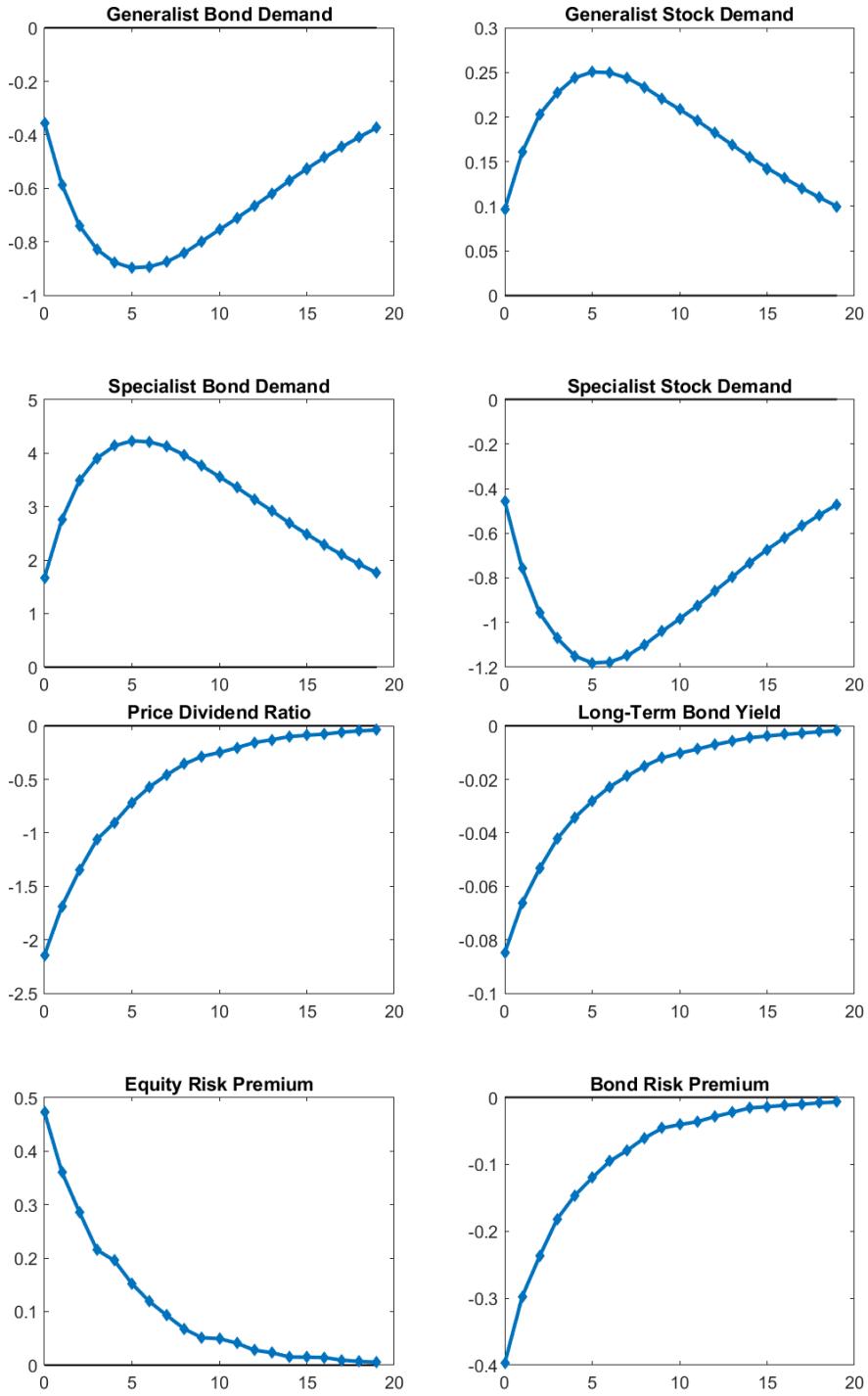

Note: Responses of portfolio shares (quantity demanded) and risk premia and asset prices to a one-standard deviation decline in specialist risk tolerance.

Figure 16: Impact of Increased Share of Hedge Funds on Stock-Bond Correlation

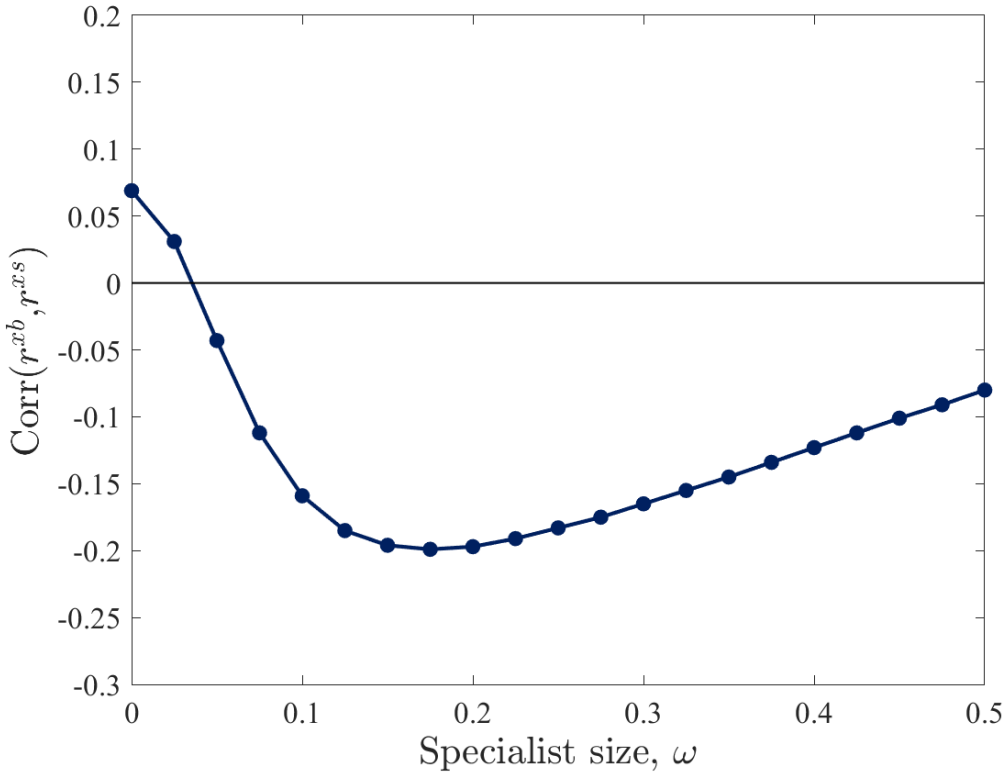

Note: Unconditional stock-bond correlation as the share of hedge funds increases.

5.5 Robustness

Appendix I examines the sensitivity of the results to various changes to the baseline parametrization. These are summarized briefly here: first, a greater degree of interest rate sensitivity to the dividend growth rate lower, all else equal, the equilibrium stock-bond correlation for any level of specialist market share. This is because, as described above, the dividend growth shock also leads to a negative stock-bond correlation which is amplified by the endogenous response of the interest rate; second for sufficiently high volatility of interest rate shocks, it is very unlikely that a negative stock-bond correlation can emerge, given the strong positive conditional correlation that this type of shock generates; finally, I examine the importance of adjustment costs of the generalist pension fund, and find that while these costs contribute to increasing quantiatively the impact of an increased market share of specialist, they play a small impact on the qualitative results.

Figure 17: Counterfactual analysis: varying ω (share of specialists) and σ^r (MP Shock volatility)

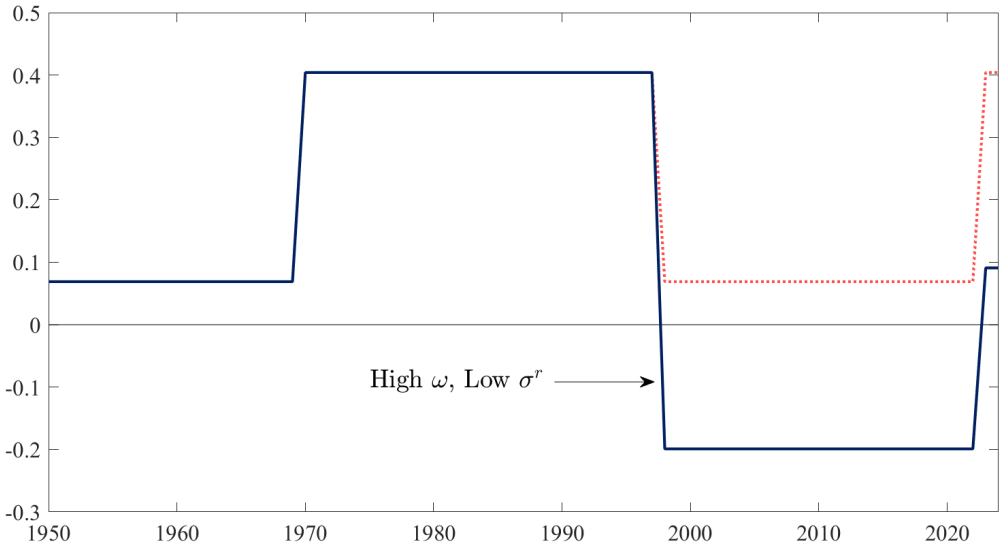

Note: Counterfactual simulation in which the share of specialist hedge funds (ω) is high and the interest rate volatility (σ^r) is low after 1998 (solid blue), versus an alternative scenario in which the interest rate volatility remains high after 1998.

5.6 Counterfactual analysis

Figure 17 presents a simple counterfactual analysis. The results above suggest that there are two conditions for a negative stock-bond correlation to emerge: first, a sufficiently high share of specialists in the market (ω), and second, a sufficiently low volatility of interest rates (σ^r). The counterfactual presents an exercise where, first, both parameters are calibrated to generate the broad patterns seen in the data. This includes a low but positive correlation during the 1950s and 1960s (driven by small interest rate volatility but small share of specialist hedge funds), a high and positive correlation during the 1970s and through the mid-1990s, as interest rate volatility increased in an environment in which the share of specialists was low. From the late 1990s we enter an era of low interest rate volatility and high share of specialists, leading to the emergence of a negative correlation.

This exercise also sheds light to the events after the COVID-19 pandemic. After 2022, the stock-bond correlation became positive again, but did not reach the levels observed prior to 1998. Through the lens of the model, this can be rationalised as a higher volatility of interest rates interacting with a still-high share of intermediaries.

6 Conclusion

This paper examines how government bonds in advanced economies transformed from moving in sync with stocks to acting as "safe" assets that appreciate when stock prices decline, and their subsequent return to behaving as risky assets in 2022. An analysis of twelve countries over the postwar period reveals that these shifts occurred simultaneously across nations and are not adequately explained by changes in output and inflation dynamics. Instead, the findings point to an increased importance of financial shocks inducing flight-to-safety behavior as the primary driver. By employing a Dynamic Factor Model with a novel identification strategy, this paper identifies these financial shocks and demonstrates how the rise of levered financial intermediaries, constrained by risk limits, amplified and propagated these shocks, altering the unconditional comovement between stocks and bonds.

These results have significant implications for understanding financial markets and informing economic policy. They highlight the crucial role of financial intermediaries and market structure in shaping asset price dynamics, suggesting that traditional macroeconomic factors may be insufficient to explain asset comovements fully. Recognizing the influence of financial shocks and intermediary behavior is essential for policymakers when designing regulatory frameworks and for investors in developing effective portfolio diversification and risk management strategies.

On the modeling side, my model is silent from the international implications of shocks to the risk tolerance of levered specialist, treating global financial markets as a closed economy. Extending the theoretical framework to a multi-country setting, and exploring the implications for exchange rates in the directions suggested by Greenwood et al. (2023a) and Gourinchas et al. (2024) is an important priority for future investigation. Moreover, empirical research could build on the macro findings by exploring the micro-level mechanisms through which financial intermediaries impact asset prices, potentially incorporating data on intermediary balance sheets and risk exposures. Additionally, examining the effects of regulatory changes and financial innovations on intermediary behavior may provide deeper insights into the evolution of asset return comovements. Understanding these dynamics is increasingly important in a global financial system where shocks can quickly propagate across borders, affecting the stability of financial markets and the broader economy.

References

ACHARYA, V. V. AND T. LAARITS (2023): "When Do Treasuries Earn the Convenience Yield?: A Hedging Perspective," Tech. rep., National Bureau of Economic Research.

ANTOLÍN-DÍAZ, J., T. DRECHSEL, AND I. PETRELLA (2024): "Advances in nowcasting economic activity: The role of heterogeneous dynamics and fat tails," *Journal of Econometrics*, 238, 105634.

ANTOLÍN-DÍAZ, J. AND J. F. RUBIO-RAMÍREZ (2018): "Narrative sign restrictions for SVARs," *American Economic Review*, 108, 2802–29.

BAELE, L., G. BEKAERT, AND K. INGHELBRECHT (2010): "The determinants of stock and bond return comovements," *The Review of Financial Studies*, 23, 2374–2428.

BAELE, L., G. BEKAERT, K. INGHELBRECHT, AND M. WEI (2020): "Flights to safety," *The Review of Financial Studies*, 33, 689–746.

BAI, J. AND P. WANG (2014): "Identification theory for high dimensional static and dynamic factor models," *Journal of Econometrics*, 178, 794–804.

——— (2015): "Identification and Bayesian estimation of dynamic factor models," *Journal of Business & Economic Statistics*, 33, 221–240.

BARRO, R. J. AND J. F. URSÚA (2008): "Macroeconomic Crises since 1870," *Brookings Papers on Economic Activity*, 2008, 255–350.

BRUNNERMEIER, M., D. PALIA, K. A. SASTRY, C. A. SIMS, ET AL. (2020): "Feedbacks: financial markets and economic activity," *Manuscript, Princeton University*.

BURKHARDT, D. AND H. HASSELTOFT (2012): "Understanding asset correlations," *Swiss Finance Institute Research Paper*.

CAMPBELL, J. Y., A. W. LO, A. C. MACKINLAY, AND R. F. WHITELAW (1998): "The econometrics of financial markets," *Macroeconomic Dynamics*, 2, 559–562.

CAMPBELL, J. Y., C. PFLUEGER, AND L. M. VICEIRA (2020): "Macroeconomic drivers of bond and equity risks," *Journal of Political Economy*, 128, 3148–3185.

CAMPBELL, J. Y. AND R. J. SHILLER (1988a): "The dividend-price ratio and expectations of future dividends and discount factors," *The review of financial studies*, 1, 195–228.

——— (1988b): "Stock prices, earnings, and expected dividends," *the Journal of Finance*, 43, 661–676.

CAMPBELL, J. Y., R. J. SHILLER, L. M. VICEIRA, ET AL. (2009): *Understanding inflation-indexed bond markets*, w15014, National Bureau of Economic Research Cambridge, MA.

CAMPBELL, J. Y., A. SUNDERAM, AND L. M. VICEIRA (2017): "Inflation Bets or Deflation Hedges? The Changing Risks of Nominal Bonds," *Critical Finance Review*, 6, 263–301.

CARRIERO, A., M. G. MARCELLINO, AND T. TORNESE (2023): "Blended identification in structural vars," *BAFFI CAREFIN Centre Research Paper*.

CHAN, J. C. AND I. JELIAZKOV (2009): "Efficient simulation and integrated likelihood estimation in state space models," *International Journal of Mathematical Modelling and Numerical Optimisation*, 1, 101–120.

CHAN, J. C. C. AND A. L. GRANT (2016): "On the Observed-Data Deviance Information Criterion for Volatility Modeling," *Journal of Financial Econometrics*, 14, 772–802.

CHERNOV, M., L. A. LOCHSTOER, AND D. SONG (2021): "The real channel for nominal bond-stock puzzles," Tech. rep., National Bureau of Economic Research.

CHOW, G. C. AND A.-L. LIN (1971): "Best linear unbiased interpolation, distribution, and extrapolation of time series by related series," *The review of Economics and Statistics*, 372–375.

COEURDACIER, N., H. REY, AND P. WINANT (2011): "The risky steady state," *American Economic Review*, 101, 398–401.

DANIELSSON, J., H. S. SHIN, AND J.-P. ZIGRAND (2004): "The impact of risk regulation on price dynamics," *Journal of Banking & Finance*, 28, 1069–1087.

DANIELSSON, J. AND J.-P. ZIGRAND (2001): "What happens when you regulate risk? Evidence from a simple equilibrium model," *Evidence from a Simple Equilibrium Model (August 2001)*.

DAVID, A. AND P. VERONESI (2013): "What ties return volatilities to price valuations and fundamentals?" *Journal of Political Economy*, 121, 682–746.

DIEBOLD, F. X. AND C. LI (2006): "Forecasting the term structure of government bond yields," *Journal of econometrics*, 130, 337–364.

DIMSON, E., P. MARSH, AND M. STAUNTON (2009): *Triumph of the optimists: 101 years of global investment returns*, Princeton University Press.

DUFFEE, G. (2018): "Expected inflation, real rates, and stock-bond comovement," *Unpublished working paper. Johns Hopkins University*.

DUFFEE, G. R. (2023): "Macroeconomic News and Stock–Bond Comovement," *Review of Finance*, 27, 1859–1882.

DUFFIE, D. (2010): "Asset price dynamics with slow-moving capital,(American Finance Association Presidential Address)," *Journal of Finance*, 65, 1238–68.

FERNÁNDEZ-VILLAVERDE, J., J. F. RUBIO-RAMÍREZ, T. J. SARGENT, AND M. W. WATSON (2007): "ABCs (and Ds) of understanding VARs," *American economic review*, 97, 1021–1026.

FLEMING, J., C. KIRBY, AND B. OSTDIEK (2003): "The economic value of volatility timing using realized volatility," *Journal of Financial Economics*, 67, 473–509.

FLEMING, M., G. NGUYEN, AND J. ROSENBERG (2024): "How do Treasury dealers manage their positions?" *Journal of Financial Economics*, 158, 103885.

GIACOMINI, R., T. KITAGAWA, AND M. READ (2021): "Identification and inference under narrative restrictions," *arXiv preprint arXiv:2102.06456*.

GOURINCHAS, P.-O., W. RAY, AND D. VAYANOS (2024): "A preferred-habitat model of term premia, exchange rates, and monetary policy spillovers," Tech. rep.

GREENWOOD, R., S. HANSON, J. C. STEIN, AND A. SUNDERAM (2023a): "A quantity-driven theory of term premia and exchange rates," *The Quarterly Journal of Economics*, 138, 2327–2389.

GREENWOOD, R., S. HANSON, AND D. VAYANOS (2023b): "Supply and demand and the term structure of interest rates," *Annual Review of Financial Economics*, 16.

GREENWOOD, R., S. G. HANSON, AND G. Y. LIAO (2018): "Asset price dynamics in partially segmented markets," *The Review of Financial Studies*, 31, 3307–3343.

GREENWOOD, R. AND D. VAYANOS (2014): "Bond supply and excess bond returns," *The Review of Financial Studies*, 27, 663–713.

HE, Z., B. KELLY, AND A. MANELA (2017): "Intermediary asset pricing: New evidence from many asset classes," *Journal of Financial Economics*, 126, 1–35.

ILMANEN, A. (2003): "Stock-bond correlations," *Journal of Fixed Income*, 13, 55–66.

JORDÀ, Ò., K. KNOLL, D. KUVSHINOV, M. SCHULARICK, AND A. M. TAYLOR (2019): "The rate of return on everything, 1870–2015," *The Quarterly Journal of Economics*, 134, 1225–1298.

JORDÀ, Ò., M. SCHULARICK, AND A. M. TAYLOR (2017): "Macrofinancial history and the new business cycle facts," *NBER macroeconomics annual*, 31, 213–263.

KEKRE, R. AND M. LENEL (2021): "The flight to safety and international risk sharing," Tech. rep., National Bureau of Economic Research.

KIM, S., N. SHEPHARD, AND S. CHIB (1998): "Stochastic Volatility: Likelihood Inference and Comparison with ARCH Models," *Review of Economic Studies*, 65, 361–93.

KOROBILIS, D. (2022): "A new algorithm for structural restrictions in Bayesian vector autoregressions," *European Economic Review*, 148, 104241.

KRISHNAMURTHY, A. AND A. VISSING-JORGENSEN (2012): "The aggregate demand for treasury debt," *Journal of Political Economy*, 120, 233–267.

LAARITS, T. (2020): "Precautionary savings and the stock-bond covariance," *NYU Stern School of Business*.

LEWIS, D. J. (2021): "Identifying shocks via time-varying volatility," *The Review of Economic Studies*, 88, 3086–3124.

LI, E. X., T. ZHA, J. ZHANG, AND H. ZHOU (2022): "Does fiscal policy matter for stock-bond return correlation?" *Journal of Monetary Economics*, 128, 20–34.

LI, L. (2002): "Macroeconomic factors and the correlation of stock and bond returns," .

LIU, Y. (2018): "The real and nominal determinants of stock and bond returns comovement," *Available at SSRN 3156301*.

LUDVIGSON, S. C., S. MA, AND S. NG (2018): "Shock restricted structural vector-autoregressions," Tech. rep., National Bureau of Economic Research.

LUSTIG, H., N. ROUSSANOV, AND A. VERDELHAN (2011): "Common risk factors in currency markets," *The Review of Financial Studies*, 24, 3731–3777.

MCCONNELL, M. M. AND G. PEREZ-QUIROS (2000): "Output fluctuations in the United States: What has changed since the early 1980's?" *American Economic Review*, 90, 1464–1476.

MERTON, R. C. (1972): "An analytic derivation of the efficient portfolio frontier," *Journal of financial and quantitative analysis*, 7, 1851–1872.

MIRANDA-AGRIPPINO, S. AND H. REY (2020): "US monetary policy and the global financial cycle," *The Review of Economic Studies*, 87, 2754–2776.

——— (2022): "The global financial cycle," in *Handbook of international economics*, Elsevier, vol. 6, 1–43.

MONTIEL OLEA, J. L., M. PLAGBORG-MØLLER, AND E. QIAN (2022): "SVAR Identification From Higher Moments: Has the Simultaneous Causality Problem Been Solved?" in *AEA Papers and Proceedings*, vol. 112, 481–85.

REY, H. (2013): "Dilemma not trilemma: the global financial cycle and monetary policy independence," Proceedings, Economic Policy Symposium - Jackson Hole. 12.

RIGOBON, R. (2003): "Identification through heteroskedasticity," *Review of Economics and Statistics*, 85, 777–792.

RIGOBON, R. AND B. SACK (2003): "Measuring the reaction of monetary policy to the stock market," *The quarterly journal of Economics*, 118, 639–669.

ROMER, C. D. AND D. H. ROMER (2023): "Presidential Address: Does Monetary Policy Matter? The Narrative Approach after 35 Years," *American Economic Review*, 113, 1395–1423.

RUBIO-RAMIREZ, J. F., D. F. WAGGONER, AND T. ZHA (2010): "Structural vector autoregressions: Theory of identification and algorithms for inference," *The Review of Economic Studies*, 77, 665–696.

SENTANA, E. (1998): "The relation between conditionally heteroskedastic factor models and factor GARCH models," *The Econometrics Journal*, 1, 1–9.

SENTANA, E. AND G. FIORENTINI (2001): "Identification, estimation and testing of conditionally heteroskedastic factor models," *Journal of Econometrics*, 102, 143–164.

SIMS, C. A. (2020): "Svar identification through heteroskedasticity with misspecified regimes," *Princeton University*.

SONG, D. (2017): "Bond market exposures to macroeconomic and monetary policy risks," *The Review of Financial Studies*, 30, 2761–2817.

SPIEGELHALTER, D. J., N. G. BEST, B. P. CARLIN, AND A. VAN DER LINDE (2002): "Bayesian Measures of Model Complexity and Fit," *Journal of the Royal Statistical Society. Series B (Statistical Methodology)*, 64, 583–639.

VAYANOS, D. AND J.-L. VILA (2021): "A preferred-habitat model of the term structure of interest rates," *Econometrica*, 89, 77–112.

Online Appendix to
"How Did Government Bonds Become Safe?"

by Juan Antolin-Diaz (LBS)

Contents

A Details on Data Construction

A.1 Baseline data set

The main dataset underlying the empirical analysis is at the monthly frequency from January 1955 to June 2024 and covers twelve advanced economies: Australia, Canada, France, Germany, Italy, Japan, New Zealand, Norway, Sweden, Switzerland, the United Kingdom, and the United States.

I outline here the variables included and the main sources, and give full details in Appendix A. The dataset includes stock and bond returns, 3-month and 10-year interest rates, exchange rates against the US dollar, commodity prices, core and headline inflation, and GDP growth. Stock return data comes from Morgan Stanley Capital International (MSCI) from Decmber 1969 onwards, and from Global Financial Data (GFD) prior to that date. Because data on government bonds differs greatly in terms of time span and maturity availability across countries, the creation of consistent series of government bond returns requires specifying and estimating an empirical model of the term structure of interest rates for each country. I apply the model of Diebold and Li (2006), adjusted to allow for arbitrary patterns of missing data, to raw data from Thomson Reuters Datastream and GFD, and construct homogeneous series of zero-coupon bond yields at the 1-month, 2-year and 10-year maturity for all the countries in my sample.[1] Returns are then computed following the approximation of Campbell et al. (1998). All return series are denominated in their domestic currency and converted into excess returns by substracting the one-month bill return of the respective country. Foreign Exchange rates are from the International Monetary Fund (IMF).[2] Commodity futures returns are from S&P Goldman Sachs Commodity Indices. I include series for the most important commodities for each asset class for which long series are available, including Brent Crude (energy), Gold (precious metals), Copper and Aluminum (Industrial metals), and an index of agricultural commodities. Whenever necessary, these are extended backwards using historical data from GFD. Inflation rates, both headline and core (excluding food and energy), as well as quarterly real GDP and consumption growth rates, are from the OECD Main Economic Indicators. These are interpolated to monthly frequency using the growth rates of industrial

[1] Further details are provided in Appendix A.

[2] For France, Germany and Italy, the Franc, Mark, and Lira are used prior to the introduction of the euro, and spliced with the euro thereafter.

production and retail sales, also from the OECD.[3]

B Specification of the Priors for the Factor Model

One of the advantages of our Bayesian approach is that an a-priori preference for simpler models can be naturally encoded by shrinking the parameters towards a more parsimonious specification. We follow the tradition of applying stronger shrinkage to more distant lags initiated by **?**. "Minnesota"-style priors are applied to the coefficients in $\mathbf{\Lambda}(L)$, $\phi(L)$ and $\rho_i(L)$. For $\phi(L)$ the prior mean is set to 0.9 for the first lag, and to zero in subsequent lags. This reflects a belief that the common factor captures a highly persistent but stationary business cycle process. For the factor loadings, $\mathbf{\Lambda}(L)$, the prior mean for the contemporaneous coefficient is set to $\hat{s}_i$, an estimate of the standard deviation of each of the variables, and to zero in subsequent lags. This prior reflects the belief that the factor is a cross-sectional average of the standardized variables. For the autoregressive coefficients of the idiosyncratic components, $\rho_i(L)$ the prior is set to zero for all lags, shrinking towards a model with no serial correlation in $u_{i,t}$, a common specification in the literature (see, e.g., **?**). In all cases, the variance of the priors is $\frac{\gamma}{h^2}$, where γ is a parameter governing the tightness of the prior, and h is equal to the lag number of each coefficient. We set $\gamma = 0.2$, the reference value used in the Bayesian VAR literature. We use a Normal diffuse prior for $\mathbf{c}$ and normalize the initial value of the stochastic trend by setting $a_0 = 0$. For the variances of the innovations to the time-varying parameters ω_a^2, ω_ε^2 and $\omega_{\eta,i}^2$ we also use priors that shrink them towards zero, i.e. towards a DFM without time-varying long-run growth and SV. In particular, for ω_a^2 we set an inverse gamma prior with one degree of freedom and scale equal to 0.001. For ω_ϵ^2 and $\omega_{\eta,i}^2$ we set an inverse gamma prior with one degree of freedom and scale equal to 0.0001.[4]

The number of lags in $\mathbf{\Lambda}(\mathbf{L})$, $\phi(L)$, and $\rho_i(L)$ is set to $m = 1$, $p = 2$, and $q = 2$. We found that $m = 1$ is enough to allow for rich heterogeneity in the dynamics. By setting $p = q = 2$, which follows **?**, the model allows for the hump-shaped responses to aggregate shocks commonly thought to characterize macroeconomic time series. With this choice we also nest the specification in **?**, which we consider as a benchmark model without heterogeneous dynamics and without outliers.

[3]The empirical model which I present below can easily be extended to handle mixed frequencies, at the cost of increased computation time. To avoid this, I use the method of Chow and Lin (1971) to transform these series to monthly frequency prior to estimation.

[4]**?** provide a number of robustness checks around the choice of priors in a Bayesian DFM.

In the Online Appendix, we evaluate the deviance information criterion (DIC, Spiegelhalter et al., 2002; Chan and Grant, 2016) for alternative choices of the lag orders m, p, q. The analysis of the DIC clearly supports models with heterogeneous lead-lag dynamics ($m > 0$), but also highlights that our baseline specification of m, p, and q is preferred over alternative ones with greater values.

C Further Details on the Estimation Algorithm

C.0.1 Detailed description of the Gibbs sampler algorithm

The algorithm has a block structure composed of the following steps.

0. Initialization

The model parameters are initialized at arbitrary starting values $\boldsymbol{\theta}^0$, and so are the sequences for the stochastic volatilities, $\{\sigma^0_{\varepsilon,t}, \sigma^0_{\eta_{i,t}}\}_{t=1}^T$. The latent components $\mathbf{c}_t, \mathbf{o}_t$, and f_t, are initialized by running the Kalman filter and smoother once, conditional on the initialized parameters. Set $j = 1$.

1. Draw outlier and idiosyncratic components conditional on estimated common factors

Obtain a draw $\{o_{i,t}\}_{t=1}^T$ and $\{u_{i,t}\}_{t=1}^T$ from $p(\{o_{i,t}, u_{i,t}\}_{t=1}^T | \boldsymbol{\theta}^{j-1}, a_t^{j-1}, f_t^{j-1}, \{\sigma^{j-1}_{\varepsilon,t}, \sigma^{j-1}_{\eta_{i,t}}\}_{t=1}^T, \mathbf{y})$ for each variable, $i = 1, \ldots, N$.

Conditioning on a_t^{j-1}, f_t^{j-1} and the loadings, λ_i^{j-1}, one can compute $\Delta y_{i,t} - c_{i,t} - \lambda_i(L) f_t = o_{i,t} - o_{i,t-1} + u_{i,t}$. Therefore, conditioning on $\boldsymbol{\rho}_i^{j-1}$, $\{\sigma^{j-1}_{\eta_{i,t}}\}_{t=1}^T$, and $\sigma^{j-1}_{o,i}$ and v_i^{j-1}, one can use the Kalman filter and simulation smoother to independently draw the outlier and idiosyncratic components. This step is independent for each of the variables in the system as such it can be run in a univariate state-space and be parallelized. The univariate state spaces are all at monthly frequency, and in the case of quarterly variables the estimation of the states spaces also produces interpolated monthly values for the quarterly variables applying the approximation in MarianoMurasawa2003. The interpolated quarterly variables are used in later steps of the Gibbs sampler. Specifically, we can retrieve monthly, outlier adjusted data as $y_{i,t}^{OA} = c_{i,t} + \lambda_i(L) f_t + u_{i,t}$.

2. Draw the parameters of the outlier component

For each variable, $i = 1, \ldots, N$, obtain a draw of $\sigma_{o,i}$ from $p(\sigma_{o,i}|\{o_{i,t}^j\}_{t=1}^T, v_i^{j-1})$ and v_i from $p(v_i|\{o_{i,t}^j\}_{t=1}^T, \sigma_{o,i}^j)$.

A fat-tailed distribution is easily obtained by a scale mixture, see **?**, **?**. Therefore, we can treat the scale mixture variable as a latent variable. Specifically, with $\psi_{i,t}$ i.i.d. inverse gamma, or $v_i/\psi_{i,t} \sim \chi^2_{v_i}$, with $z_{i,t} \sim N(0, \sigma^2_{o,i})$ one has that $o_{i,t} = \sqrt{\psi_{i,t}} z_{i,t} \sim t_{v_i}(0, \sigma^2_{o,i})$. Taking the sample $\{o_{i,t}^j/\sqrt{\psi_{i,t}^{j-1}}\}_{t=1}^T$ and posing an inverse-gamma prior $p(\sigma^2_{o,i}) \sim IG(s_{o,i}, \nu_{o,i})$ the conditional posterior of $\sigma^2_{o,i}$ is also drawn from an inverse-gamma distribution. We choose the scale $s_{o,i} = 0.1$ and degrees of freedom $\nu_{o,i} = 1$ for the monthly variables. For the quarterly variables where only one in three data points is available, we choose a more conservative prior with $\nu_{o,i} = 30$ degrees of freedom.

Conditioning on $\sigma_{o,i}^j$, given the conjugate inverse gamma prior, the conditional posterior of $\psi_{i,t}|v$ is also an inverse gamma. A draw $\psi_{i,t}^j$ can be obtained from $p(\psi_{i,t}^j|o_{i,t}^j, \sigma_{o,i}^j, v_i^{j-1}) \sim IG\left(\frac{v_i^{j-1}+1}{2}, \frac{2}{(o_{i,t}^j/\sigma_{o,i}^j)^2+2}\right)$. The degree of freedom v_i are discrete with probability mass proportional to the product of t distribution ordinates $p(v_i^j|o_{i,t}^j, \sigma_{o,i}^j) = p(v)\prod_{t=1}^T \frac{v^{-1/2}\Gamma(v+1/2)}{\Gamma(1/2)\Gamma(v/2)}(v + (o_{i,t}^j/\sigma_{o,i}^j)^2)^{-(v+1)/2}$, where $p(v)$ denotes the prior distribution for the degree of freedom (see **?**). We use a weakly informative prior for v which we assume to follow a Gamma distribution $\Gamma(2, 10)$ discretized on the support [3; 40]. This prior was proposed and analyzed by **?**. The lower bound at 3 enforces the existence of a conditional variance for the outlier component.

3. Draw the common factor and trend component conditional on model parameters and SVs

Obtain a draw $\{a_t^j, f_t^j\}_{t=1}^T$ from $p(\{a_t, f_t\}_{t=1}^T|\{o_{i,t}^j\}_{t=1}^T, \boldsymbol{\theta}^{j-1}, \{\sigma_{\varepsilon,t}^{j-1}, \sigma_{\eta_i,t}^{j-1}\}_{t=1}^T, \mathbf{y})$.

Having computed the outlier adjusted series and interpolated the quarterly series in Step 1 of the algorithm, this step produces a draw of the entire state vector $\mathbf{x}_t$ (which includes the long-run growth component, a_t, and the common factor, f_t) of the state-space representation described in Section C.0.2, and using the precision filter as described in the Section C.0.3.[5]

[5]Like **?**, we initialize the Kalman Filter step from a normal distribution whose moments are independent of the

4. Draw the variance of the time-varying GDP growth component

Obtain a draw $\omega_a^{2,j}$ from $p(\omega_a^2|\{a_t^j\}_{t=1}^T)$.

Taking the sample $\{a_t^j\}_{t=1}^T$ drawn in the previous step as given, and posing an inverse-gamma prior $p(\omega_a^2) \sim IG(S_a, v_a)$ the conditional posterior of ω_a^2 is also drawn from an inverse-gamma distribution. We choose the scale $S_a = 10^{-3}$ and degrees of freedom $v_a = 1$.

5. Draw the autoregressive parameters of the factor VAR

Obtain a draw $\mathbf{\Phi}^j$ from $p(\mathbf{\Phi}|\{f_t^j, \sigma_{\varepsilon,t}^j\}_{t=1}^T)$.

Taking the sequences of the common factor $\{f_t^j\}_{t=1}^T$ and its stochastic volatility $\{\sigma_{\varepsilon,t}^{j-1}\}_{t=1}^T$ from previous steps as given, and posing a non-informative prior, the corresponding conditional posterior is drawn from the Normal distribution, see, e.g. **?**.[6] Like **?**, or **?**, we reject draws which imply autoregressive coefficients in the explosive region.

6. Draw the factor loadings and constant terms

Obtain a draw of $\boldsymbol{\lambda}^j$ and $\boldsymbol{c}^j$ from $p(\boldsymbol{\lambda}, \boldsymbol{c}|\rho^{j-1}, \{f_t^j, \sigma_{\eta_{i,t}}^{j-1}\}_{t=1}^T, \mathbf{y})$.

Conditional on the draw of the common factor $\{f_t^j\}_{t=1}^T$, the measurement equations reduce to n independent linear regressions with heteroskedastic and serially correlated residuals. By conditioning on $\boldsymbol{\rho}^{j-1}$ and $\sigma_{\eta_{i,t}}^{j-1}$, the loadings and constant terms can be estimated using GLS. When necessary, we apply linear restrictions on the loadings. In order to ensure the identification of the model, we set the loading of the GDP equation associated to the (contemporaneous) common factor to unity (**?**).

model parameters, in particular $\mathbf{x}_0 \sim N(0, 10^4\mathbf{I})$.

[6] In the more general case of more than one factor, this step would be equivalent to drawing from the coefficients of a Bayesian VAR.

7. Draw the serial correlation coefficients of the idiosyncratic components

Obtain a draw of $\boldsymbol{\rho}^j$ from $p(\boldsymbol{\rho}|\lambda^{j-1}, \{f_t^j, \sigma_{\eta_{i,t}}^{j-1}\}_{t=1}^T, \mathbf{y})$.

Taking as given the idiosyncratic components and the sequence for the stochastic volatility of the i^{th} component, $\{\sigma_{\eta_{i,t}}^{j-1}\}_{t=1}^T$, the standardized idiosyncratic component is obtained, which follows an autoregression with homoskedastic residuals whose conditional posterior can be drawn from the Normal distribution.

8. Draw the stochastic volatilities

Obtain a draw of $\{\sigma_{\varepsilon,t}^j\}_{t=1}^T$ and $\{\sigma_{\eta_{i,t}}^j\}_{t=1}^T$ from $p(\{\sigma_{\varepsilon,t}\}_{t=1}^T|\boldsymbol{\Phi}^j, \{f_t^j\}_{t=1}^T)$, and from $p(\{\sigma_{\eta_{i,t}}\}_{t=1}^T|\boldsymbol{\lambda}^j, \boldsymbol{\rho}^j, \{f_t^j\}_{t=1}^T, \mathbf{y})$ respectively.

Finally, we draw the stochastic volatilities of the innovations to the factor and the idiosyncratic components independently, using the algorithm of Kim et al. (1998), which uses a mixture of normal random variables to approximate the elements of the log-variance.[7]

Increase j by 1 and iterate until convergence is achieved.

C.0.2 Construction of the state space system for Step 3 of the Gibbs sampler

For expositional clarity, in this section we abstract from the heterogeneous dynamics. Recall that in our main specification we choose the order of the autoregressive dynamics in factor and idiosyncratic components to be $p = 2$ and $q = 2$, respectively. Let the $n \times 1$ vector $\mathbf{y}_t$, which contains the (outlier adjusted and de-meaned) n_q interpolated quarterly and n_m monthly variables (i.e. $n = n_q + n_m$).[8] Therefore the time index t is always monthly, both for the quarterly and the monthly variables. The state space system is defined so that the system is written out in terms of

[7] This is a more efficient alternative to the exact Metropolis-Hastings algorithm previously proposed by **?**. For the general case in which there is more than one factor, the volatilities of the factor VAR can be drawn jointly, see primiceri2005time.

[8] The interpolation of the quarterly variables is performed in step 1 of the Gibbs sampler.

the *quasi-differences* of the indicators, $\tilde{\mathbf{y}}_t$, defined as

$$\tilde{\mathbf{y}}_t = \begin{bmatrix} y^q_{1,t} - \rho_{1,1} y^q_{1,t-1} - \rho_{1,2} y^q_{1,t-2} \\ \vdots \\ y^q_{n_q,t} - \rho_{n_q,1} y^q_{n_q,t-1} - \rho_{n_q,2} y^q_{n_q,t-2} \\ y^m_{1,t} - \rho_{n_q+1,1} y^m_{1,t-1} - \rho_{n_q+1,2} y^m_{1,t-2} \\ \vdots \\ y^m_{n_m,t} - \rho_{n,1} y^m_{n_m,t-1} - \rho_{n,2} y^m_{n_m,t-2} \end{bmatrix},$$

Given this re-defined vector of observables, we cast our model into the following state space form:

$$\begin{aligned} \tilde{\mathbf{y}}_\mathbf{t} &= \mathbf{H}\mathbf{x}_t + \tilde{\boldsymbol{\eta}}_\mathbf{t}, & \tilde{\boldsymbol{\eta}}_\mathbf{t} &\sim N(0, \tilde{\mathbf{R}}_\mathbf{t}) \\ \mathbf{x}_t &= \mathbf{F}\mathbf{x}_{t-1} + \mathbf{e}_t, & \mathbf{e}_t &\sim N(0, \mathbf{Q}_t) \end{aligned}$$

where the state vector is defined as $\mathbf{x}'_t = [a_t, a_{t-1}, a_{t-2}, f_t, f_{t-1}, f_{t-2}]$. We order GDP, GDI and consumption growth as the first three variables in $\tilde{\mathbf{y}}_\mathbf{t}$ and assume they share a common low frequency component. Therefore in Equation (**??**) we set $\mathbf{b} = (1\ 1\ b_c\ 0\ \ldots\ 0)'$. Setting $\lambda_1 = 1$ for identification, the matrices of parameters $\mathbf{H}$ and $\mathbf{F}$, are then constructed as shown below:

$$\mathbf{H} = \begin{bmatrix} \mathbf{H}_a & \mathbf{H}_\lambda \end{bmatrix},$$

where the respective blocks of $\mathbf{H}$ are defined as

$$\mathbf{H}_a = \begin{bmatrix} 1 & -\rho_{1,1} & -\rho_{1,2} \\ 1 & -\rho_{2,1} & -\rho_{2,2} \\ b_c & -b_c\rho_{3,1} & -b_c\rho_{3,2} \\ & \mathbf{0}_{(n-3)\times 3} & \end{bmatrix}, \qquad \mathbf{H}_\lambda = \begin{bmatrix} 1 & -\rho_{1,1} & -\rho_{1,2} \\ \lambda_2 & -\lambda_2\rho_{2,1} & -\lambda_2\rho_{2,2} \\ \vdots & \vdots & \vdots \\ \lambda_n & -\lambda_n\rho_{n,1} & -\lambda_n\rho_{n,2} \end{bmatrix},$$

and

$$\mathbf{F} = \begin{bmatrix} \mathbf{F}_1 & \mathbf{0} \\ \mathbf{0} & \mathbf{F}_2 \end{bmatrix},$$

where the respective blocks of $\mathbf{F}$ are defined as

$$\mathbf{F}_1 = \left[\begin{array}{cc} 1 & \mathbf{0}_{1\times 2} \\ \hline \mathbf{I}_2 & \mathbf{0}_{2\times 1} \end{array}\right] \qquad\qquad \mathbf{F}_2 = \left[\begin{array}{ccc} \phi_1 & \phi_2 & 0 \\ \hline & \mathbf{I}_2 & \mathbf{0}_{2\times 1} \end{array}\right].$$

The innovations to the transition equation are denoted as

$$\mathbf{e}_t \quad = \quad \begin{bmatrix} v_{a_t} & \mathbf{0}_{2\times 1} & \epsilon_t & \mathbf{0}_{2\times 1} \end{bmatrix}',$$

with covariance matrix $\mathbf{Q}_t = diag(\omega_a^2, \mathbf{0}_{1\times 2}, \sigma_{\epsilon,t}^2, \mathbf{0}_{1\times 2})$. Whereas the covariance matrix of the measurement equation is defined as $\tilde{\mathbf{R}}_t = diag(\sigma_{\eta_{1,t}}^2, \ldots, \sigma_{\eta_{n,t}}^2)$.

C.0.3 Efficient precision sampler with missing observations

In order to make the algorithm more efficient we use the vectorized version of the Kalman filter/smoother (sometimes referred to as precision sampler, see Chan and Jeliazkov, 2009). The vectorized approach leads to substantial gains in computational time.

Following DurbinKoopman2012, we can express any state space model in its vectorized form:

$$\begin{aligned} \mathbf{y} &= \overline{\mathbf{H}}\mathbf{x} + \eta, \qquad \eta \sim N(0, \overline{\mathbf{R}}) \\ \overline{\mathbf{F}}\mathbf{x} &= \mathbf{x}^* + \mathbf{e}, \qquad \mathbf{e} \sim N(0, \overline{\mathbf{Q}}) \end{aligned} \tag{26}$$

where $\mathbf{y}' = [\mathbf{y}_1', ..., \mathbf{y}_T']$, $\mathbf{x}' = [\mathbf{x}_1', ..., \mathbf{x}_T']$ and $\mathbf{x}^* = [\mathbf{x}_0', \mathbf{0}_{1\times k(T-1)}]$. $\mathbf{x}_0$ is the initialization for the state vector and its variance is initialized at $\mathbf{P}_0$. The system's matrices are organized as

$$\overline{\mathbf{H}} = \begin{bmatrix} \mathbf{H}_1 & & & \\ & \mathbf{H}_2 & & \\ & & \ddots & \\ & & & \mathbf{H}_T \end{bmatrix}, \quad \overline{\mathbf{R}} = \begin{bmatrix} \mathbf{R}_1 & & & \\ & \mathbf{R}_2 & & \\ & & \ddots & \\ & & & \mathbf{R}_T \end{bmatrix},$$
$$\overline{\mathbf{F}} = \begin{bmatrix} \mathbf{I}_k & & & \\ -\mathbf{F}_1 & \mathbf{I}_k & & \\ & \ddots & \ddots & \\ & & -\mathbf{F}_{T-1} & \mathbf{I}_k \end{bmatrix}, \quad \overline{\mathbf{Q}} = \begin{bmatrix} \mathbf{P}_0 & & & \\ & \mathbf{Q}_1 & & \\ & & \ddots & \\ & & & \mathbf{Q}_{T-1} \end{bmatrix}. \tag{27}$$

In Proposition 1 we extend the results of Chan$jeliazkov09tothecaseweretherearemissingobservations.$

Proposition 1. *Let* $\mathbf{J}$ *be the diagonal selection matrix selecting the full rank portion of the generic time* t *covariance matrix of the transition equation and* $\mathbf{\Xi}$ *a diagonal matrix with ones corresponding to the existing elements in* $\mathbf{y}$ *and zero for the missing elements. Define* $\overline{\mathbf{J}}=(\mathbf{I}_T \otimes \mathbf{J})$, $\widetilde{\mathbf{F}} = \overline{\mathbf{J}}'\overline{\mathbf{F}}\overline{\mathbf{J}}$, $\widetilde{\mathbf{Q}} = \overline{\mathbf{J}}'\overline{\mathbf{Q}}\overline{\mathbf{J}}$, $\widetilde{\mathbf{H}} = \overline{\mathbf{H}}\overline{\mathbf{J}}$, *and* $\widetilde{\mathbf{R}}^{-1} = \mathbf{\Xi}'\overline{\mathbf{R}}^{-1}\mathbf{\Xi}$. *The state vector* $\mathbf{x} \sim \mathbf{N}(\varkappa, \mathbf{P})$ *with*

$$\begin{aligned} \mathbf{P} &= \mathbf{K} + \widetilde{\mathbf{H}}'\widetilde{\mathbf{R}}^{-1}\widetilde{\mathbf{H}} \\ \varkappa &= \mathbf{P}^{-1}\left(\mathbf{K}\widetilde{\mathbf{F}}^{-\mathbf{1}}\mathbf{x}^* + \widetilde{\mathbf{H}}'\widetilde{\mathbf{R}}^{-1}\mathbf{y}\right) \end{aligned}$$

where $\mathbf{K} = \widetilde{\mathbf{F}}'\widetilde{\mathbf{Q}}^{-1}\widetilde{\mathbf{F}}$.

The precision algorithm takes advantage of the sparse and banded structure of many of the very large matrices that enter into the posterior for the states. The introduction of $\mathbf{J}$ allows us to deal with the presence of a rank deficient system for the state variables, arising from the presence of multiple lags in the dynamics of the factors,[9] whereas $\mathbf{\Xi}$ deals with the missing observations.[10] Research on precision sampling algorithms for state space models with mixed frequency data is fast evolving. See for example **?** and **?** for recent contributions in this area. In particular, the

[9] $\mathbf{J}$ is a k-dimensional diagonal matrix with zeros corresponding to singular columns and one for the nonsingular columns of $\mathbf{Q}_t$, where the latter denotes the covariance matrix of the transition equation innovations of the (original) state space model.

[10] In MATLAB, the use of the 'backslash' operator as opposed to the standard inverse operator guarantees further efficiency in computation. Given a $k \times k$ non-singular sparse matrix $\mathcal{S}$ and a $k \times 1$ vector x, we have that $\mathcal{S}^{-1}x \equiv \mathcal{S}\backslash x$, which denotes the unique solution for z to the system $\mathcal{S}z = x$. Defining the Cholesky factor $\mathcal{C}$, such that $\mathcal{C}\mathcal{C}' = \mathcal{S}$,$\mathcal{S}^{-1}x = \mathcal{C}'\backslash(\mathcal{C}\backslash x)$, and this solves two triangular systems by forward substitution followed by back substitution (see also **?**).

precision-based method of **?** is applicable to a wide range of state-space models with missing data patterns.

D Empirical Fit of the Factor Model

Figure D.1: Fit of the Model: Stock Returns

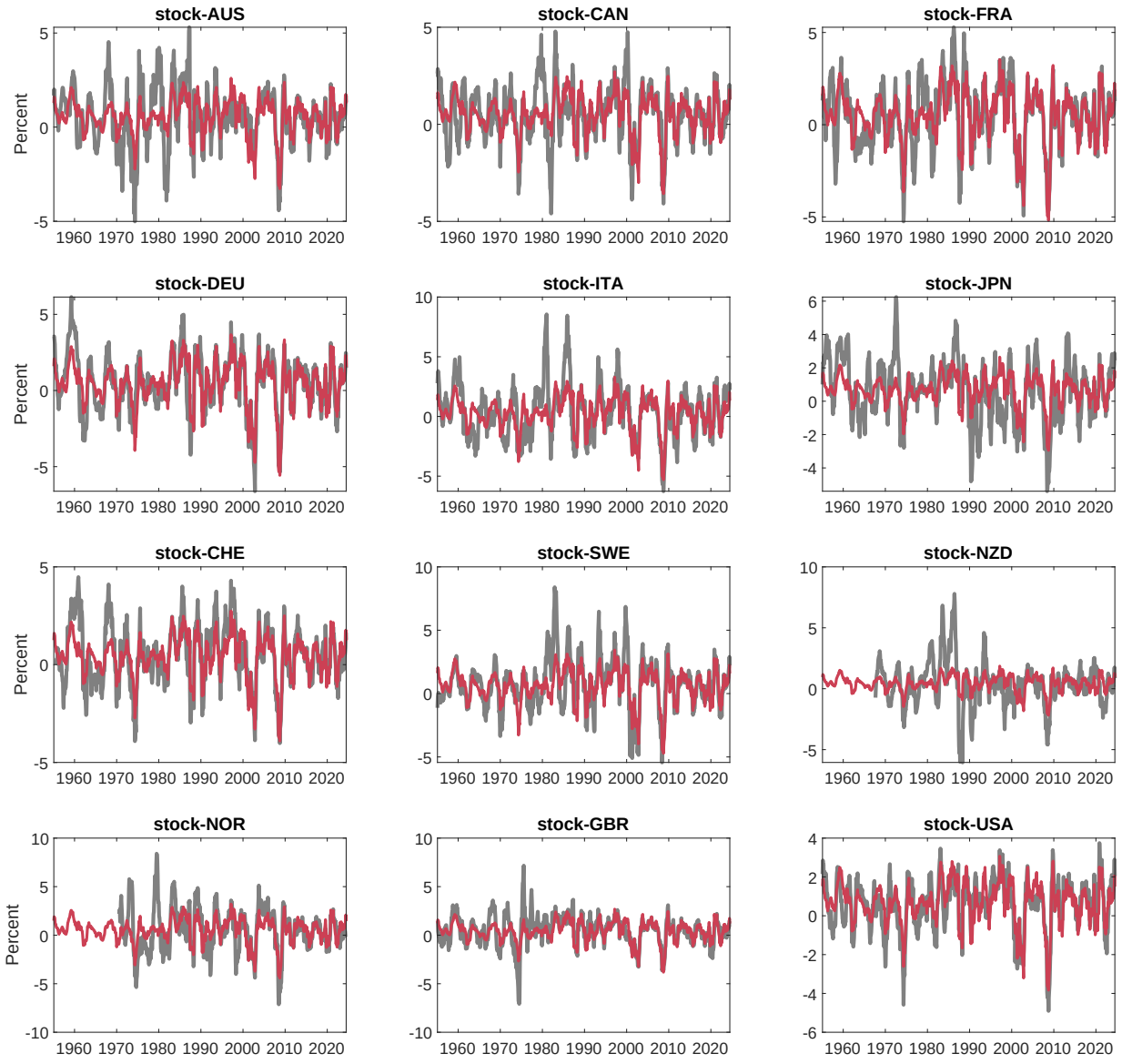

Figure D.2: Fit of the Model: Long-Term Bond Yields

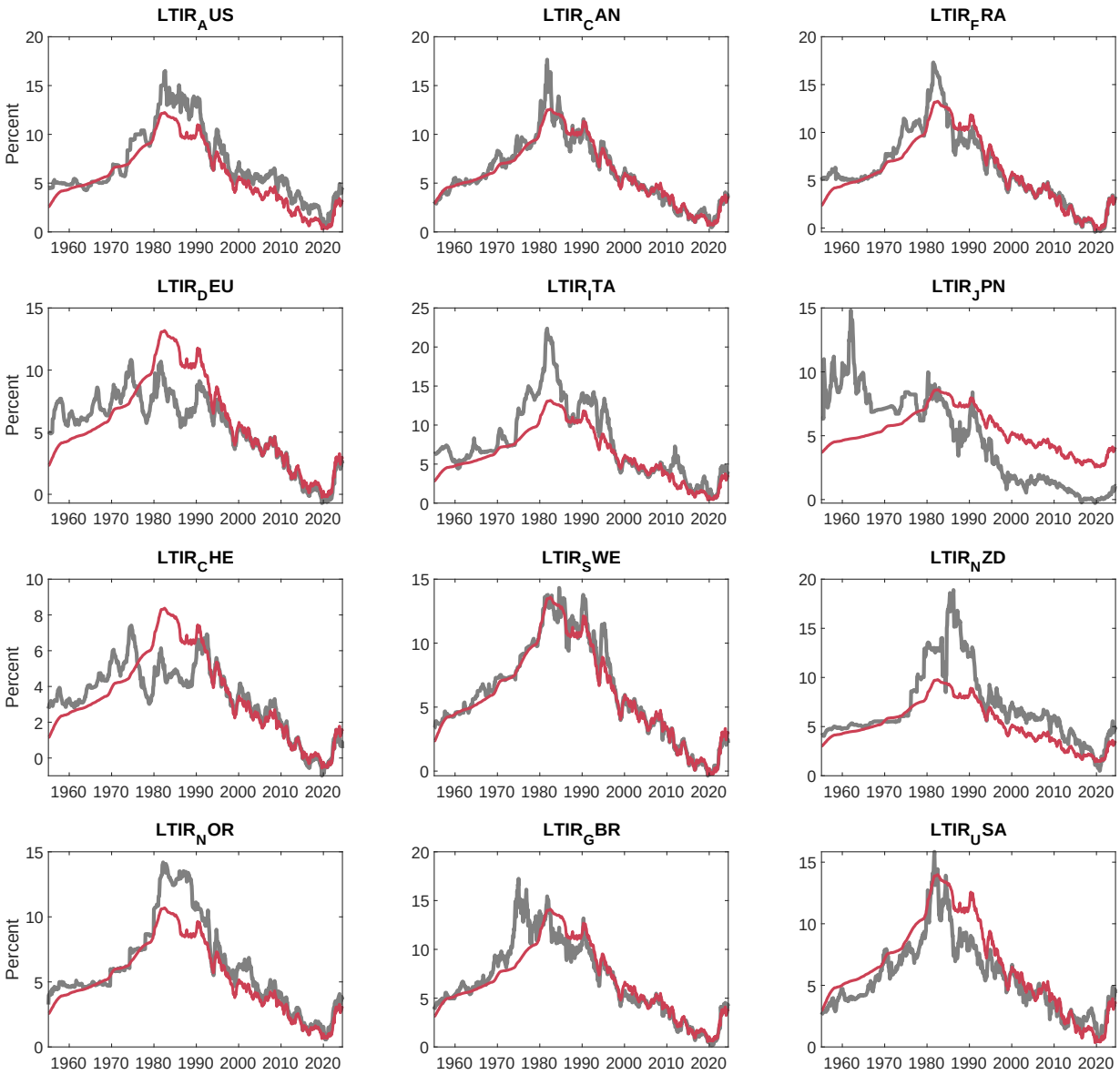

E Shock Time Series and Volatilties of Remaining Shocks

Figure E.1: TIME SERIES AND VOLATILITIES OF OTHER SHOCKS

(a) Aggregate Demand Shock

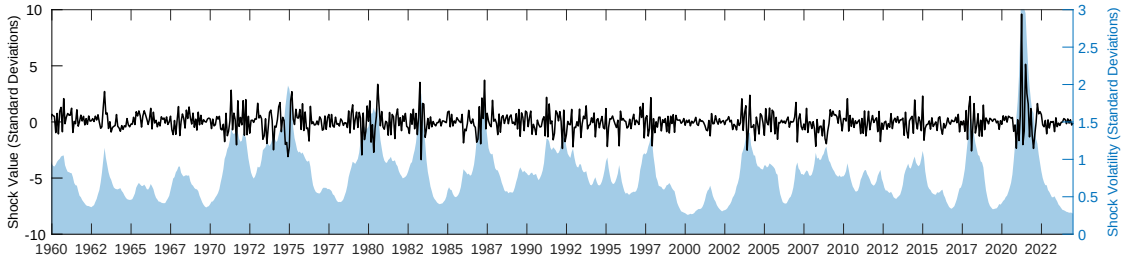

(b) Aggregate Supply Shock 1

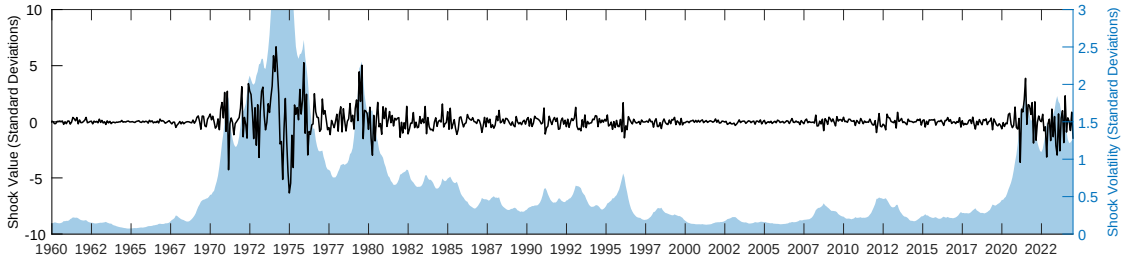

(c) Food Price Shock

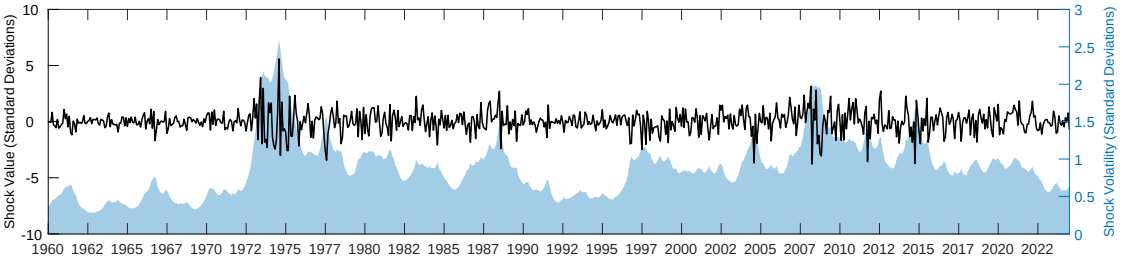

(d) Aggregate Supply Shock 2

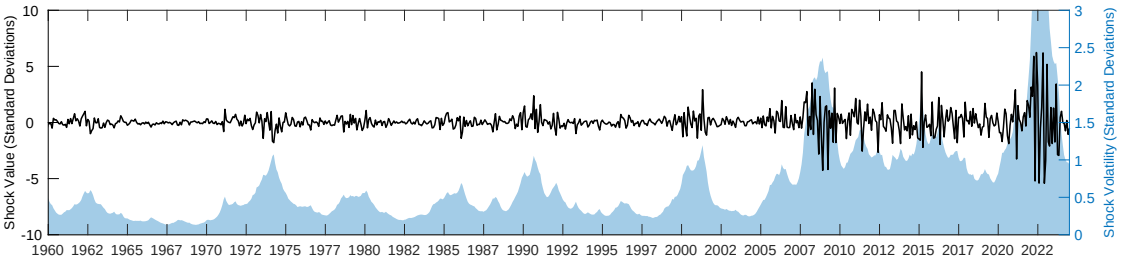

Note:

F Additional Impulse Responses

Figure F.1: Impulse Responses to a Long-Rate Monetary Shock

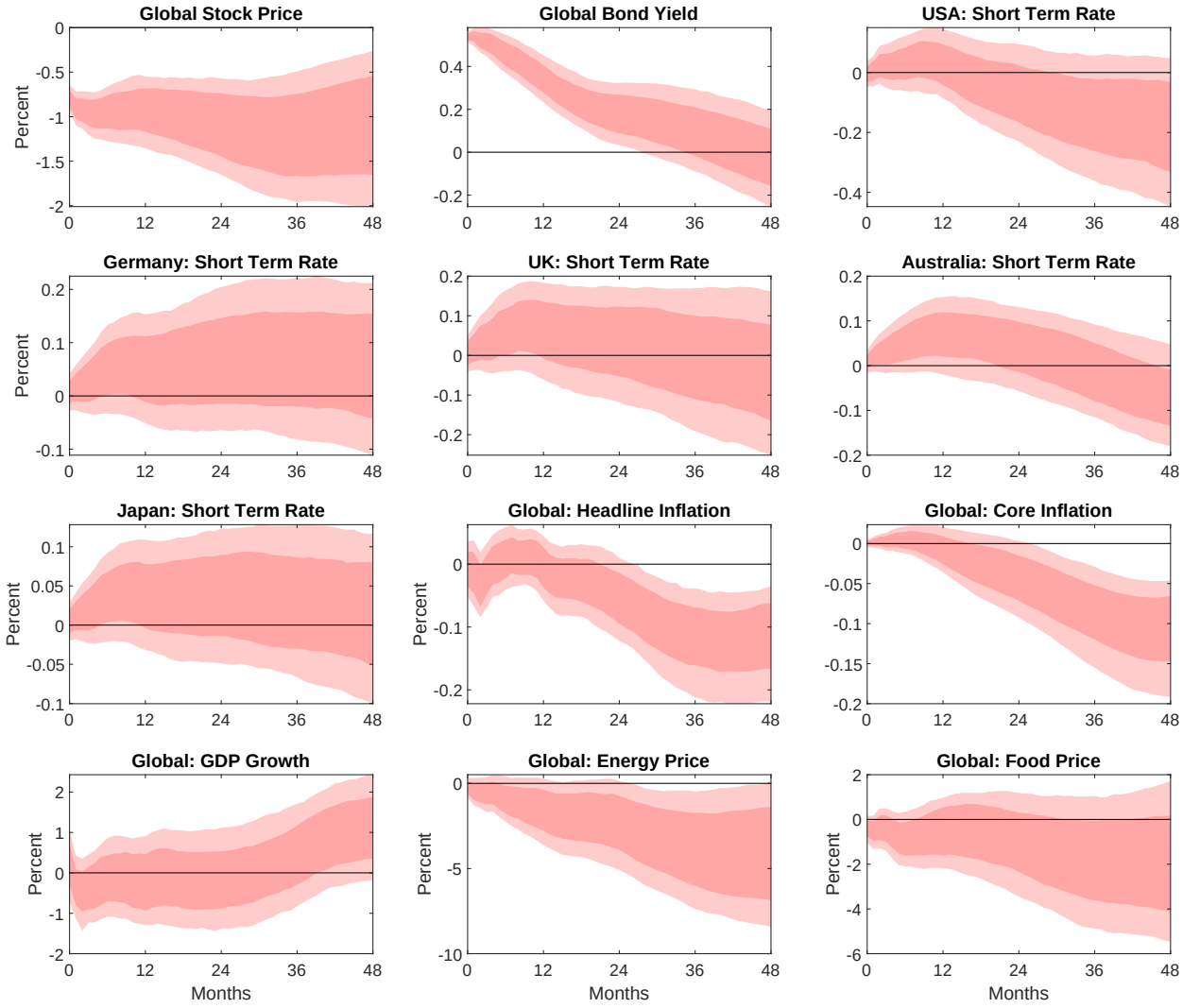

Note: Responses of selected variables to the term premium shock.

Figure F.2: Impulse Responses to an Oil Supply Shock

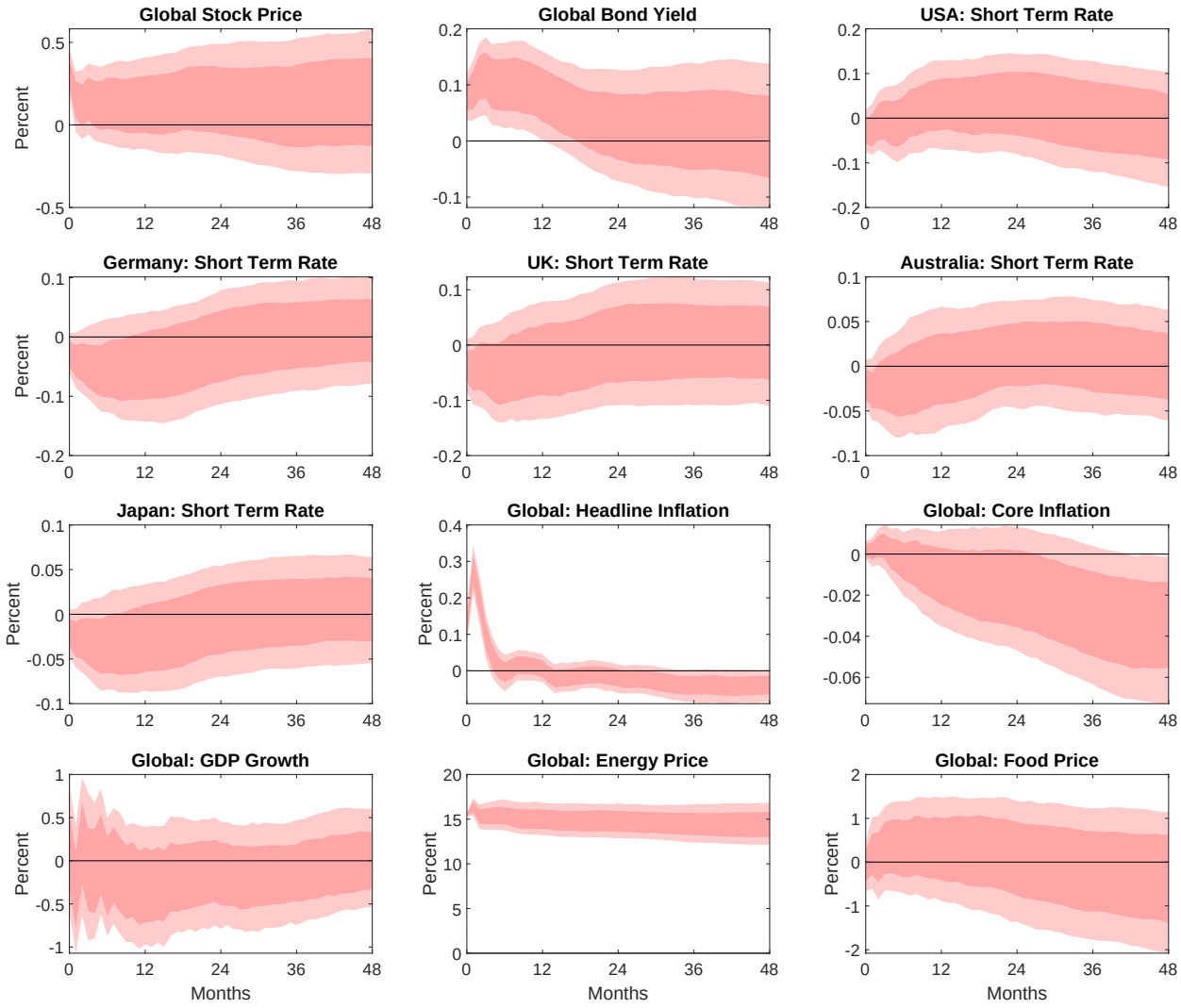

Note: Responses of selected variables to the food supply shock.

Figure F.3: Impulse Responses to an Aggregate Demand Shock

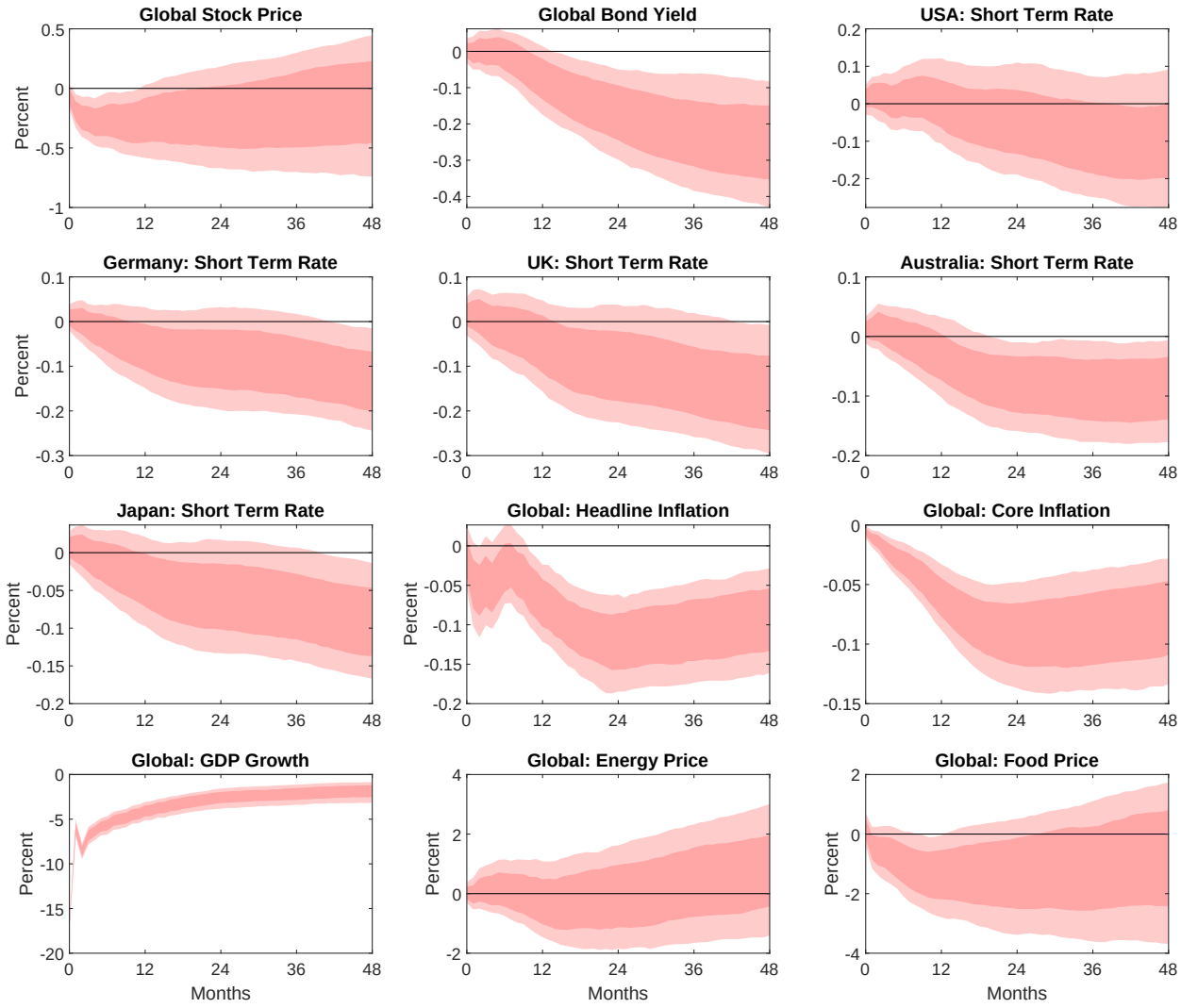

Note: Responses of selected variables to the aggregate demand shock.

Figure F.4: Impulse Responses to an Aggregate Supply Shock

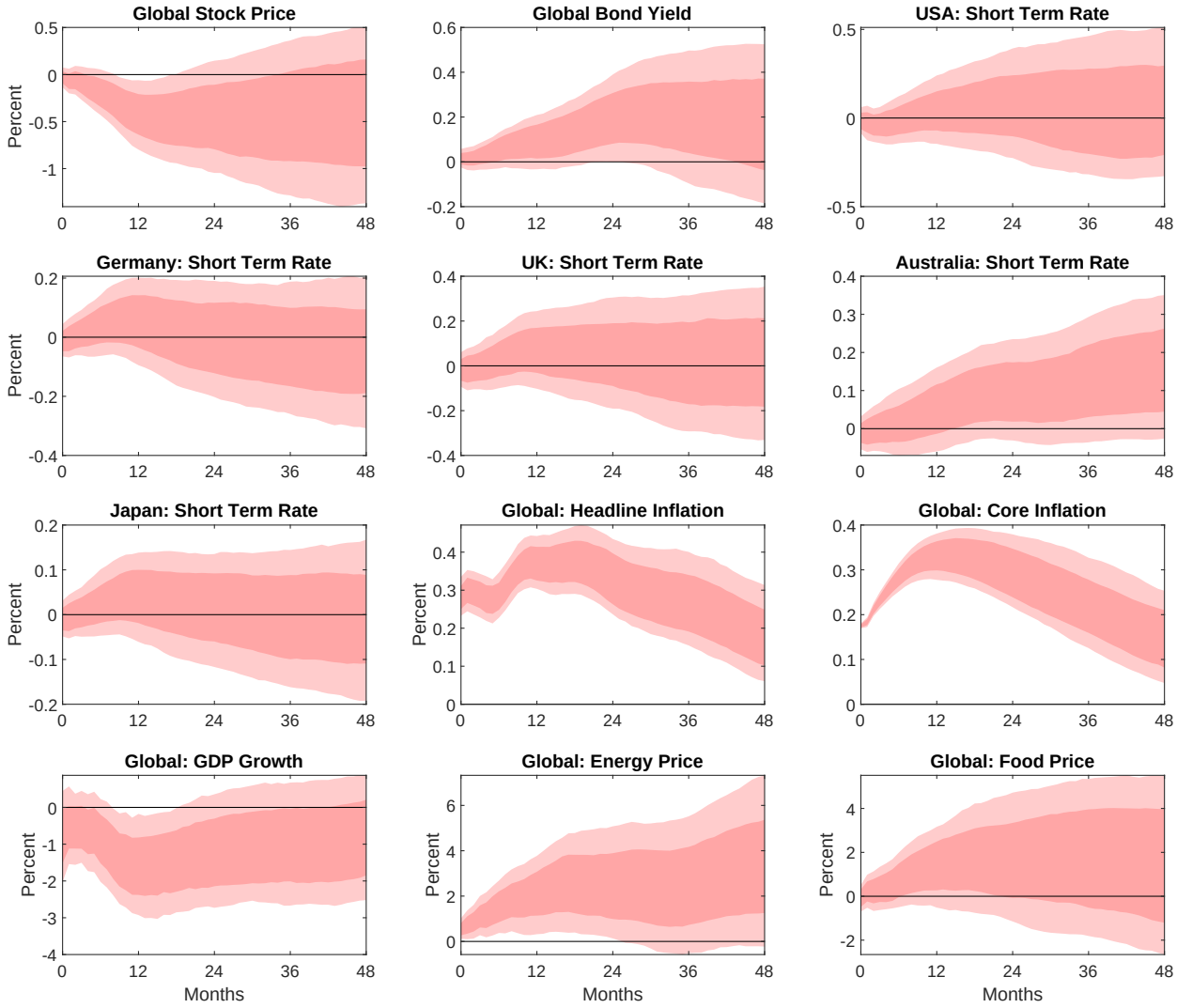

Note: Responses of selected variables to the aggregate supply shock.

Figure F.5: Impulse Responses to a Food Supply Shock

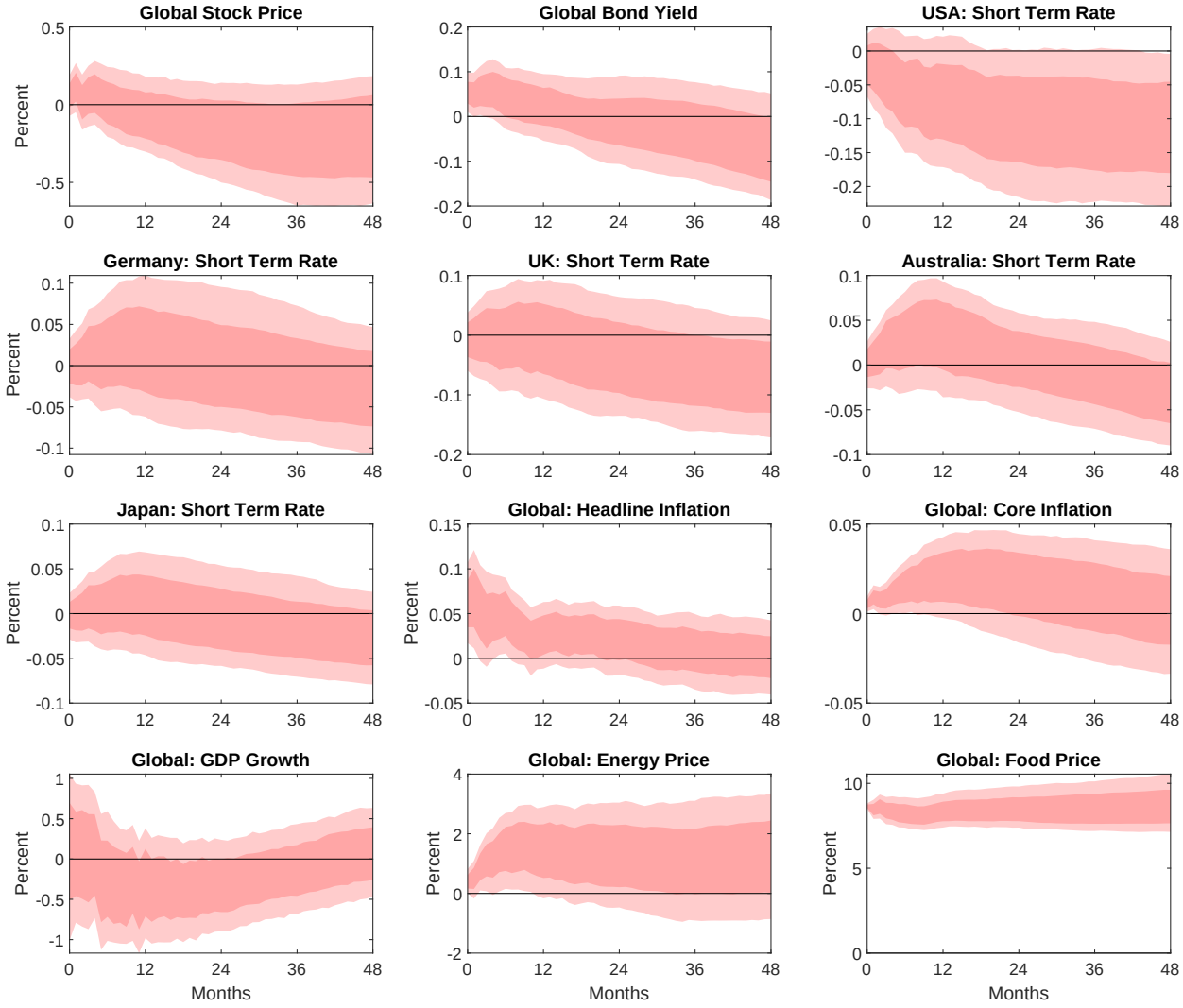

Note: Responses of selected variables to the food supply shock.

G Phillips Curve Correlation Decomposition

Figure G.1: HISTORICAL CORRELATION DECOMPOSITION: STOCK-BOND CORRELATION

(a) Stock-Bond Correlation: Fraction Attributed to Flight-to-Safety Shocks

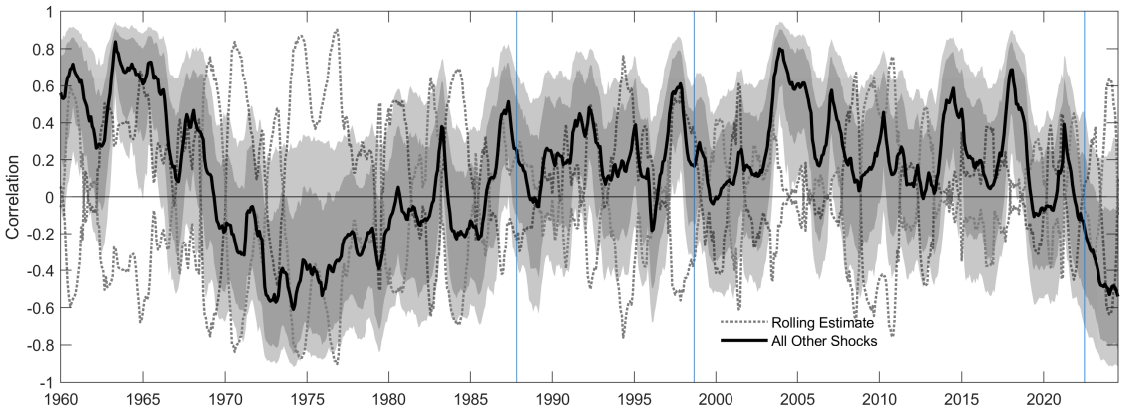

(b) Stock-Bond Correlation: Fraction Attributed to Aggregate Demand Shocks

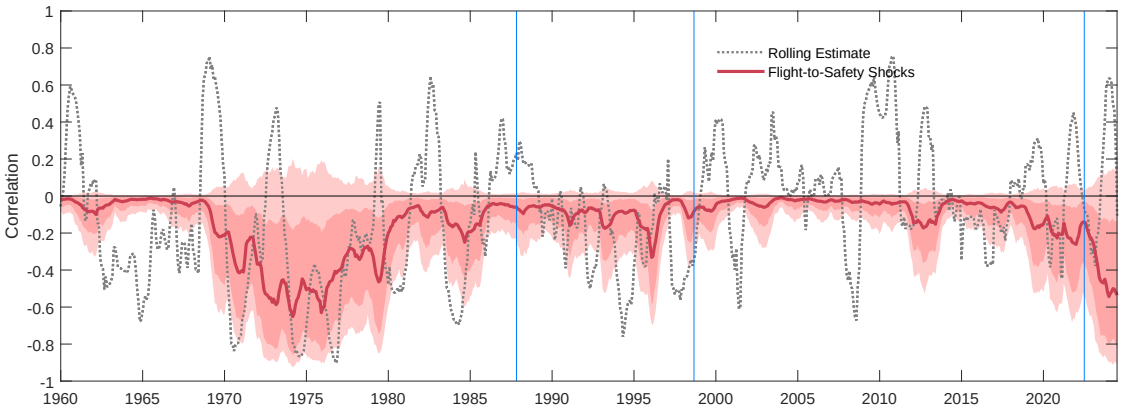

(c) Stock-Bond Correlation: Fraction Attributed to Aggregate Supply Shocks

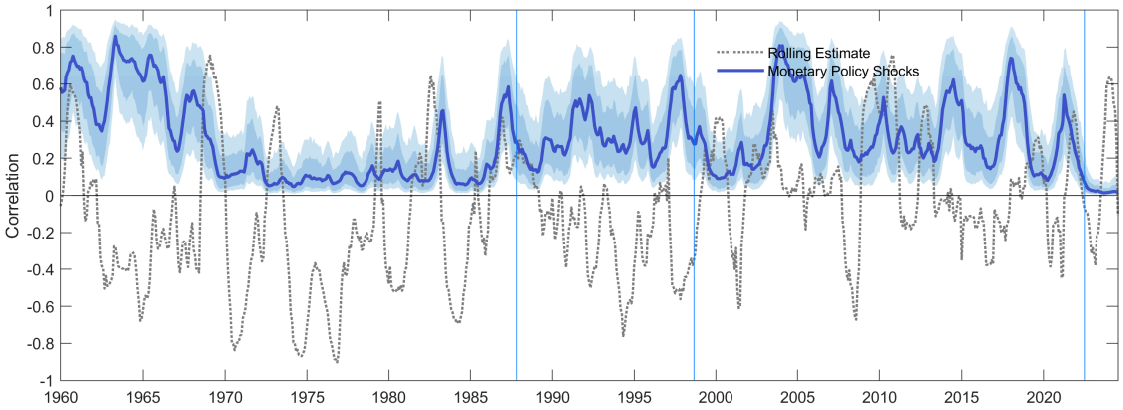

Note: Estimates of stock-bond correlation across twelve advanced economies from January 1955 to June 2024, using monthly data. Each panel presents the posterior median correlation (thick solid line) along with the associated 68% highest posterior density (HPD) interval and 90% interval derived from the global factor model. The posterior estimates account for the portion of the correlation explained by global shocks. The dotted line represents a simple 12-month rolling correlation.

H Steady state of the Model

We solve for the stochastic steady state given a guess of the variances and covariances:

$$
\begin{aligned}
r^{xb} &= [\omega\gamma + \tau(1-\omega)]^{-1}\left(V_b\bar{s}^b + C_{bs}\bar{s}^s\right) && (28)\\
r^{xs} &= \frac{1}{V_b}\left[\frac{V_bV_s - C_{bs}^2}{\tau(1-\omega)} + [\omega\gamma + \tau(1-\omega)]^{-1}C_{bs}^2\right]\bar{s}^s + [\omega\gamma + \tau(1-\omega)]^{-1}C_{bs}\bar{s}^b && (29)\\
y &= \bar{r} + r^{xb} && (30)\\
dp &= (1-\rho)^{-1}\left[r + r^{xs} - \Delta d - \kappa\right] && (31)\\
d^{b,h} &= \gamma\frac{r^{xb}}{V_b} && (32)\\
D_b &= \frac{\tau}{V_bV_s - C_{bs}^2}\left[V_sr^{xb} - C_{bs}r^{xs}\right] && (33)\\
D_s &= \frac{\tau}{V_bV_s - C_{bs}^2}\left[V_br^{xs} - C_{bs}r^{xb}\right] && (34)
\end{aligned}
$$

For the initial guess, we consider a model with no time variation in risk premia. Iterating forward on the return equation, and denoting $\hat{x}$ the deviation of a variable from its unconditional mean, we have $\mathbb{E}_t r^{xb}_{t+1} - r^{xb} = \mathbb{E}_t r^{xs}_{t+1} - r^{xs} = 0$, and:

$$
\begin{aligned}
\hat{y}_t &= (1-\theta)\sum_{s=0}^{\infty}\theta^s\mathbb{E}_t\hat{r}_{t+s} = \left(\frac{1-\theta}{1-\theta\phi_r}\right)r_t\\
\text{Var}_t(r^{xb}_{t+1}) &= \text{Var}_t\left[\left(\frac{\theta}{1-\theta}\right)\hat{y}_t\right] = \left(\frac{\theta}{1-\theta\rho_r}\right)^2\sigma_r^2\\
\hat{dp}_t &= \sum_{s=0}^{\infty}\rho^s\mathbb{E}_t(\hat{r}_{t+s} - \Delta\hat{d}_{t+s+1}) = \left(\frac{1}{1-\rho\phi_r}\right)r_t - \left(\frac{\phi_d}{1-\rho\phi_d}\right)\Delta d_t\\
\text{Var}_t(r^{xs}_{t+1}) &= \text{Var}_t\left[-\rho\hat{dp}_{t+1} + \Delta d_{t+1}\right] = \text{Var}_t\left[-\left(\frac{\rho}{1-\rho\phi_r}\right)r_{t+1} + \left(\frac{1}{1-\rho\phi_d}\right)\Delta d_{t+1}\right]\\
&= \left(\frac{1}{1-\rho\phi_d}\right)^2\sigma_d^2 + \left(\frac{\rho}{1-\rho\phi_d}\right)^2\sigma_r^2 - 2\left(\frac{\rho}{1-\rho\phi_r}\right)\left(\frac{1}{1-\rho\phi_d}\right)\text{Cov}_t(r_{t+1}, d_{t+1})\\
\text{Cov}_t(r^{xb}_{t+1}, r^{xs}_{t+1}) &= \left(\frac{\theta}{1-\theta\phi_r}\right)\left(\frac{\rho}{1-\rho\phi_r}\right)\sigma_r^2 - \left(\frac{\theta}{1-\theta\phi_r}\right)\left(\frac{1}{1-\rho\phi_d}\right)\text{Cov}_t(r_{t+1}, d_{t+1})
\end{aligned}
$$

I Sensitivity Analysis

This section analyzes the sensitivity of the quantitative results to the values of certain key parameters. In particular, I examine the impact of the volatility of interest rate shocks (σ_r), the endogenous

Figure I.1: Sensitivity Analysis, higher interest rate volatility

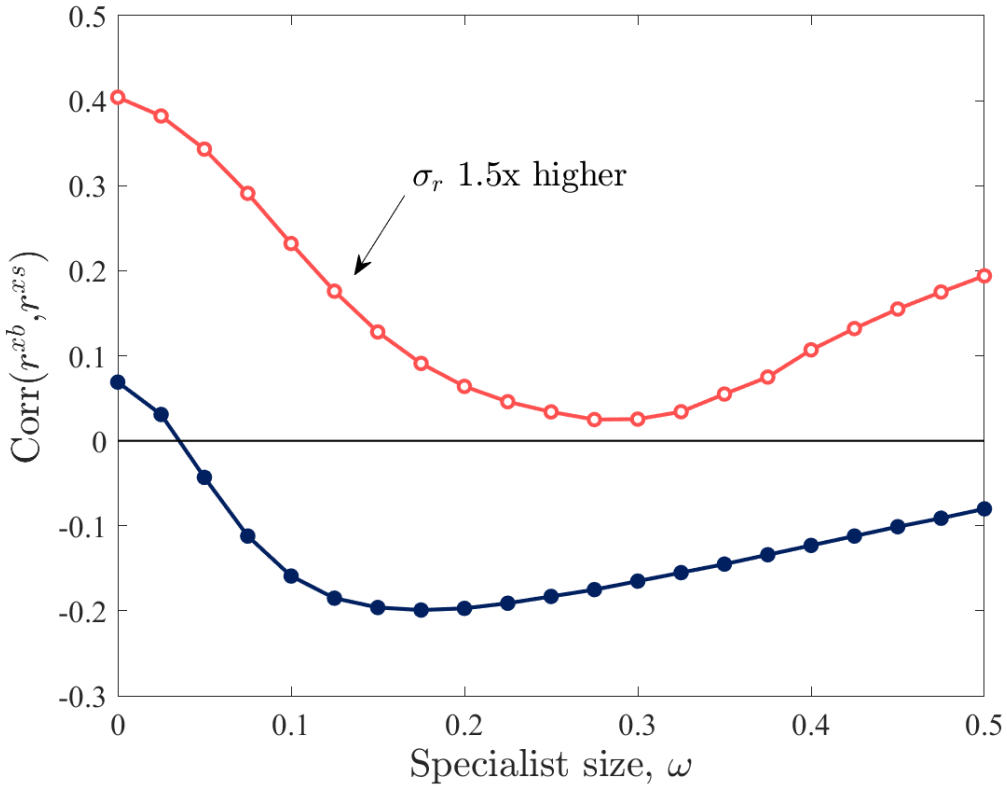

Note: Unconditional stock-bond correlation as the share of hedge funds increases.

response of the real interest rate to dividend growth (captured by the sensitivity parameter β_d), and the degree of adjustment costs in the pension funds portfolio (α).

Starting with the volatility of interest rate shocks, Figure I.1 looks at the impact of increasing the sensitivity of interest rate shocks. Given that this class of shocks leads to a strong movement of equity and bond returns in the same direction, as discussed in the main text, the higher the volatility of interest rate shocks, the less likely that a negative stock-bond correlation emerges in equilibrium. The figure shows how, for an increase of 50% in this parameter, there is no level of ω, the hedge-fund market share, that leads to an unconditionally negative correlation. Therefore, these results show, as discussed in the text, that interest rate volatility being sufficiently low is a necessary condition for the negative correlation to appear.

Figure I.2 examines the sensitivity of the results to the endogenous response of the real interest rate to dividend growth shocks. All else equal, dividend growth shocks lead to an equilibrium negative stock-bond correlation through a "cash-flow" channel as long as this sensitivity is not zero.

Figure I.2: Sensitivity Analysis, lower endogenous response of dividends

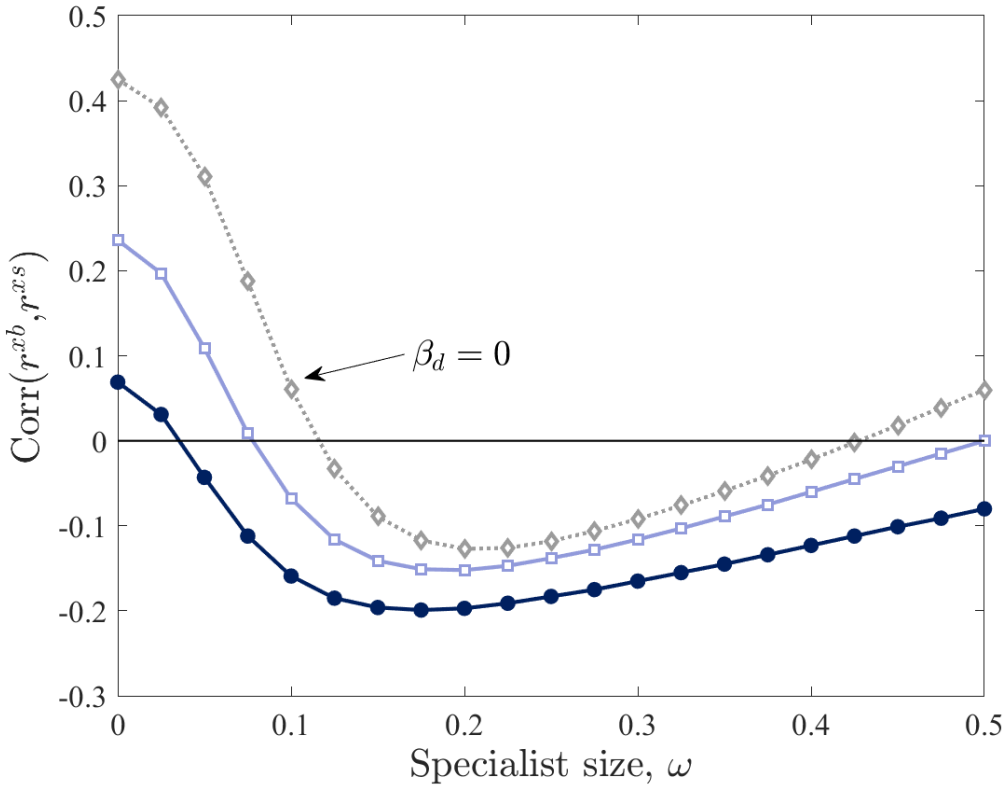

Note: Unconditional stock-bond correlation as the share of hedge funds increases.

The higher the sensitivity, the more likely it is that a negative correlation emerges unconditionally. However, as the figure shows, even in a situation in which this channel is entirely shut down, for a sufficiently large share of specialist hedge funds, the γ-shocks alone are capable of generating a negative unconditional comovement.

Finally, Figure I.3 examines the importance of the adjustment costs for the pension funds portfolios. While the qualitative conclusions of the main paper are not greatly affected by removing the adjustment costs, the figure shows how, the higher the adjustment costs for pension funds, the more the γ-shocks propagate and the more pronounced the negative equilibrium stock-bond correlation.

Figure I.3: Sensitivity Analysis, higher interest rate volatility

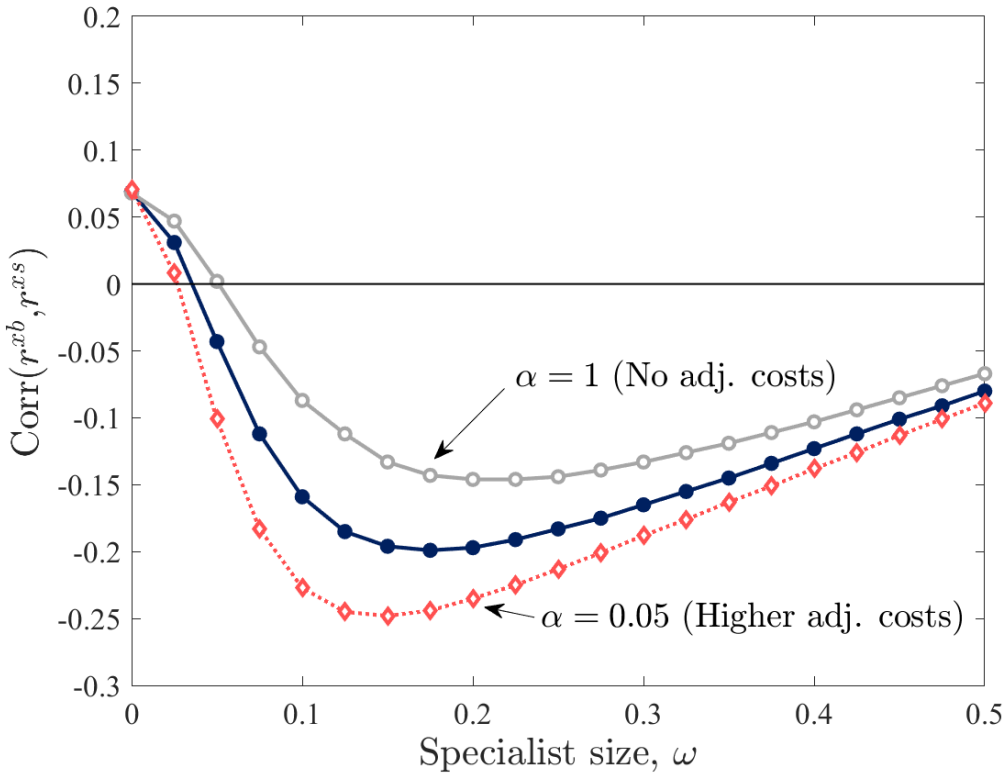

Note: Unconditional stock-bond correlation as the share of hedge funds increases.